POLITECNICO DI MILANO

School of Industrial Processes Engineering

Master of Science in Materials Engineering and Nanotechnology

Synthesis and characterization of ferroelectric Nb-doped PZT thin films

Supervisor: Ing. Luca Magagnin

Master degree thesis by:

Riva Luca

Matricola n°: 779865

Academic year: 2012/2013

ABSTRACT

This thesis deals with the processing and characterization of Nb-doped Lead Zirconate Titanate (PNZT) sol-gel films. PZT has the perovskite structure (general formula, $A^{II}B^{IV}O_3$) and it is one of the materials with the best piezoelectric and ferroelectric property. For this reason it is suitable for potential applications in microelectronic industry as actuators, capacitors, transducers, sensors and for their implementation into MEMS devices. Using donor dopant such as Nb^{5+} on the B-site is one of mechanisms thought to promote domain wall motion in PZTs. Niobium increases the electrical resistance of PZT films and produces polarization hysteresis loops with low coercive fields and large remanent polarizations. However, their effects on the piezoelectric properties of PZT films have not been extensively and systematically studied. The aim of the work was to reduce the number of steps in the film processing by simplifying the production procedures and to use the less hazardous chemicals, as 2-Methoxyethanol based solution, to make the PNZT thin sol-gel films attractive for the industrial applications. First of all, a new route to synthesize stable and homogeneous sol-gel precursors solutions has been developed. Lead(II) acetate trihydrate ($Pb(CH_3CO_2)_2 \cdot 3H_2O$, Niobium(V) ethoxide ($C_{10}H_{25}NbO_5$), Zirconium propoxide $Zr(OCH_2CH_2CH_3)_4$ (70 wt% in propanol) and Titanium isopropoxide [$Ti((CH_3)_2CHO)_4$] are used as precursors materials and acetic acid and propanol as solvents. Four different solutions have been prepared varying the Nb composition. The first solution was prepared adding 0% of Nb to produce a simple PZT solution, in the second 1% of Nb was added, in the third solution there was 2% of Nb and 3% of Nb in the last one. These solutions have been spin coated on $Pt/TiO_2/SiO_2/Si$. For each kind of solution, a proper thermal treatment has been defined to obtain dense, uniform and cracks free PZT films that possess a fully perovskite crystallographic structure. This thermal treatment has been divided in three step: the first at 150°C for 5 minutes, the second at 370°C for 5 minutes, the third step need a temperature able to transform the metastable phase into a full perovskite phase and the temperature is different for each one of the solution used (due to the influence of Niobium): 650°C for the solution 0% Nb, 700°C for the solution 1% Nb, 750°C for the solution 2% Nb and 825°C for the solution 3 %Nb. The films morphology has been analyzed using SEM and optical microscope and the crystallographic structure has been studied using grazing incident X-ray diffraction. The influence of substrate texture and properties and of the performed heat treatment on the films

crystallization mechanism has been discussed. For the solution with 0%, 1%, 2% of Niobium, dense, uniform and crack free PZT films with a fully perovskite crystallographic structure and preferentially oriented towards the (110) plane direction, have been successfully deposited. For the solution with 3% of Niobium good density and homogeneity was very hard to obtain due to the high temperature used for the annealing process. The electrical features of these films have been analyzed calculating the C-V and the ε-V curves, from which the ferroelectric behavior of these films has been confirmed. The values of the dielectric constant obtained were 656 for the PZT thin film, 399 for the PNZT 1%Nb, 451 for the PNZT 2%Nb and 153 for the PNZT 3%Nb.

ABSTRACT

Lo scopo di questa tesi è la sintesi, la deposizione e la successiva analisi delle fasi di un film sottile di PNZT (piombo zirconio titanio drogato niobio). Il PZT semplice ha una struttura perovskitica (formula generale , $A^{II}B^{IV}O_3$) e possiede tra le più alte proprietà piezoelettriche e ferroelettriche ed è largamente utilizzato nell'industria elettronica per produrre sensori, come quelli presenti nei dispositivi airbag o negli accelerometri, attuatori, capacitori, trasduttori. Il drogaggio di questo materiale con un elemento "donatore" come il Nb^{5+} sul sito B del cristallo è uno dei meccanismi pensati per migliorare il movimento dei domini nei PZT. Il Niobio aumenta la resistenza elettrica del film di PZT e produce un ciclo di isteresi con un minor campo coercitivo e una più ampia polarizzazione rimanente. Tuttavia i sui effetti sulle proprietà piezoelettriche dei film di PZT non sono state ancora studiate in maniera approfondita e sistematica. Le linee guida che sono state seguite per sviluppare un metodo efficiente per la produzione di questo tipo di film sottile sono state la semplificazione dei processi produttivi, partendo dalla sintesi della soluzione sol-gel fino al trattamento termico, e l'utilizzo di precursori chimici meno tossici e pericolosi del comunemente usato 2-Me. Usando Piombo Acetato tri-idrato, Zirconio protossido, etossido di Niobio e Titanio isopropossido come precursori dei metalli, acido acetico e propanolo come solvente, quattro tipologie di soluzioni sono state preparate in questo lavoro a seconda della quantità di Niobio contenuto nella soluzione. La prima soluzione è stata preparata senza l'utilizzo dell'etossido di Niobio in modo da ottenere i precursori per la produzione di un film di PZT non drogato, le tre restanti soluzioni contenevano rispettivamente 1%, 2% e 3% di Niobio. dopo numerose prove, un metodo per sintetizzare soluzioni sol-gel di PNZT omogenee e stabili su lunghi periodi è stato definito. I sol gel preparati sono stati depositati utilizzando la tecnica di spin coating su $Pt/TiO_2/SiO_2/Si$. Per ogni tipo di soluzione è stato messo a punto un diverso trattamento termico per cercare di ottenere film densi, uniformi e senza alcun tipo di cricche. Questo trattamento termico è stato suddiviso in tre step: il primo a 150°C per 5 minuti, il secondo a 370°C per 5 minuti. Per il terzo step necessario per la formazione di una fase perovskitica stabile a causa dell'influenza del Niobio sono state utilizzate quatto temperature differenti, 650°C per la soluzione 0%Nb, 700°C per la soluzione 1%Nb, 750°C per la soluzione 2%Nb e 825°C per la soluzione 3%Nb. La durata del processo di cristallizzazione è stata ottimizzata in modo tale da ottenere una struttura cristallina a perovskite

in tutto il film e di evitare la formazione di cricche e l'interdiffusione di elementi tra il substrato e il deposito. La morfologia dei film depositati è stata studiata attraverso l'uso del microscopio ottico e della microscopia elettronica (SEM). L'influenza del drogaggio del Niobio e del tempo di ricottura sul meccanismo e sulla tipologia di cristallizzazione dei film è stato analizzato e discusso attraverso l'analisi di diffrazione a raggi-X. Per i substrati contenenti rispettivamente 0%, 1% e 2% di Niobio film sottili con buona morfologia e con la giusta struttura cristallina sono stati ottenuti con successo. Per i provini contenenti un drogaggio del 3% di Niobio, a causa delle alte temperature raggiunte nella fase di ricottura, la probabilità di ottenere substrati senza cricche è stata piuttosto bassa. I film depositati hanno mostrato durante il processo di cristallizzazione una crescita di strutture a rosetta identificate come porzioni di materiale cristallizzato la cui estensione cresce aumentando il tempo di ricottura. I film depositati hanno mostrato, per tutti i tipi di substrato usati, la formazione di una struttura policristallina con una forte crescita preferenziale del piano (110) e le condizioni per cui sono state ottenute diverse orientazioni preferenziali sono state analizzate e discusse. Matrici di capacitori sono state ottenute da questi film, depositando su di essi elettrodi d'oro attraverso la tecnica di cold spattering, in modo tale da ottenere una struttura metallo/PZT/metallo su cui è possibile effettuare misure elettriche. La caratterizzazione elettrica dei film è stata effettuata misurando le curve C-V e ε-V dei capacitori fabbricati. Queste hanno mostrato, per tutti i dispositivi analizzati, una forma a farfalla tipica dei materiali ferroelettrici, confermando cosi l'effettiva ferroelettricità dei film depositati. Le costanti dielettriche per ogni diversa tipologia di soluzione sono state ricavate dalle misure di capacità e i valori ottenuti sono 656 per il film di PZT 399 per il film di PNZT 1%Nb 451 per il film di PNZT 2%N e 153 per il PNZT 3%Nb.

ACKNOWLEDGEMENTS

First of all I would like to thank my supervisor, Ing. Luca Magagnin, for his constant help and support during all the thesis project period. I would also like to express my particular gratitude to all the staff of the Surface Engineering and Advanced Coatings lab, Simona, Fabio, Lorenzo, Ferdi, Rosario, Federico and Roberto for their help, support and technical exchanges. I wish to thank Dario Picenoni, Mattia Ronchi and Stefano Dellea for all of the SEM, XRD analysis and for the capacitance measures. I would like to thank my family for their support throughout my university education. Finally I would like to thank my friends and university mates, especially Nano, Moment, Valeria, Federica for her help in the English translation, Andre, Atto, Bobo, Chiara, Corra, Edo, Filo, Giorgia, Giulia, Guido, Jappy, Manu, Marco, Michele, Nicla, Omar, Paolo, Riky, Soro and Vale.

CONTENTS

ABSTRACT 2
ACKNOWLEDGEMENTS 6
LIST OF FIGURES 9
LIST OF TABLES 11
1 INTRODUCTION 12
1.1 RESEARCH GOAL 12
2 PIEZOELECTRICITY, FERROELECTRICITY AND PYROELECTRICITY 17
2.1 INTRDUCTION 17
2.2 PIEZOELECTRICITY 19
2.2.1 PIEZOELECTRIC MATERIALS 19
2.2.2 PHYSICAL PRINCIPLE 21
2.3 PYROELECTRICITY 24
2.4 FERROELECTRICITY 25
2.5 PIEZOELECTRIC FOR HARVESTING ACTUATING AND SENSING 28
3 SOL-GEL PROCESS 32
3.1 INTRODUCTION 32
3.1.1 SOL 32
3.1.2 GEL 33
3.2 SOL-GEL FOR PZT 36
3.2.1. CARBOXYLIC ACID BASED SOL-GELS 37
3.2.2 METHOXYETHANOL BASED SOL-GELS 39
3.2.3 SOL-GELS BY THE USE OF DIFFERENT METAL ALKOXIDES 40
4 LEAD ZIRCONATE TITANATE 41
4.1 CRYSTAL STRUCTURE 41
4.1.1 PZT 41
4.1.2 DOPED PZT 47
4.2 DEPOSITION METHODS 48
4.2.1 PHYSICAL VAPOR DEPOSITION 49
4.2.2 CHEMICAL VAPOR DEPOSITION 51
4.2.3 CHEMICAL SOLUTION DEPOSITION 51

5 EXPERIMENTAL PROCEDURES 53
5.1 SOL-GEL PROCESS 53
5.1.1 PZT 56
5.1.2 PNZT 1%Nb 56
5.1.3 PNZT 2%Nb 56
5.1.4 PNZT 3%Nb 57
5.2 PREPARATION OF THE PT SUBSTRATE AND DEPOSITION 57
5.2.1 CHOICE OF THE SUBSTRATE 57
5.2.2 DEPOSITION 60
5.3 HEATING TREATMENT 63
5.3.1 THERMAL ANALYSIS 64
5.3.2 CRYSTALLIZATION MECHANISMS 65
5.3.3 HEATING SEQUENCE 66
5.3.4 EFFECT OF NIOBIUM ON HEATING TEMPERATURE 70
5.3.5 STRESSES EVOLUTION DURING HEATING 71
5.4 TOP ELECTRODES DEPOSITION 73
6 RESULTS AND DISCUSSION 75
6.1 PZT 76
6.1.1 DIFFRACTION ANALYSIS FOR PZT FILMS 79
6.2 PNZT 1% Nb 83
6.2.1 DIFFRACTION ANALYSIS FOR PNZT 1%Nb 85
6.3 PNZT 2% Nb 91
6.3.1 DIFFRACTION ANALYSIS FOR PNZT 2%Nb 95
6.4 PNZT 3%Nb 100
6.4.1 DIFFRACTION ANALYSIS FOR PNZT 3%Nb 104
6.5 COMPOSITION ANALYSIS 108
6.6 ELECTRICAL CHARACTERIZATION 111
6.6.1 ELECTRICAL CHARACTERIZATION OF PZT FILMS 112
6.6.2 ELECTRICAL CHARACTERIZATION OF PNZT 1%Nb FILMS 113
6.6.3 ELECTRICAL CHARACTERIZATION OF PNZT 2%Nb FILMS 115
6.6.4 ELECTRICAL CHARACTERIZATION OF PNZT 3%Nb FILMS 117
7 CONCLUSIONS AND FURTHER WORKS 121
REFERENCES 124

LIST OF FIGURES

Fig. 1:The direct (left) and converse (right) piezoelectric effect [7] 17
Fig. 2: Scheme of crystal classes in function of pyroelectric, piezoelectric and ferroelectric properties [8] 18
Fig. 3: structure of polyvinylidene diflouride (PVDF) [11] 21
Fig. 4: a)piezoelectric crystal b) deformed piezoelectric crystal [12] 22
Fig. 5: phase diagram of PZT illustrating how the Zr/Ti ratio and temperature affects the phase of the ceramic. [10] 23
Fig. 6: effect of poling treatment in Weiss domain [12] 24
Fig. 7: Polarization of a ferroelectric ceramic in response to the change of an outer electric field strength, E. [15] 26
Fig. 8: Direct and converse piezoelectric effect [17] 29
Fig. 9: Piezoelectric cantilever stack [17] 30
Fig. 10: Overview of the sol gel process. [20] 35
Fig. 11: Firing schedule example for PZT sol gel. 36
Fig. 12: Flow chart of Yi and Sayer recipe [21] 39
Fig. 13: PZT perovskite structure, b) PZT pyrochlore structure [27] 42
Fig. 14: Phase diagram of $PbZrO_3$-$PbTiO_3$ solid solution [4] 43
Fig. 15: (a) PZT Cubic structure above Tc (b) Movement of Ti or Zr ions below Tc [8] 44
Fig. 16: Piezoelectric coefficients of $Pb(Zr,Ti)O_3$ ceramics as a function of composition close to the morphotropic phase boundary [28] 45
Fig. 17: Drawings of (100), (110) and (111) plains [8] 46
Fig. 18: schematic rapresentation of the sol-gel solution preparation 55
Fig. 19: schematic example of spin coating [26] 61
Fig. 20: in the figure are reported different kind of defects that can be arise during spin coating: a)comets; b) striations; c) concentric circles; d) cracks 63
Fig. 21: schematic process of the thermal treatment 70
Fig. 22: optical microscope image of a cracked PZT Nb-doped film onto Pt substrate 72
Fig. 23: a) PZT capacitors stack structure b):electric scheme of two capacitors in series 73
Fig. 24: electrode deposited ont PNZT film 74
Fig. 25: Optical microscope images of double layer PZT films deposited on Pt/TiO2/Si substrate and annealed for 30 min at 650°C 77
Fig. 26: SEM of PZT single layer deposited on $Pt/TiO_2/Si$ substrate and annealed at 650°C for 30 min.. 78
Fig. 27: cross section of a PZT thin film annealed at 650°C for 30minutes 79
Fig. 28: XRD of PZT films deposited on Pt/TiO2/Si substrate annealed at 650°C for 5 min 80
Fig. 29: XRD of PZT films deposited on Pt/TiO2/Si substrate annealed at 650°C for 10 min 81
Fig. 30: XRD of PZT films deposited on Pt/TiO2/Si substrate annealed at 650°C for 30 min 81
Fig. 31: PNZT 1%Nb double layer annealed at 700°C for 30 minutes. 83
Fig. 32: SEM images of double PNZT1%Nb layer derived from propanol based solution annealed at 700°C for 30min 84
Fig. 33: cross section of single PNZT1%Nb film 85
Fig. 34: XRD of PNZT 1%Nb films deposited on Pt/TiO2/Si substrate annealed at 650°C for 5 min 86

Fig. 35: XRD of PNZT 1%Nb films deposited on Pt/TiO2/Si substrate annealed at 650°C for 10 min.... 86
Fig. 36: XRD of PNZT 1%Nb films deposited on Pt/TiO2/Si substrate annealed at 650°C for 20 min.... 87
Fig. 37: XRD of PNZT 1%Nb films deposited on Pt/TiO2/Si substrate annealed at 650°C for 30 min.... 87
Fig. 38: XRD of PNZT 1%Nb films deposited on Pt/TiO2/Si substrate annealed at 700°C for 10 min.... 88
Fig. 39: XRD of PNZT 1%Nb films deposited on Pt/TiO2/Si substrate annealed at 700°C for 20 min.... 89
Fig. 40: XRD of PNZT 1%Nb films deposited on Pt/TiO2/Si substrate annealed at 700°C for 30 min.... 89
Fig. 41: island of different morphology into PNZT film annealed at 700°C for 30 minutes. 91
Fig. 42:: crack into PNZT 2%Nb annealed at 750°C for 30min. 92
Fig. 43: PNZT 2%Nb double layer annealed at 750°C for 30 minutes. 93
Fig. 44: SEM images of double PNZT2%Nb layer derived from propanol based solution annealed at 750°C for 30 min..... 94
Fig. 45: cross section of single PZT film 95
Fig. 46: XRD of PNZT 2%Nb films deposited on Pt/TiO2/Si substrate annealed at 700°C for 20 min.... 96
Fig. 47: XRD of PNZT 2%Nb films deposited on Pt/TiO2/Si substrate annealed at 700°C for 40 min.... 96
Fig. 48: XRD of PNZT 2%Nb films deposited on Pt/TiO2/Si substrate annealed at 700°C for 50 min.... 97
Fig. 49: XRD of PNZT 2%Nb films deposited on Pt/TiO2/Si substrate annealed at 700°C for 1 hour 97
Fig. 50: XRD of PNZT 2%Nb films deposited on Pt/TiO2/Si substrate annealed at 750°C for 10 min.... 98
Fig. 51: XRD of PNZT 2%Nb films deposited on Pt/TiO2/Si substrate annealed at 750°C for 20min..... 99
Fig. 52: XRD of PNZT 2%Nb films deposited on Pt/TiO2/Si substrate annealed at 750°C for 30min..... 99
Fig. 53: island of different morphology into PNZT3%Nb film annealed at 700°C for 30 minutes. 101
Fig. 54: cracks in a film of PNZT3%Nb 102
Fig. 55: microcracks in a film of PNZT3%Nb 102
Fig. 56: PNZT 3%Nb double layer annealed at 825°C for 30 minutes 103
Fig. 57: SEM images of double PNZT3%Nb layer derived from propanol based solution annealed at 825°C for 30 min. 103
Fig. 58: cross section of single PNZT3%Nb film 104
Fig. 59: XRD of PNZT 3%Nb films deposited on Pt/TiO2/Si substrate annealed at 700°C for 30min... 105
Fig. 60: XRD of PNZT 3%Nb films deposited on Pt/TiO2/Si substrate annealed at 700°C for 40min... 105
Fig. 61: XRD of PNZT 3%Nb films deposited on Pt/TiO2/Si substrate annealed at 700°C for 50min... 106
Fig. 62: XRD of PNZT 3%Nb films deposited on Pt/TiO2/Si substrate annealed at 700°C for 1h..... 106
Fig. 63: XRD of PNZT 3%Nb films deposited on Pt/TiO2/Si substrate annealed at 825°C for 10min... 107
Fig. 64: XRD of PNZT 3%Nb films deposited on Pt/TiO2/Si substrate annealed at 825°C for 20min... 107
Fig. 65: XRD of PNZT 3%Nb films deposited on Pt/TiO2/Si substrate annealed at 825°C for 30min... 108
Fig. 66: Composition of a single layer of PZT anneal at 650°C for 30min..... 109
Fig. 67: composition of three double layer of PNZT (1%,2%,3%) anneal respectively at 700°C, 750°C, 825°C for 30min..... 110
Fig. 68: C-V curve for 1µm PZT substrate annealed at 650°C for 30min 112
Fig. 69: ε-V curve for 1µm PZT substrate annealed at 650°C for 30min 113
Fig. 70: C-V curve for 1µm PNZT 1%Nb substrate annealed at 700°C for 30min 114
Fig. 71: ε-V curve for 1µm PNZT 1%Nb substrate annealed at 700°C for 30min 115
Fig. 72: C-V curve for 1µm PNZT 2%Nb substrate annealed at 750°C for 30min 116
Fig. 73: ε-V curve for 1µm PNZT 2%Nb substrate annealed at 750°C for 30min 117
Fig. 74: C-V curve for 1µm PNZT 3%Nb substrate annealed at 825°C for 30min 118
Fig. 75: curve for 1µm PNZT 3%Nb substrate annealed at 825°C for 30min 119

LIST OF TABLES

Tab. 1: different example for PZT substrate 58
Tab. 2: Composition of a single layer of PZT anneal at 650°C for 30min. 109
Tab. 3: composition of three double layer of PNZT (1%,2%,3%) anneal respectively at 700°C, 750°C, 825°C for 30min 110
Tab. 4: mean value and maximum value of dielectric constant 120

CHAPTER 1

1 INTRODUCTION

1.1 RESEARCH GOAL

The purpose of this study is to develop a reproducible method to synthesize a Nb doped Lead Zirconate Titanate (PNZT) thin films for ferroelectric and piezoelectric applications using sol gel technique. Starting from PNZT sol gel precursor solution synthesis, different routes will be studied to find which is the one that permit to obtain the best electrical features from the ferroelectric film. The role of this type of material in the electronic devices and MEMS industry is gathering great attention for the production of high density memories, actuators, transducers and sensors thanks to the ability to integrate this type of films inside the silicon chip, increasing in this way the miniaturization of the whole device with all the resulting benefits, as low power consumption and high frequency response. Micro electromechanical systems (MEMS) based on piezoelectric thin films have gained importance in recent times because of the efficient transformation between mechanical and electrical forms of energy in piezoelectric materials. Piezoelectric MEMS devices attracted particular attention because of vibration energy harvesting. They are one of the best candidates for exploiting environmental energy when daylight is absent, and piezoelectric energy conversion is especially efficient at low frequencies as compared with electromagnetic conversion, also giving higher voltages [1]. Lead zirconate titanate (PZT) thin films that have a composition $Pb(Zr_{0.52}Ti_{0.48})O_3$, near the morphotropic phase boundary, have been investigated extensively in the recent years. They have been used in ferroelectric memory applications and micro-electro-mechanical systems (MEMS). The most common applications of PZT thin films are accelerometers, ferroelectric random access memories (FeRAM), amplifiers, thermal imaging and non-volatile memories. PZT materials which have a perovskite structure possess a number of properties which make them suitable

candidates for memory applications. With some compositional modifications like adding dopants, modifiers or using other compositions, the properties can be improved for specific applications [2]. A particular characteristic of these materials, on which this thesis is focused, is the piezoelectricity. The piezoelectricity is the ability of some material, called piezoelectrics, of producing a mechanical output when subjected to an electrical input, and vice versa of creating free charges in response of a mechanical stimulus. Piezoelectric materials have been used since the very beginning of the XX century. They were used in ultrasonic devices or in phonograph. They are now present in many simple macroscopic devices either sensors or actuators. With the rise of Micro-Electro-Mechanical-Systems (MEMS) a new focus is on piezoelectricity. The great advantage of the piezoelectric phenomenon is that it does not exhibit failure modes associated with charge storage and it is reversible and linear (properties which electrostatic capacitors do not have)[3]. On the other hand the importance in miniaturize actuators is related to the less invasive size of small devices, in fact the smaller is the devices size, the less is the energy used for the actuation operations. This fact suggests to use materials with high energy density as piezoelectrics. Moreover, one can expect larger force output from piezoelectric MEMS actuators than that available from electrostatic actuators now being employed in MEMS. Furthermore, micromachined piezoelectric actuators are capable of sub-microsecond response times and can operate at low bias voltages (5-15V) while consuming only microwatts of power [4]. Piezoelectric materials show also high acoustic quality. One can summarize their advantages as follows:

- Strong forces, or alternatively large excursions in bending structures;
- Low voltage because of high dielectric constant;
- High efficiency in energy conversion
- High-speed and high-frequency
- High acoustic qualities
- Linear behavior

In spite of these promising properties, piezoelectric materials have some disadvantages. Because of the small ultimate strain (usually less than 10%) and high stresses (several MPa) of piezoelectrics materials, their use is only suitable for applications with large forces but small displacements. Moreover, the most popular piezoelectric material (PZT) contains Lead which is

toxic. Researchers are now trying to develop some new Lead-free piezoelectric materials as the Barium Titanate (BTO) or the Polyvinylidene fluoride (PVDF) which is a synthetic polymer that exhibits low piezoelectricity. Until now, such researchers are far from reaching results comparable to that of PZT and the process temperature used in Lead containing material is still lower than that of Lead free material as BTO. The problem of integration of small amount of piezoelectric materials (as thin films or as bulk) in MEMS is the major challenge researchers are dealing with. The complications are given both by the technological feasibility to deposit thin layers of piezoelectric materials on silicon substrate and by the reduction of the technologically caused constraints, like thickness deviation and deformation by residual stress. Another important problem is that polycrystalline PZT thin films deposited on substrates show high energy loss and low piezoelectric response compared with bulk PZT materials, mainly due to the clamping effect of substrates and limited film thickness effects . Some previous studies have shown that Nb-doping is effective in enhancing the piezoelectric response of PZT bulk materials, mainly due to the increased mobility of domains and reduced coercive field. Lead oxide evaporation in PZT materials annealed at crystallized temperature always seems to occur with Lead and oxygen vacancies. The introduction of Nb doping leads to reduction of oxygen vacancies by its excess oxygen atoms and thus domain-wall pinning reduces. However, few reports have been reported on Nb-doped PZT films to elucidate the mechanisms of the enhanced properties by such doping, especially for broad compositional range with preferred orientation [5]. In the perovskite structure, Nb^{5+} substitutes for Zr^{4+}/Ti^{4+} site. By the substitution of Nb^{5+} ion on perovskite lattice, additional positive charge is introduced and Pb^{2+} vacancies are created to maintain charge neutrality. For every two atoms of Nb^{5+} introduced into the lattice, one Pb^{2+} vacancy occurs. Such Nb-doped PZT materials have been reported to possess increased dielectric constants, lower coercive fields and square hysteresis loops.[2]. There are essentially three approaches to form devices: the first one is based on the deposition of piezoelectric thin films on silicon substrates with appropriate insulating and conducting layers followed by surface or silicon bulk micromachining to form the micro-machined transducers (additive approach); the second one is the direct bulk micromachining of single crystal or polycrystalline piezoelectrics and piezoceramics which are thereafter appropriately electroded to form micro-machined transducers (subtractive approach) and the third one is the based on the integration of micro-machined structures in silicon via bonding techniques onto bulk piezoelectric substrates (integrative approach). The most common approach is the additive one, based on the deposition of thin oxide film. The best route to create this kind of piezoelectric film is the sol-gel method. The sol–gel method has been widely studied as a new route for the preparation of ceramics, due

to its advantages such as: the mixing of reactants on a molecular level, a better control of the stechiometry higher-purity raw materials, easy formation of ultra-fine and crystallization powders with controlled morphology and grain size. It should display considerable stability in solution to guarantee the reproducibility of the materials preparation and it has to be easy to be purified to provide sufficient chemical quality of the final products. Generally, physical methods have shown considerable success in the growth of high quality ultrathin oxide films but these methods are expensive and unfavorable when large substrate surfaces need to be deposited. Chemical methods appear to be more suitable for easier fabrication of larger areas, simpler composition control and better thin film homogeneity as well as for lowering the synthesis temperature. Unfortunately, some problems, such as microstructural instability, could appear as a result of high temperature or long annealing time when chemical methods are used for ultrathin film preparation. In other words, it was found that oxide thin films with thickness below the critical value break up and form nanoislands after high temperature processing. This type of micro structural instability might have a negative influence on ferroelectric properties and needs to be avoided in the preparation of ultrathin films[3]. One of the major advantages attributed to the use of chemical methods is the ability to produce fine active powders with high surface areas. Ceramics derived from powders of this type are typically characterized by lower sintering temperatures and fine microstructures. Furthermore, the ability to process this class of materials at low temperatures has allowed the use of less expensive materials in thick film capacitor applications, and sol–gel derived films, integration directly onto semiconductors without deleterious interactions. The development of sol–gel technology has, at very early step, put forward a request on the development of precursor compounds that are easily transformed into chemically reactive forms or hydrated oxides on hydrolysis [6]. Therefore, the ferroelectric ceramics thin films and their ferroelectric, dielectric and piezoelectric properties are important to be reviewed by providing an insight into different processes which may affect the behavior of ferroelectric devices and specific applications. Among the available piezoelectric materials, Lead zirconate titanate Pb $(Zr_xTi_{(1-x)})O_3$, also called simply PZT as already mentioned, is the most popular due to its superior dielectric constant, piezoelectric constants, and thermal stability. PZT finds broad application as capacitor, transducer, sensor and actuator. The increasing need of miniaturization of such devices and their implementation onto a silicon chip leads to the development of micro-electromechanical systems (MEMS). To exploit the good PZT properties in a wide range of piezoelectric actuator applications in MEMS devices thick films are needed from some microns to several 10's micron. This kind of thick films are not easy to be obtained via sol gel technique because of film cracking above a critical thickness of few microns. Many

attempts were undertaken to increase the single layer thickness and so to reduce the quantity of processing steps. When the thickness of a single layer increases, it simultaneously increases the internal stress into the film which easily leads to cracking. It's thus fundamental to define a procedure to deposit dense, thick and free from cracks PZT films that has to be as simple as possible and guarantee good electrical properties.

CHAPTER 2

2 PIEZOELECTRICITY, FERROELECTRICITY AND PYROELECTRICITY

2.1 INTRDUCTION

Crystal geometry includes 7 mayor crystal systems: cubic, hexagonal, orthorhombic, monoclinic, tetragonal, triclinic and trigonal. These crystal groups can be subdivided into point groups (crystal classes) according to their symmetry with respect to a point. In total, there are 32 such classes and 11 of them posses a center of symmetry. If a uniform stress is applied to a centrosymmetrical crystal the resulting small movement of charge is symmetrically distributed around the center of symmetry and so the relative displacement is fully compensated. The remaining 21 non-centrosymmetric classes, all except one, exhibit polarity when subject to stress because the charge displacement is not compensated. The polarity is linear with stress and the reversal of the stimulus results in a reversal of the response. This effect is termed piezoeffect and the materials that possess this property are defined as piezoelectric material.

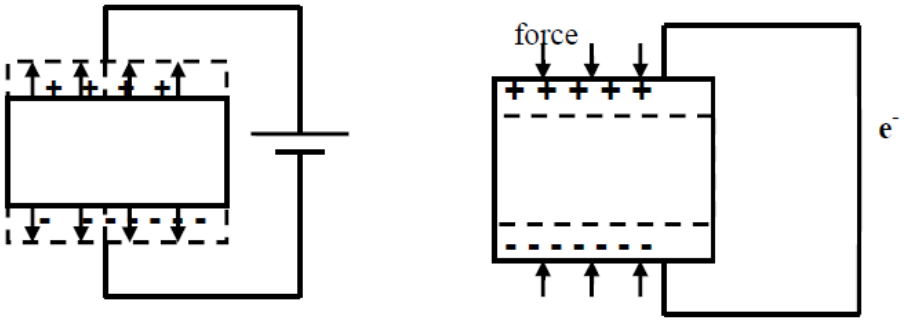

Fig. 1:The direct (left) and converse (right) piezoelectric effect [7]

The piezoelectric effect was discovered by Pierre and Jacques Curie in the late 1800 and occurs in materials with dipole moments resulting from non-centrosymmetric crystal structures. The direct piezoelectric effect occurs when a charge is generated due to a change in the dipole movement caused by the application of a mechanical stress to the crystal. Coupled with some electrode it actually works as a transducer which produces charge (voltage) at the electrode upon the application of stress, exploiting the direct piezoelectric effect. The converse piezoelectric effect occurs when a strain is generated on the crystal by the application of an electric field. Quartz crystals in bulk resonators are examples of natural piezoelectric crystals. In Fig. 1 the direct and converse piezoelectric effect are depicted. 10 out of 20 of the piezoelectric crystal classes have a unique polar axis. Crystals belonging to these classes are called polar because they possess a spontaneous polarization or electric moment per unit volume. The spontaneous polarization in such crystals is temperature dependent and its existence can be detected by observing the flow of charge towards and from the surface on change of temperature. This is the pyroelectric effect and the 10 polar classes that have a unique polar axis are often referred to as the pyroelectric classes. Finally, the spontaneous polarization vector can be reversed, thus it's possible to reverse the barycenter of positive and negative charges. The materials that possess this property are called ferroelectrics.

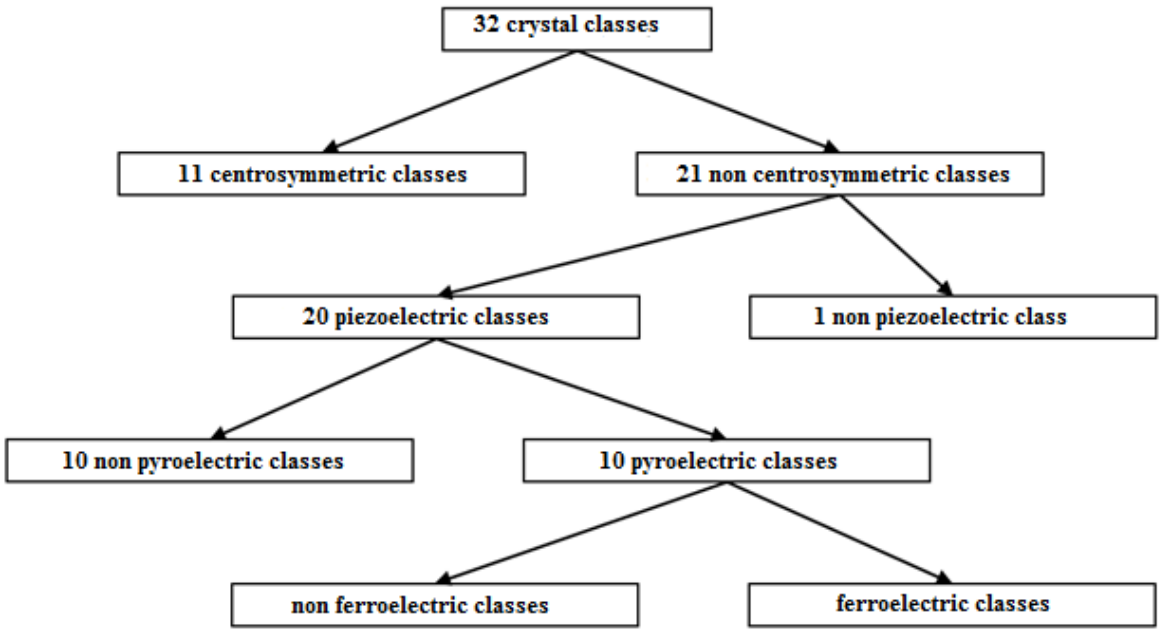

Fig. 2: Scheme of crystal classes in function of pyroelectric, piezoelectric and ferroelectric properties [8]

2.2 PIEZOELECTRICITY

The world piezoelectricity comes from Greek and means “electricity by pressure”. This name was proposed by Hankel in 1881 to name the phenomenon that was discovered a year before by Pierre and Jacques Curie[9]. They observed that in certain types of crystals electrical energy was converted into mechanical energy or viceversa. We can distinguish:

direct piezoelectric effect, that is the phenomena where charges are generated when appropriate stresses are applied to the crystals;

converse piezoelectric effect, that is the phenomena where crystal contract or expand subject to an applied electric field. [10]. The piezoelectric effect is exhibit by a number of naturally-occurring crystals, for instance quartz, tourmaline and sodium potassium tartrate

2.2.1 PIEZOELECTRIC MATERIALS

This section summarizes the current status of piezoelectric materials: single-crystal materials, piezoceramics, piezopolymers and piezocomposites.

Single crystal: the most popular single-crystal materials are quartz, lithium niobate ($LiNbO_3$) and lithium tantalite ($LiTaO_3$). The single crystals are anisotropic, exhibiting different material properties depending on the cut of the materials and direction of bulk. Quartz is a well-known piezoelectric materials. α-Quartz belongs to the triclinic crystal system with point group 32 and has a phase transition at 537◦C to its β-form, which is not piezoelectric. LiNbO3 and LiTaO3 belong to an isomorphous crystal system and are composed of oxygen octahedron. These materials have high electromechanical coupling coefficients for surface acoustic wave. In addition, large single crystals can easily be obtained from their melt using the conventional Czochralski technique. Thus both materials occupy very important positions in the surface acoustic wave (SAW) device application field.

Polycrystalline Materials: barium titanate ($BaTiO_3$) is one of the most thoroughly studied and most widely used piezoelectric materials. The dielectric and piezoelectric properties of ferroelectric ceramic $BaTiO_3$ can be affected by its own stoichiometry, microstructure, and by dopants entering onto the A or B site in solid solution. Modified ceramic $BaTiO_3$ with dopants such as Pb or Ca ions have been developed to stabilize the tetragonal phase over a wider temperature range and are used as commercial piezoelectric materials. Piezoelectric Pb(Ti,Zr)O3

solid solutions (PZT) ceramics have been widely used because of their superior piezoelectric properties. The crystalline symmetry of this solid-solution system is determined by the Zr content. Lead titanate also has a tetragonal ferroelectric phase of perovskite structure. With increasing Zr content, *x*, the tetragonal distortion decreases and at $x > 0.52$ the structure changes from the tetragonal 4*mm* phase to another ferroelectric phase of rhombohedral 3*m* symmetry. The line dividing these two phases is called the *morphotropic phase boundary* (MPB). The electrical property of a PZT film can be modified by the introduction of dopants. According to the defect chemistry of the perovskite structure, introduction of charged impurities can change the degree of oxygen vacancy. If trivalent acceptors are substituted in the B site of PZT films, oxygen vacancies are generated in the PZT structure. On the other hand, donor doping is considered to be one of the most suitable way to compensate the oxygen vacancies. When the pentavalent donors are introduced into the PZT structure, the amount of oxygen vacancies will decreased. Additionally, the introduced foreign elements can influence the structure and lattice energy of PZT, since the ionic sizes and charges of dopants are different from those of Ti(IV) or Zr(IV). In order to modify the ferroelectric property of PZT, pentavalent Nb(V) as a donor element and trivalent Sc(III) as an acceptor element, are generally used. It is thought that these elements can substitute the B site of perovskite structure in the PZT film, since their ionic size are similar to those of Ti(IV) or Zr(IV).

Polymers: Polyvinylidene difluoride, PVDF (Fig.3) or PVF2, is piezoelectric when stretched during fabrication. Thin sheets of the cast polymer are then drawn and stretched in the plane of the sheet, at least in one direction, and frequently also in the perpendicular direction, to transform the material into its microscopically polar phase. Crystallization from the melt forms the non-polar α-phase, which can be converted into the polar β-phase by uniaxial or biaxial drawing operation.

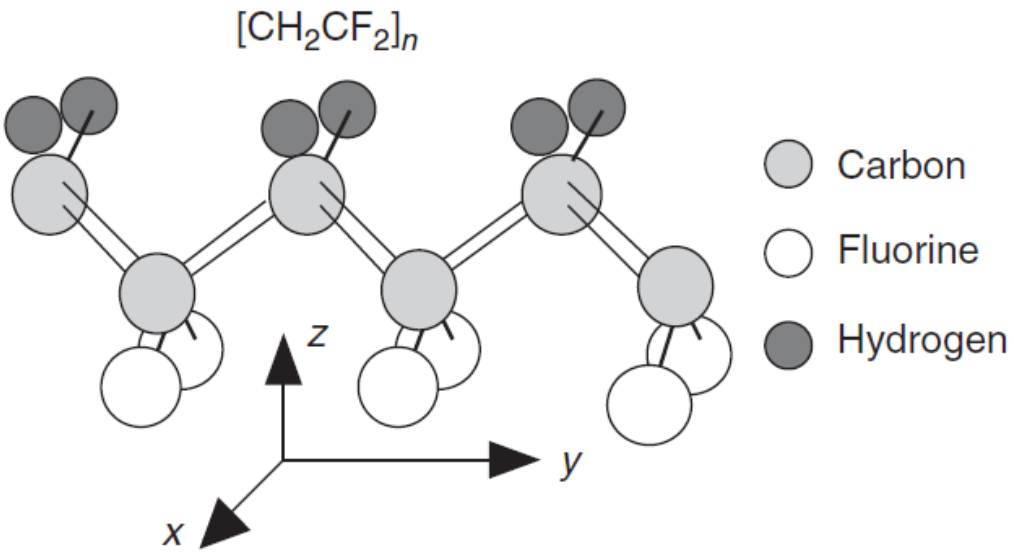

Fig. 3: structure of polyvinylidene diflouride (PVDF) [11]

Composites: piezocomposites comprised of a piezoelectric ceramic and a polymer phase are promising materials because of their excellent and readily tailored properties. The geometry for two-phase composites can be classified according to the dimensional connectivity of each phase into 10 structure; 0–0, 0–1, 0–2, 0–3, 1–1, 1–2, 1–3, 2–2, 2–3 and 3–3 [15]. A 1–3 piezocomposite, such as the PZT rod/polymer composite is a more promising candidate. The advantages of this composite are high coupling factors, low acoustic impedance, good matching to water or human tissue, mechanical flexibility, broad bandwidth in combination with a low mechanical quality factor and the possibility of making undiced arrays by structuring the electrodes. [11]

2.2.2 PHYSICAL PRINCIPLE

For a crystal to exhibit the piezoelectric effect, its structure should have no center of symmetry. A stress (tensile or compressive) applied to such a crystal will alter the separation between the positive and negative charge sites in each elementary cell leading to a net polarization on the crystal surface. The effect is practically linear, i.e. the polarization varies directly with the applied stress, and direction-dependent, so that compressive and tensile stresses will generate electric fields and hence voltages of opposite polarity. It's also reciprocal, so that if the crystal is exposed to an electric field, it will experience an elastic strain causing its length to increase or

decrease according to the field polarity. Besides the crystal mentioned above, an important group of piezoelectric materials are the piezoelectric ceramics, among which PZT is an example. These are polycrystalline ferroelectric materials with the perovskite crystal structure that is a tetragonal/rhombahedral structure very close to the cubic one. They have the general forumula $A^{2}+B^{1}+O^{2-}{}_{3}$, in which "A" denote a large divalent metal ion such as Barium or Lead, and "B" denotes a tetravalent metal ion such as Titanium or Zirconium (Fig.4).

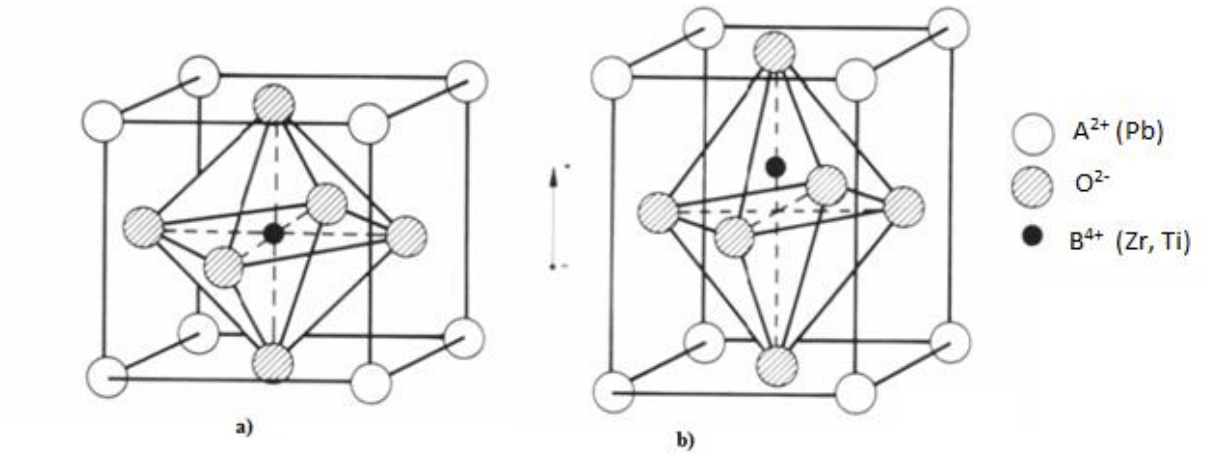

Fig. 4: a) piezoelectric crystal b) deformed piezoelectric crystal [12]

Depending on the atomic ratio of Zirconium to Titanium, PZT can exist either in the tetragonal, rhombohedral or orthorhombic phase at room temperature (Fig.5). PZT-type piezoelectric ceramics are solid solutions of Lead zirconate and lead titanate which have compositions near the morphotropic phase boundary (MPB). This boundary separates the tetragonal *(T)* and rhombohedra1 *(R)* ferroelectric phases of the solid solutions. [13] In these phases, the unit cell elongate in one direction, causing the central atom (Zr or Ti) to shift towards one of the oxygen atoms in the direction of elongation. As a result, one end of the long axis is more positive than the other end. Hence dipole moment or a polarization is produced in the unit cell.

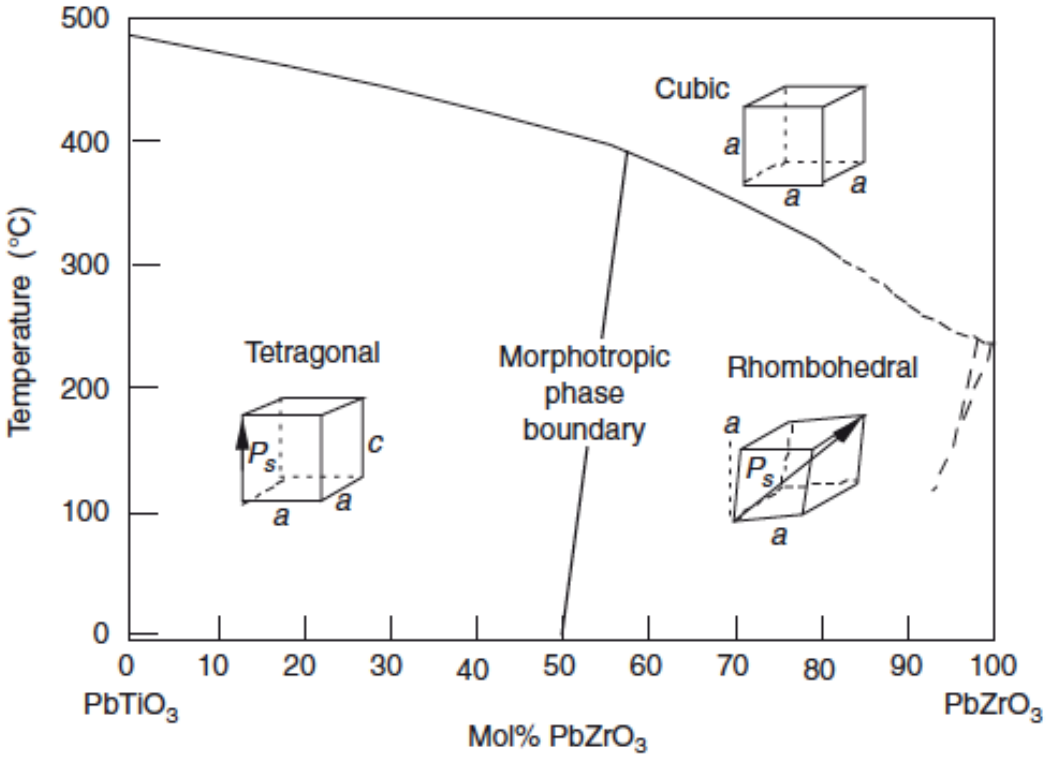

Fig. 5: phase diagram of PZT illustrating how the Zr/Ti ratio and temperature affects the phase of the ceramic. [10]

Materials such PZT can be considered as a mass of minute crystallites. Above a temperature known as Curie point, these crystallites exhibit simple cubic symmetry. This structure is centrosymmetric with positive and negative charge sites coinciding, so there are no dipoles present in the material (which is said to exhibit paraelectric behavior). Below the Curie point, however, the crystallites take as we said a tetragonal symmetry in which the positive and the negative charge sites no longer coincide. The dipole are not randomly oriented throughout the material. Neighboring dipoles align with each other to form region of local alignment known as Weiss domains. Within a Weiss domain, therefore, all the dipole are aligned, giving a net dipole moment to the domain, and hence a net polarization (dipole moment per unit volume). The direction of polarization between neighboring Weiss domains within a crystallite can differ by 90° or 180°, and owning to the random distribution of Weiss domains throughout the materials, no overall polarization or piezoelectric effect is exhibited. The ceramic may be made piezoelectric in any chosen direction by a poling treatment which involves exposing it to a strong electric field at a temperature slightly below the Curie point. Under the action of this field, domains most nearly aligned with the field will grow at the expense of the other domains. When

the field is removed the dipoles remain locked in approximate alignment, giving the ceramic materials a residual polarization and a permanent deformation (Fig.6). Therefore the poling treatment is usually the finally treatment of PZT component manufacture.

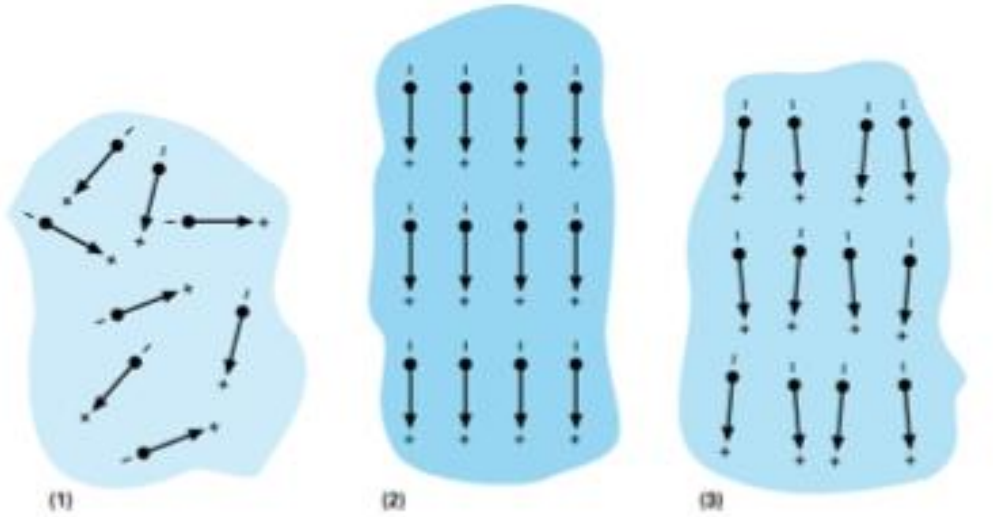

Fig. 6: effect of poling treatment in Weiss domain [12]

The piezoelectric effect can be described with the constitutive equation, in matrix notation, as:

direct piezoelectric effect: $\mathbf{D_i = d_{ip} X_p + \varepsilon_{ij} Ej}$

converse piezoelectric effect: $\mathbf{S_p = s_{pq} X_q + d_{pi} E_i}$

where *D* is the electric displacement, *d* is the piezoelectric coefficient, *X* is the stress, ε is the relative permittivity, *E* is the electric field, *S* is the elastic strain and *s* is the elastic compliance. The subscript i(=1,2 or 3) denotes the x_1, x_2 or x_3 direction, while the subscript p or q denotes the longitudinal components (1,2 or 3) and the shear components (4,5 or 6).

2.3 PYROELECTRICITY

Pyro-electricity originates from the temperature dependence of the spontaneous polarization. When the temperature of the crystal is changed, electric charge induced by the change of spontaneous polarization appears on the surface of the crystal. Pyro-electricity is a property inherent in crystals with unique polar axes that are, consequently, without a center of symmetry. However, as opposed to piezoelectricity not all symmetry groups (point groups) lacking a center

of symmetry are pyroelectric, whereas all pyroelectrics are also piezoelectrics. [14] The differential of electric displacement D with three independent variables can be written

$$dD = \left(\frac{\partial D}{\partial X}\right)^{E,T} dX + \left(\frac{\partial D}{\partial E}\right)^{X,T} dE + \left(\frac{\partial D}{\partial T}\right)^{X,E} dT$$

where X, E and T are stress, electric field and temperature, respectively. The coefficients of the first two terms are due o the direct piezoelectric effect and relative permittivity. We define as pyroelectric coefficient ,p, under constant stress and electric field the coefficient of the last term

$$p = -\frac{\partial D}{\partial T}$$

D can also be written as

$$D = \varepsilon_o E + P$$

Where P is the resulting polarization including the spontaneous polarization $_{P_S}$ and the polarization induced by electric field and stress, and ε_o is the relative permittivity of the free space. Under zero electric field and stress, the equation written above become

$$D = P_s$$

Therefore, we can write p as

$$P = -\frac{\partial Ps}{\partial T}$$

2.4 FERROELECTRICITY

By definition, ferroelectrics – that is, materials showing one or more ferroelectric phases in a realizable range of pressure and temperature – are materials in which, in the ferroelectric phase, the crystal is spontaneously electrically polarized and the polarization has more than one possible equilibrium orientation that results in a domain structure. To establish true ferroelectricity in a

material, it must be confirmed that the polarization can be reoriented between the different orientation (domain) states by a realizable electric field. Ferroelectricity was discovered by Valasek in Rochelle salt in 1921. One of the important characteristics of the ferroelectrics is the polarization hysteresis P-E loop.

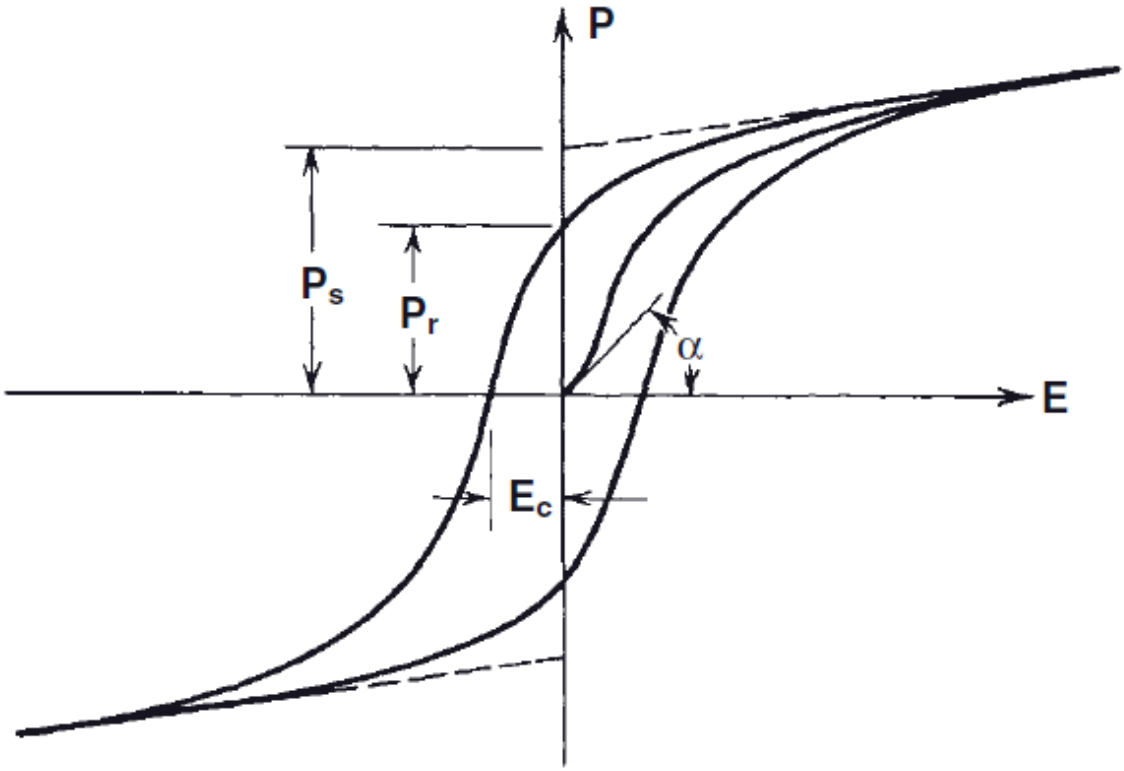

Fig. 7: Polarization of a ferroelectric ceramic in response to the change of an outer electric field strength, E. [15]

In figure 7 we can see a typical P-E loop in ferroelectrics materials. The electric field and the polarization P are connected in a dielectric medium by the relation

$$D=\varepsilon_o E + P.$$

For a ferroelectric materials however, P, is itself a function of E as shown in the figure. In this plot, the hysteresis effect, familiar form ferromagnetics, is quite evident. If an initial unpolarized sample is subjected to an increasing electric field at a temperature slightly below its Curie point, the dipoles become increasingly aligned with the field and the polarization follow the initial curve shown in the figure 7. When the field has increased beyond a certain value, no further increase in polarization will be observed because the dipoles are then all aligned with the field.

The materials is then said to have reached its saturation polarization P_s. If the field is now reduced to zero, the dipoles become less strongly aligned, since in the absence of an external field they're bound to certain preferred direction within the individual crystallites. They do not, however return to their original alignment since there are several preferred direction within the crystallites and the dipoles remain in the ones most closely aligned with the original field. Since there is still, therefore , a very high degrees of alignment the polarization does not fall back to zero but to a value somewhat lower than the saturation polarization known as the remaining polarization P_r . If the field is now increased in the opposite direction, the polarization of the sample initially falls to zero and then increased in the negative direction until it reaches a saturation polarization $-P_s$. If the field is again reduced to zero, the polarization falls to the remaining polarization $-P_r$ and finally, if the field is increased to the positive direction again, the polarization will fall to zero and eventually return to P_s. the distinction between P_r and P_s is that P_r is the resultant net polarization after the application of an electric field (poling) while P_s is rather a conceptual quantity referring to the polarization that a ferroelectric material possesses spontaneously.[16] Most ferroelectric materials undergo a structural phase transition from higher temperature paraelectric phase into a lower temperature ferroelectric phase, and the temperature where this transition takes place is called the Curie point, Tc. When the temperature is close to the Curie point, thermodynamic properties (such as spontaneous polarization, specific volume, and entropy) show anomalies, and the structure of the crystal changes. For example, the dielectric constant in most ferroelectric crystals has a very large value near their Curie point, which is usually referred to as the "dielectric anomaly ". Above the Curie point the dielectric permittivity falls off with temperature according to the Curie-Weiss law:

$$\varepsilon = \varepsilon_0 + \frac{C}{T - T_0} \approx \frac{C}{T - T_0}$$

where C is the Curie-Weiss constant and T_0 is the Curie-Weiss temperature. T_0 may be different from the Curie point Tc. In the case of a first-order phase transition, $T_0 < Tc$, while for the second–order phase transition $T_0 = Tc$. Representative ferroelectric materials include: barium titanate $BaTiO_3$, Lead zirconate titanate $Pb(Ti,Zr)O_3$ (PZT), Lead titanate ($PbTiO_3$), Lead lanthanum zirconate titanate (PLZT), $Pb(ZnNb)O_3$ and ferroelectrics like Lead Magnesium Niobate (PMN) which have been developed and utilized for a variety of applications. Generally, these materials have a high dielectric constant and are characterized by large piezoelectric,

pyroelectric and electro-optic effects as well as nonlinear optical effects. On the basis of these unique properties, ferroelectric materials have been applied to produce active elements of various devices. Generally, there is a considerable interest in ferroelectric crystals as transducer materials for their spontaneous polarization and the strong sensitivity that is attributed to their higher electromechanical coupling than piezoelectric crystal, such as quartz. While ferroelectric materials have a higher electromechanical coupling, they are not as stable as the single crystal piezoelectric materials. Both the poly and the single crystals are made of brittle materials, which limit their practical size for high frequency ultrasonic applications where thin films on wafer are required. [6]

2.5 PIEZOELECTRIC FOR HARVESTING ACTUATING AND SENSING

Energy harvesting refers to effective energy conversion techniques for recycling energy released from the natural environment. Offering benefits such as energy savings and a stable and constant power supply, these techniques have recently attracted considerable attention as energy sources that do not involve batteries. Solar, piezoelectric, and thermoelectric devices belong to the field of energy harvesting systems. Solar energy is very dependent on the weather and shade. Thermoelectric devices suffer from very low energy density in general environmental conditions. In this regard, harvesting techniques that exploit piezoelectric phenomenon, where mechanical energy from the environment is converted into electric power, have been investigated due to their notable advantages, including relatively high energy density and being less influenced by weather. PZT-based piezoelectric ceramics have been adopted in the production of energy harvester devices because of their high piezoelectric constant and electromechanical coupling coefficient [Application of CIP processing and sol-gel surface coating to PZN-PZT piezoelectric ceramics for use as energy harvesters]. Good harvesters must have an adequate electro-mechanical conversion efficiency to compete against damping and other loss mechanisms. During deformation of the elastic harvesting structure, a fraction of the elastic energy stored in the piezoelectric material is transformed to electrostatic energy. Only from this part of the energy, electrical power can be supplied to an external circuit. PZT thin films are thus good candidates. However, they exhibit large capacitances as a result of large dielectric constants and small film thickness, thus preventing the development of large voltages across thin films. For

this reason, interdigitated electrodes (IDE) were proposed instead of the parallel plate configuration (PPE). Piezoelectric transduction is an alternative to electrostatic transduction for MEMS resonators and offers the potential advantage of increased electromechanical coupling strength, inherently linear performance, and an elimination of the need for small electrode gaps potentially leading to larger power handling. As already mentioned , the direct piezoelectric effect occurs when a charge is generated due to a change in the dipole movement caused by the application of a mechanical stress to the crystal. The converse piezoelectric effect occurs when a strain is generated on the crystal by the application of an electric field. The direct and the converse piezoelectric effect are illustrated in Figure 8. The equations of state relating the electric and elastic variables for the piezoelectric element are

$$S_1 = s^E_{11}T_1 + s^E_{12}T^2 + s^E_{13}T_3 + d_{31}E_3 \quad (1)$$

for strain generated in the x direction by an applied stress and electric field in the z direction and

$$D_3 = d_{31}(T_1 + T_2) + d_{33}T_3 + \varepsilon_3 E_3 \quad (2)$$

for the electric charge generated by an applied stress and electric field. In (1) and (2) S is the strain, T is the stress, s^E is the elastic compliance, d is the piezoelectric constant, E is the electric field intensity, D is the electric charge generated and ε is the material permittivity. To obtain a complete description for all of the directions a matrix can be constructed using the equations above.

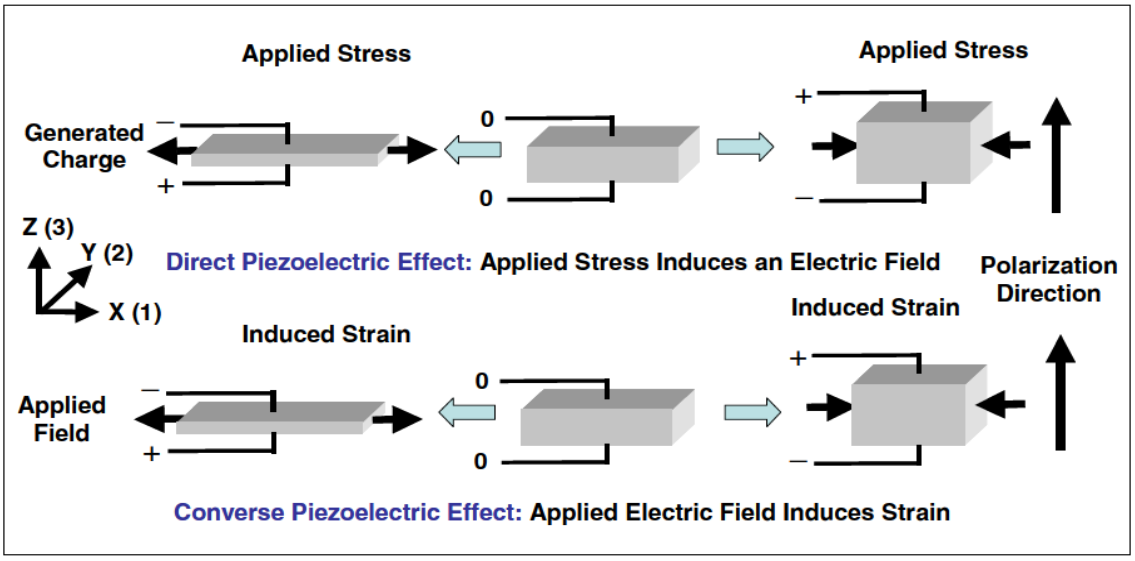

Fig. 8: Direct and converse piezoelectric effect [17]

Therefore from (1), in the absence of an applied stress, an applied electric field in the z direction results in a strain in the x direction via the piezoelectric coupling coefficient d_{31}. Likewise, from (2) in the absence of an electric field, an applied stress in the x direction results in a charge in the z direction via the piezoelectric coupling coefficient d_{31}. The efficiency of this conversion of mechanical energy to charge or charge to mechanical energy is given by the piezoelectric coupling coefficient

$$k^2 = \frac{Electrical\ Energy\ Converted\ to\ Mechanical\ Displacement}{Electrical\ Energy\ Input} \tag{3}$$

If an additional material layer is used to move the piezoelectric material off of the neutral axis of a beam, the induced strain in the piezoelectric material when an electric field is applied generates a moment that causes the beam to bend.

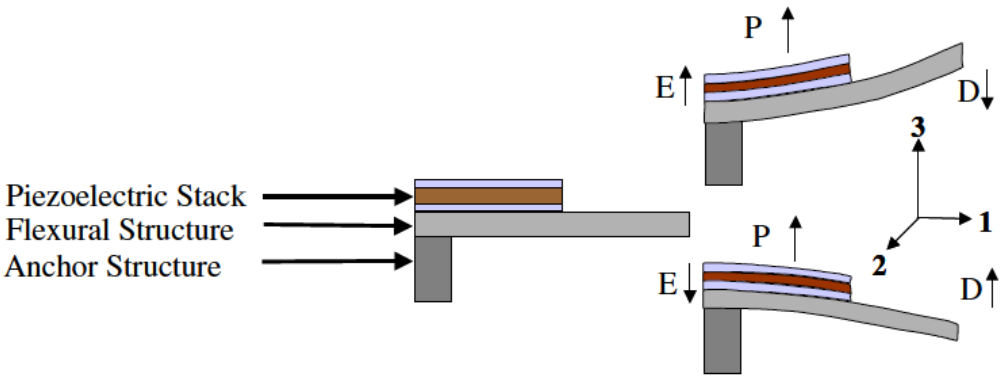

Fig. 9: Piezoelectric cantilever stack [17]

If the input electric field is an RF signal that matches the natural resonant frequency of the beam, the resultant strain from the converse piezoelectric effect can induce resonance of the beam and vice versa.

$$\varepsilon_{\max} = d_{31}\left(\frac{V}{t_p}\right) \quad (4)$$

The maximum force that can be generated when the piezoelectric element is held in the zero strain condition is given by

$$F_{max} = d_{31}EbV \quad (5)$$

where *E* is the Young's modulus of the piezoelectric element, *b* is the width of the element, and *V* is the applied voltage. In almost all applications, the piezoelectric element is mounted or attached to a substrate. The inclusion of a substrate can cause a reaction force to the piezoelectric-induced strain that reduces the actual amount of induced strain from the maximum that can be achieved. Moreover, also when the piezoelectric element is attached to a surface, like in the case of a cantilever beam, the equations of the bending moment and of the strain on the top of the surface can be extrapolated and these depend not only on the voltage applied to the element but also on the thickness and stiffness of both beam and the piezoelectric layer. If the oxide beam is too stiff, the actuator will not induce any displacement. On the other hand, if the beam is too soft, it will only stretch under the drive electrode. For these reason a complete mechanical analysis of the whole system is necessary to increase the performance of the device.

CHAPTER 3

3 SOL-GEL PROCESS

3.1 INTRODUCTION

3.1.1 SOL

A colloid is a suspension in which the dispersed phase is so small (1-1000nm) that gravitational forces are negligible and interactions are dominated by short range forces, such as Van der Waals attraction and surface charges. The inertia of the dispersed phase is small enough to exhibits Brownian motion, a random walk driven by momentum imparted by collision with molecules of the suspending medium. A sol is a colloidal suspension of solid particles in a liquid. An aerosol is a colloidal suspension of particles in a gas and an emulsion is a suspension of liquid droplets in another liquid. All of this types of colloids can be used to generate polymers or particles from which ceramics materials can be made. In the sol gel process, the precursors (starting compound) for the preparation of a colloid consist of a metal or metalloid element surrounded by various ligands. The class of precursors most widely used in sol- gel research is alkoxide. An alkane is a molecule containing only carbon and hydrogen linked exclusively by single bonds, as in methane (CH_4) and ethane (C_2H_6). An alkyl is a ligand derived from the remotion of one hydrogen from an alkane molecule producing, for example, methyl ($^*CH_3$) or ethyl ($*C_2H_5$) where the * indicates an electron that is available to form a bond. An alcohol is a molecule formed by the addition of hydroxyl (OH) group to an alkyl (or other) molecule, as in methanole (CH_3OH) or ethanol (C_2H_5OH). An alkoxy is a ligand formed by removing a proton from the hydroxyl on an alcohol, as in methoxy ($*OCH_3$) or ethoxy ($*OC_2H_5$). Metal alkoxides are members of the family of metallorganic compounds, which has an organic ligand attached to a metal or metalloid atom. Metal alkoxides are popular precursor because they react readily with water. The reaction is called hydrolysis, because a hydroxyl ion becomes attached to the metal atom, as in the following reaction:

$$Si(OR)_4 + H_2O \rightarrow HO\text{-}Si(OR)_3 + ROH.$$

The R represent a proton or other ligand, and ROH is an alcohol; the bar (-) is used to indicate a chemical bond. Depending on the amount of water and catalyst present, hydrolysis may go to completion (so that the OR groups are replaced by OH),

$$Si(OR)_4 + 4H_2O \rightarrow Si(OH)_4 + 4ROH$$

Or stop while the metal is only partially hydrolyzed. Two partially hydrolyzed molecules can be linked together in a condensation reaction, such as

$$(OR)_3Si\text{-}OH + HO\text{-}Si(OR)_3 \rightarrow (OR)_3Si\text{-}O\text{-}Si(OR)_3 + H_2O$$

Or

$$(OR)_3Si\text{-}OR + HO\text{-}Si(OR)_3 \rightarrow (OR)_3Si\text{-}O\text{-}Si(OR)_3 + ROH$$

By definition, condensation liberates a small molecules, such as water or alcohol. This type of reaction can continue to build larger and larger molecule by the process of polymerization. When a particulate sol aggregates, it common form fractal structures. A *mass fractal* is distinguished from a conventional Euclidean object by the fact that the mass (m) of the fractal increases with its radius (r) according to

$$m \alpha r^{df}$$

where d_f is called the mass fractal dimension of the object. For a Euclidean object $m \alpha r^3$, but for a fractal $d_f < 3$ so its density ($p \alpha m/r^3$) decreases as the object gets bigger. A *surface fractal* has a surface area, S, that increase faster than r^2

$$S \alpha r^{ds}$$

Where d_s is called surface fractal dimension.

3.1.2 GEL

If a monomer can make more than two bonds, then the size of the molecule has got no limits. If one molecule reaches a macroscopic dimension so that it extends throughout the solution, the substance is said to be a gel. The gel point is the time at which the last bond is formed that

completes this giant molecule. Thus a gel is a substance that contains a continuous solid skeleton enclosing a continuous liquid phase. The continuity of the solid structure give elasticity to the gel. The characteristics feature of the gel is obviously not the type of bonding: polymeric gels are covalently linked, gelatin gels form by entanglement of chain, and particulate gels are established by Van der Waals forces. The bonds may be reversible or permanent. [18] A gel has been defined as a two component system of a semisolid nature, rich in liquid. We interpret a gel to consist of continuous solid and fluid phases of colloidal dimension. Continuity means that one could travel through the solid phase from one side of the sample to the other one without having to enter in the liquid. Since both phase are of colloidal dimension, a line segment originated in a pore and running perpendicularly into the nearest solid surface must re-emerge in another pore closer than 1 μm [19]. Bond formation does not stop at the gel point. In the first place, the network is initially compliant so segment of the gel network can still move close enough together to allow further condensation. Moreover, there still a sol within the gel network and those smaller polymers or particles continue to attach themselves to the network[18]. The hydrolysis and condensation reactions are reversible. If these reactions reach the equilibrium, so the speed of the two is the same, the solution will never gel in a sealed container. Such solution is called a stable sol-gel. By varying the amount of water/alcohol, it is possible to control the speed of each reaction and shift the equilibrium in both directions. If one were to remove alcohol from a stable sol-gel, this would decrease the speed of the reverse reactions, and would shift the equilibrium toward hydrolysis and condensation. If enough alcohol is removed from the solution, it will eventually gel. This is actually desired for the fabrication of thin films. If the chemical reactions are controlled properly, the solution will become a structured liquid containing a matrix of metalorganic chains. When the sol-gel is spread out over a surface (either by dip coating or spinning), the solvent evaporates, the equilibrium of the reaction is shifted towards hydrolysis and condensation and the solution gels, creating a branched polymeric network into the thin film, that is rigid enough for handling. Controlling the evaporation rate of the solvent it is possible to produce also Aerogels, that is a suspension of particles in a gas which forms when the solvent is evaporated in supercritical conditions, and Xerogels, that is a solid with high porosity that forms from a gel when the solvent is extracted slowly with unhindered shrinkage. If the drying of the solvent is followed by heat treatment, it is possible to create dense films or dense ceramic. These procedures are summarized in fig.10.

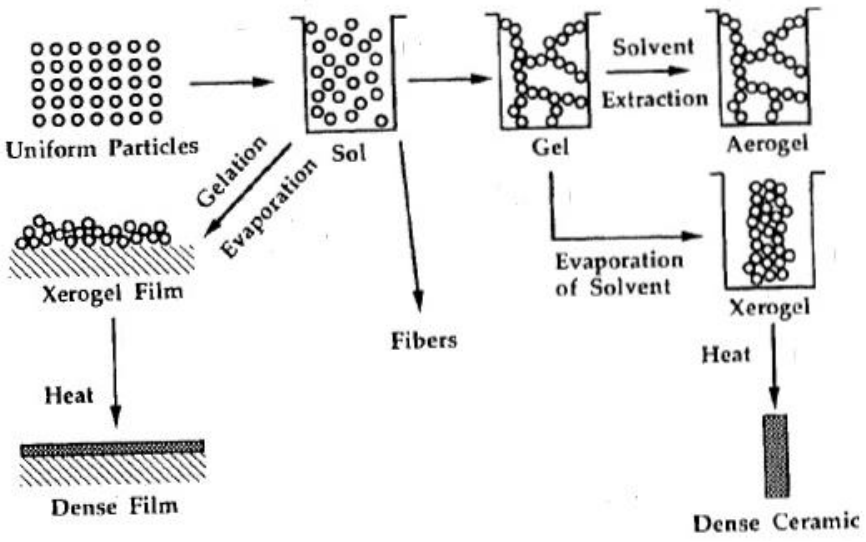

Fig. 10: Overview of the sol gel process. [20]

The thermal treatment for the production of PZT films, once that the solution has been spinned on the wafer, can be divided into three steps. The first step is the drying of the film. This is usually accomplished on a hot plate in air, at temperatures ranging from 100°C to 200°C depending on the composition of the film. During this stage, the excess solvent is eliminated and the film shrinks and densifies as it loses liquid. After drying, the film is much denser, and any remaining liquid is held in by capillary action. After drying, the as-deposited film is an amorphous gel of metallorganic compounds. In order to eliminate the organic components and the residual liquid, the film is pyrolysed, which involves heating in the range of approximately 300-500°C to burn the organic compounds off. This step is often referred into the literature as the "firing" stage because in this stage the organic component is carbonized and oxidized. After this stage the film is amorphous but with the PZT composition. It is quite flexible, mechanically tough, but capable of being patterned by photolithography with an appropriate etch. After the firing of the film, the amorphous metallorganic gel should often be converted, as in the case of PZT, into a crystalline layer of inorganic metal oxide compounds to exploit the material properties. This step is often referred to as annealing and is a thermal treatment performed at high temperature (550°-700°C for PZT) that guarantees the elimination of all the organic traces and the crystallization of the film. The temperatures used to crystallize thin films are much lower than the sintering temperatures of the same bulk material made from ceramic powders and this is a great benefit when planning an industrial procedure for oxides film production. This final step

is usually performed using a rapid thermal annealer (RTA), which produces films with better properties and reduces cracking, but can be done also in a conventional furnace.

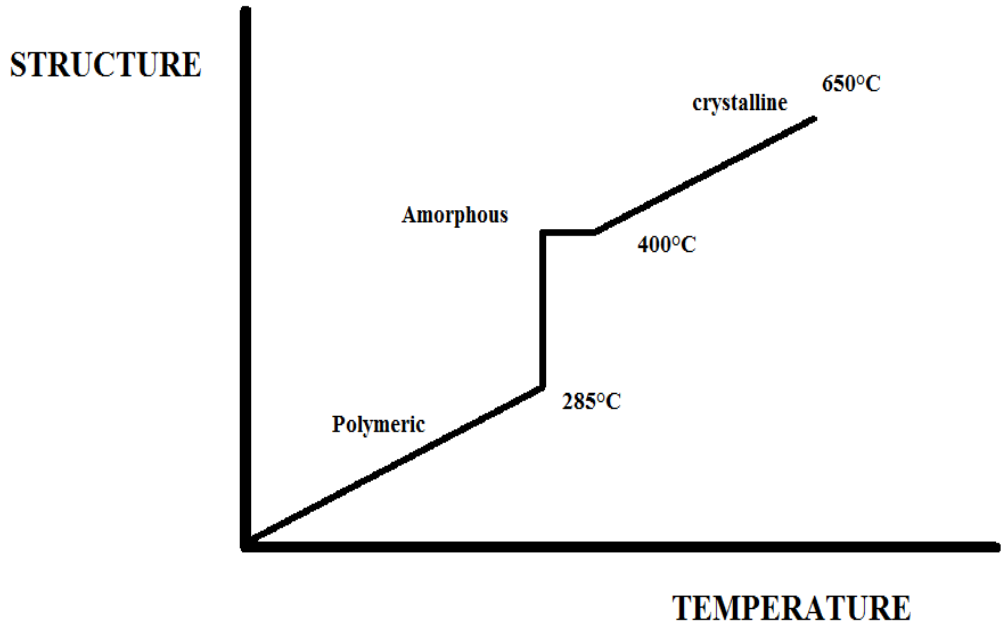

Fig. 11: Firing schedule example for PZT sol gel.

3.2 SOL-GEL FOR PZT

In this work we use sol-gel method in order to obtain thin film of PZT and PNZT. The Lead zirconate titanate is mostly deposed by means of sol-gel technique because this method assures the highest piezoelectric properties of the final thin layer. In the conventional sol-gel method, the film is prepared simply by depositing the precursor solution on substrates using common processes such as dipping, spinning, or spraying. Then film is pyrolyzed at high temperature to remove the unwanted organic materials. In our work the layer of PZT is firstly deposed by spin coating on the wafer substrate, after 5 minutes of drying on a heating plate at 150°C the laminated stack is calcined for 5 minutes at 350°C and than the calcinated layers are annealed in

an oven at temperature higher than 650 °C. Repeating this operation many times we can obtain different kinds of thickness.

3.2.1. CARBOXYLIC ACID BASED SOL-GELS

Carboxylic acid based sol-gel is present with many variations in literature. The original solution is prepared by dissolving Lead acetate trihydrate [$Pb(OOCCH_3)$,+$3H_2O$] in acetic acid [CH3COOH]. The Zirconium propoxide [$Zr(O(CH_2)_2CH_3)_4$] (70 wt% in propanol) and the Titanium isopropoxide [$Ti((CH_3)_2CHO)_4$] are then added to carboxylic acid/Lead acetate mixture to form the sol gel. This route uses less toxic agents compared to the 2-Me process and it was first initiated by Yi and Sayer at Queen's University in 1988 [21][22] and then developed by many researchers. This route is based on the use of carboxylic acids, as acetic acid or acetylacetone, as chelating agents and of water or alcohol as solvent. It is often referred to as "chelate" process because the use of carboxylic acids, such as acetic acid or acetylacetone, impacts heavily on the molecular modifications of the precursors with chelating ligands. Typically, the carboxylic acid groups coordinate to the metal species in a bidentate fashion for Zirconium and in a monodentate fashion for Titanium as reported in [21] , and frequently it acts as bridging ligands, linking metals together to form oligomers and small polymers. Chelation of the metal alkoxides by these carboxylate groups results in the formation of precursors that possess reduced sensitivity toward hydrolysis in respect to with the unmodified chemicals, as reported in many literatures. Reducing the tendency of metal alkoxides towards hydrolysis is of fundamental relevance, since when Titanium isopropoxide and Zirconium propoxide are added into a solution of water or alcohol, precipitates due to their high hydrolysis and condensation tendency. In order to prepare a useable sol or gel, Titanium iso-propoxide and Zirconium propoxide must be chemically modified to change their hydrolysis and condensation behavior. The gelation behavior of Titanium and Zirconium alkoxides can be modified by acetic acid, and this has been attributed to the formation of chelates or to the nucleophilic substitution of a propoxide group with an acetate group that is less sensitive towards hydrolysis [21]. While chelate processes are simple and rapid, the chemistry involved in solution preparation is quite complex due to the number of reactions that occur. Key reactions were found to be chelation, esterification, hydrolysis and condensation. The complexity of the reactions results in a diminished ability to control the precursor structure compared to true sol-gel approaches, and thus the gain in process simplicity comes at a cost [23]. Another drawback of chelate processes is that continued reactivity in the precursor solution after synthesis, can result in a change in

precursor characteristic over time (weeks to months) and thereby a degradation in film properties [24]. This occurs because constituent groups such as acetate, even if less susceptible to hydrolysis than alkoxy groups, may still be attacked by water, resulting in a change in the molecular structure, and other reactions result in continued oligomerization of the chemical species, eventually causing precipitation [25]. Yi and Sayer in their work chose as carboxylic acid the acetic acid. The basis of this sol-gel rests with the property of acetic acid to slow the hydrolysis and condensation reactions of transition metal alkoxides by forming more stable metal alkoxo-acetylates. The original solution is prepared by dissolving Lead acetate trihydrate ($Pb(CH_3CO_2)_2 \cdot 3H_2O$) in acetic acid ($CH_3COOH$). This is followed by de-hydratation of the solution since water may cause non uniform gelation of Titanium isopropoxide and Zirconium propoxide. The Zirconium propoxide $Zr(OCH_2CH_2CH_3)_4$ (70 wt% in propanol), and the Titanium isopropoxide [Ti $((CH_3)_2CHO)_4$] are then sequentially added to the acetic acid / Lead acetate mixture to form the sol-gel after than the solution was cooled to room temperature. In this type of sol-gel, the order of metal alkoxides addition has a fundamental importance because of the different hydrolysis / condensation reaction speeds of these compounds [21][22]. The higher reaction speed of the Titanium isopropoxide leads to the formation of large Titanium alkoxide chains which create local in homogeneities, or in some cases, the formation of precipitates in the solution when it is the first metal alkoxide added to the acetic acid / Lead acetate mixture. To prevent this phenomenon, the Zirconium propoxide is usually added first and allowed to react with the acetic acid / Lead acetate mixture to form Zirconium propoxide di-acetate before the addition of the Titanium isopropoxide. Water is added to the solution to provide excess reagent to the hydrolysis reaction and to control the viscosity [26]. Exothermic reactions between the acetic acid and the metal alkoxides warm the solution during its preparation. As it cools down, the Lead acetate re-crystallizes in the solution due to the common ion effect with the excess acetic acid. Lactic acid added to the sol-gel before cooling prevents the appearance of these crystals by reacting with, thus effectively removing, the excess acetic acid by a process known as esterification. This assures high solution stability over a long period. In order to improve the drying behavior of the film and to avoid cracking, Ethylene Glycol and Glycerol are finally added . A flow chart of the whole process is represented in fig.12.

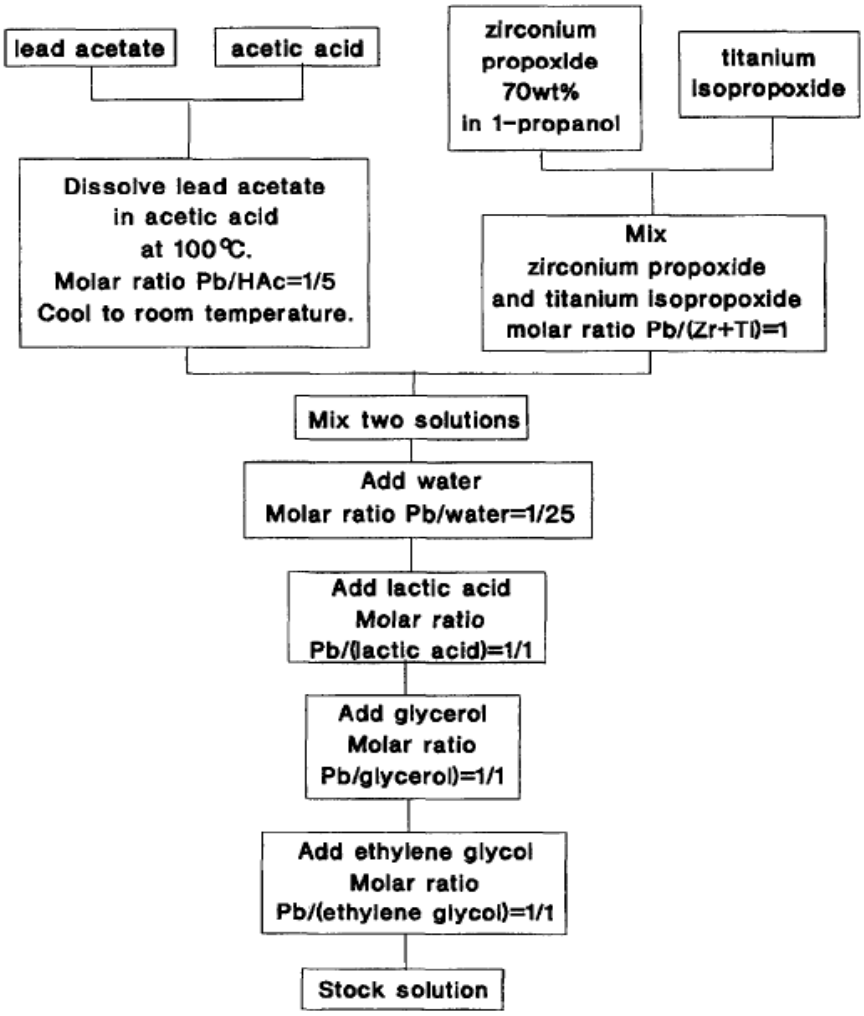

Fig. 12: Flow chart of Yi and Sayer recipe [21]

A single crack free layer of about 0.5 µm thickness can be prepared with this solution by spin coating. Thinner films were prepared by adding some combination of water and propanol to dilute the solution. It has been demonstrated that lowering the concentration of the solution helps to produce crack free films. The addition of propanol also lowers the surface tension of the solution and can improve the wettability for some substrates. Thicker films were built up by multilayer coating.

3.2.2 METHOXYETHANOL BASED SOL-GELS

Another important sol-gel process is based on the solvent 2-metthoxyethanol. The 2-Me reacts with the metal alkoxides to effectively act as a chelating agent which prevents the complete hydrolysis of metal alkoxides on the addition of water. The hydrolysis and condensation

reactions are controlled by the amount of 2-Me/water added. This kind of sol-gel approach leads to a better crystallization than those fabricated from acetic acid. This has been attributed to the smaller colloidal molecules of the 2-Me. Another important aspect is that with this process we have a lower viscosity, this facilitates the removal of the organic compounds and thus lowers the temperature required to crystallize the PZT. However 2-Me has recently been eliminated from all commercial sol-gel processing in the semiconductor industry in the United State because of its carcinogenic nature.

3.2.3 SOL-GELS BY THE USE OF DIFFERENT METAL ALKOXIDES

The original acetic acid process developed by Yi utilized Titanium and Zirconium propoxide as the precursor alkoxides. Although the use of different metal alkoxides in the sol-gel follow the same basic hydrolysis and condensation reactions, the fact that the reaction speed may differ under the same conditions for different alkoxides will change the properties of the sol-gel. Studies on transition metal alkoxides ($m(OR)_n$ M=Zr, Ti) have shown that hydrolysis rate decreases with increasing size of the alkyl group. The condensation reaction is also dependent on the size of the alkyl group. Under mild hydrolysis condition, $Ti(OR)_4$ forms TiO_2 precipitate if the alkyl group is an ethyl (C_2H_5) or a propyl (C_3H_7) group, while under same conditions, polymers are formed for butyl (C_4H_9) group. The same has been noted for Zirconium alkoxides. Control over the speed of the hydrolysis/condensation reactions by replacing one metal alkoxide for another may improve the structure and homogeneity of the sol-gel. Titanium isopropoxide has a greater reaction speed compared to the Zirconium propoxide which can lead to the formation of titaniurn alkoxide clusters in the solution. These local inhomogeneities can result in the formation of large clusters of Titanium oxide in the film which will require higher temperatures and longer anneal times to crystallize. Substituting Titanium isopropoxide with the slower reacting Titanium butoxide is believed to reduce the size of these cluster and improve the homogeneity of the sol-gel. To sum up, the main limitation of the conventional sol-gel method is that the sol gel derived films tend to crack when a certain thickness is reached. Cracking is produced by stresses in the films during drying, firing, annealing and cooling. The defects in the films can also act as centers for crack initiation. Shrinkage during firing of the films is another cause for cracking. Moreover, the conventional sol-gel method is a time-consuming method for making thick films.

CHAPTER 4

4 LEAD ZIRCONATE TITANATE

4.1 CRYSTAL STRUCTURE

4.1.1 PZT

One of the intensively studied ferroelectric materials system is the solid solution of Lead zirconate ($PbZrO_3$) and Lead titanate ($PbTiO_3$). This solid solution ceramic is abbreviated as PZT and normally written as $Pb(Zr_xTi_{1-x})O_3$ [4] .Although the properties and structure of bulk Lead zirconate titanite have been widely studied and well established, there is much interest and consequently, many research into thin film PZT. PZT is a perovskite type (ABO_3) ferroelectric material well known for excellent dielectric and pyroelectric properties and for having the highest values of piezoelectric coefficients. The basic crystal structure of PZT is of the perovskite type (ABO_3) illustrated in figure 13a, but often the non-ferroelectric pyrochlore phase is obtained after crystallization, figure 13b. Pyrochlore is a ternary compound with an $A_2B_2O_7$ stoichiometry, where A is a larger and trivalent cation and B is a smaller and tetravalent cation. The pyrochlore structure is related to the fluorite structure

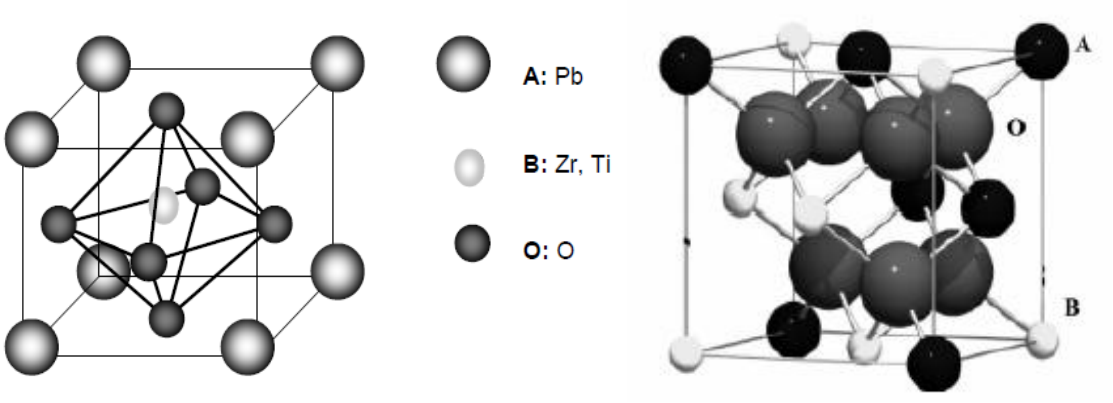

(a) **(b)**

Fig. 13: PZT perovskite structure, b) PZT pyrochlore structure [27].

Pyrochlore phase arises due to Lead deficiency in the deposit and un-equilibrated oxygen transport and it is considered to be transient or metastable. During the crystallization process, oxygen and Pb react readily to form PbO. A shortage of Pb will keep the oxygen gain greater than the oxygen loss allowing the metastable pyrochlore to stabilize. By adding excess Lead (10-20%), the volatility of PbO can be compensated but too much Lead will cause the oxygen loss to be greater than the gain, transforming the metastable pyrochlore in a fine pyrochlore matrix. The latter case is the most common, although it is possible to achieve complete pyrochlore transformation to perovskite through an approximate balance between oxygen loss and gain. The presence of a pyrochlore phase affects strongly the properties of the material changing its micro structure and in particular it decreases the electrical and piezo-electrical performances. For all these reasons it's important to find a processing method that eliminates, or strongly reduces, the presence of pyrochlore phase and this it's done well balancing the oxygen gain and loss, tailoring the Lead quantity. The sub-solidus phase diagram for $PbZrO_3$-$PbTiO_3$ is shown in Figure 14. The $PbZrO_3$-$PbTiO_3$ system exhibits multiple ferroelectric, anti-ferroelectric, and paraelectric phases, along with various symmetries, including tetragonal, rhombohedral, orthorhombic and cubic.

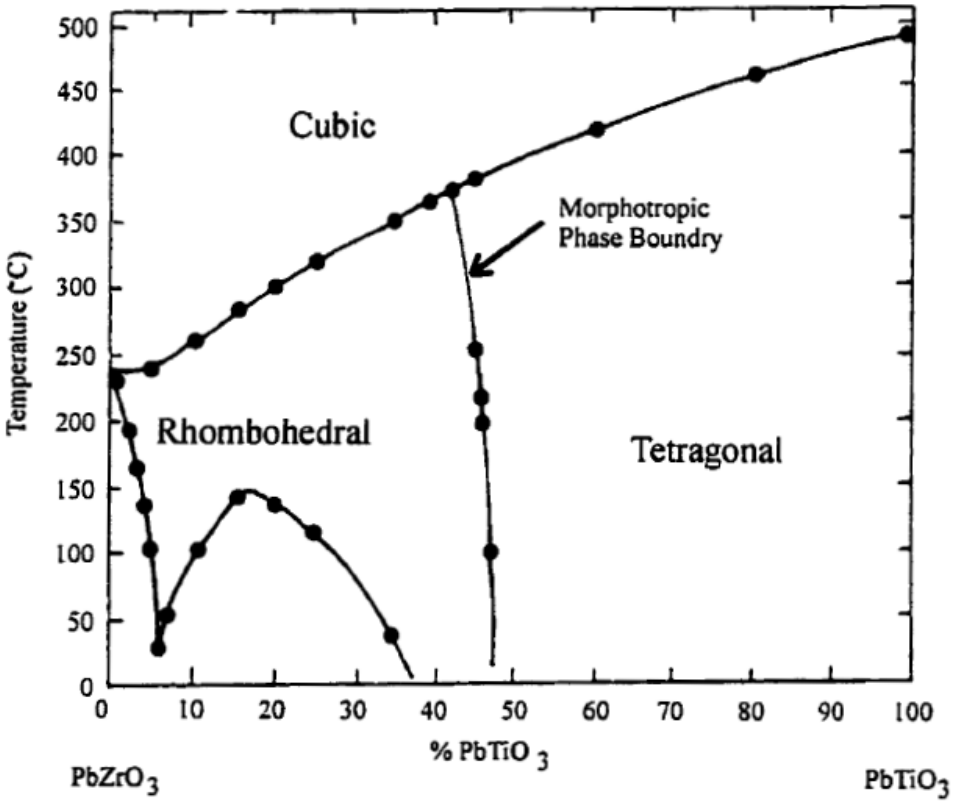

Fig. 14: Phase diagram of $PbZrO_3$-$PbTiO_3$ solid solution [4]

Ferroelectric properties of PZT depend on the Zr/Ti ratio below the Curie temperature (Tc). The Curie temperature varies from 230 °C to 490°C depending upon the Zr/Ti ratio. Above the Curie temperature of PZT, paraelectric cubic phase exists and the Zr/Ti atoms are located at the exact center of the unit cell, regardless of the composition and so it exhibits zero polarization (figure 15a). Below the Curie temperature the centers of positive and negative charges don't compensate due to the Zr or Ti ions shift and for this reason the PZT possesses a finite polarization Fig. 15b. This final polarization can be modified by an external field.

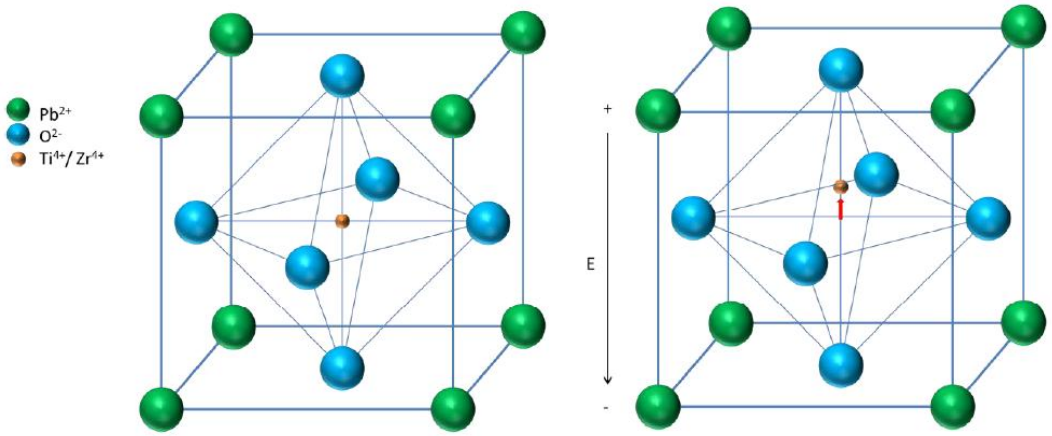

a) b)

Fig. 15: (a) PZT Cubic structure above Tc (b) Movement of Ti or Zr ions below Tc [8]

Deviations from the ideal cubic perovskite structure start to occur when PZT is cooled below the Curie point. When the PZT is cooled below the Tc, it moves from a cubic to a tetragonal or rhombohedral phase, depending on the Zr/Ti ratio, that are still very close to the cubic phase, fig.15a. For an high Ti concentration (Ti > 48%), below the Curie point, the ferroelectric phase is tetragonal. In this case, the Zr/Ti atom displaces off center and a distortion of the TiO_6 octahedral occurs along one of the six <00*l*> directions. These six directions yield six possible domain configurations separated by either 90° or 180 ° domain walls. The direction of the Zr/Ti displacement is the tetragonal *c*-axis in the resulting unit cell. Due to this distortion, as mentioned before, a dipole is created since the centers of positive and negative charge no longer coincide and this atomic displacement is the source of the spontaneous polarization (figure 15b). For higher Zr concentrations (Zr > 52%), PZT is rhombohedral below the Curie temperature. The rhombohedral distortion occurs when the Zr or Ti atom moves towards the face-center of the oxygen octahedral (the cubic <111> direction). In this case there are eight equivalent directions in which the Zr/Ti atom can move. The most widely studied composition of PZT occurs at the boundary between the tetragonal and rhombohedral phases. This is known as the morphotropic phase boundary (MPB) and its composition is approximately 52 mol% of $PbZrO_3$ and 48 mol% of $PbTiO_3$ at room temperature. This composition bounds the abrupt structural change between the rhombohedral and tetragonal phases and exhibits greatly enhanced dielectric and piezoelectric properties. The values of these characteristic coefficients show a peak at the MPB, explaining why these compositions are technologically so interesting. At the MPB composition, the free energy of the rhombohedral and tetragonal phases are equal and it is probable that an

electric field may easily cause switch between tetragonal and rhombohedral domain states. There are thus effectively 14 available directions (8 from the rhombohedral and 6 from the tetragonal) along which polarization may be reoriented, leading to a large effective remanent polarization for compositions near the MPB. The large remanent polarization at MPB in randomly oriented PZT also helps to increase the peak in the piezoelectric coefficients at MPB. Good-quality single crystals of PZT with near MPB compositions are not available due to the phase separation, therefore comparable measurements could not be made on single-domain single crystals. Calculations using the thermodynamic phenomenological theory have shown, however, that a peak in the piezoelectric coefficients and dielectric permittivity should be expected at MPB in mono-domain single crystals.

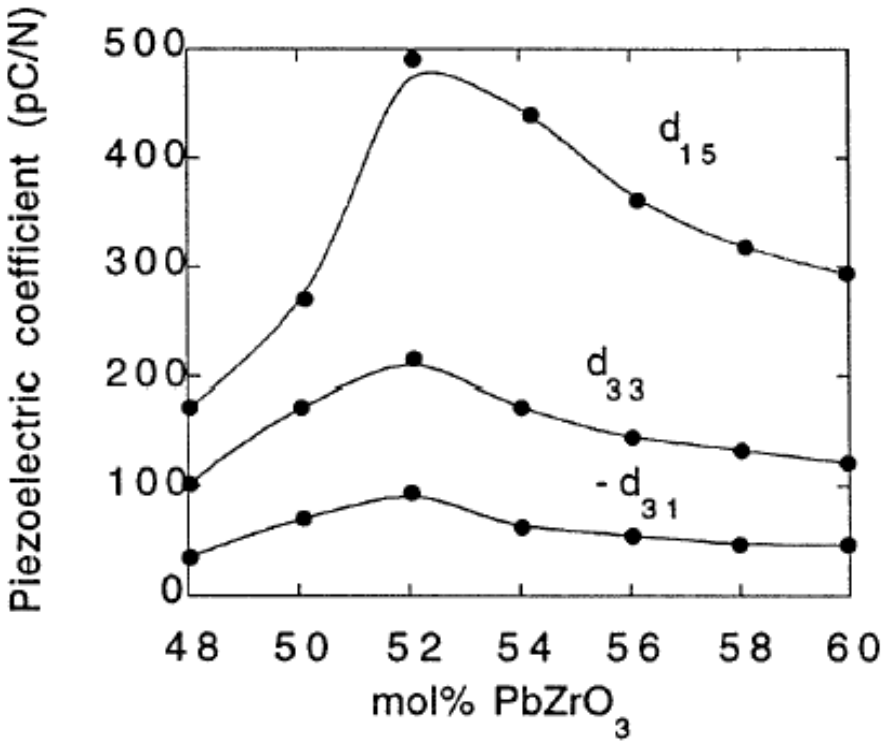

Fig. 16: Piezoelectric coefficients of $Pb(Zr,Ti)O_3$ ceramics as a function of composition close to the morphotropic phase boundary [28]

When in the perovskite phase, the PZT can be orientated in three different major directions: <100>, <110> and <111>. It's necessary, moreover obtaining a perovskite phase that have good ferroelectric and piezoelectric properties, obtain the PZT preferentially oriented in one of the above directions. In fact the electrical properties of the PZT depend on the crystal orientation and so accordingly to the final use of the device and on the properties required, it's necessary to grow

PZT crystals oriented in the direction that enhances those required properties. PZT orientation is described starting from the plane that is parallel to the surface of the substrate. Miller indices (h,k,l) are used to indicate the different crystallographic planes. When the plane is parallel to a certain direction, the value of the Miller index for that direction is 0. The <100>, <110> and <111> planes are illustrated in figure 17. The a_1, a_2 et a_3 axes are defined referring to the cubic perovskite phase. The a_3 axis correspond to the c axis when the PZT is in the tetragonal phase.

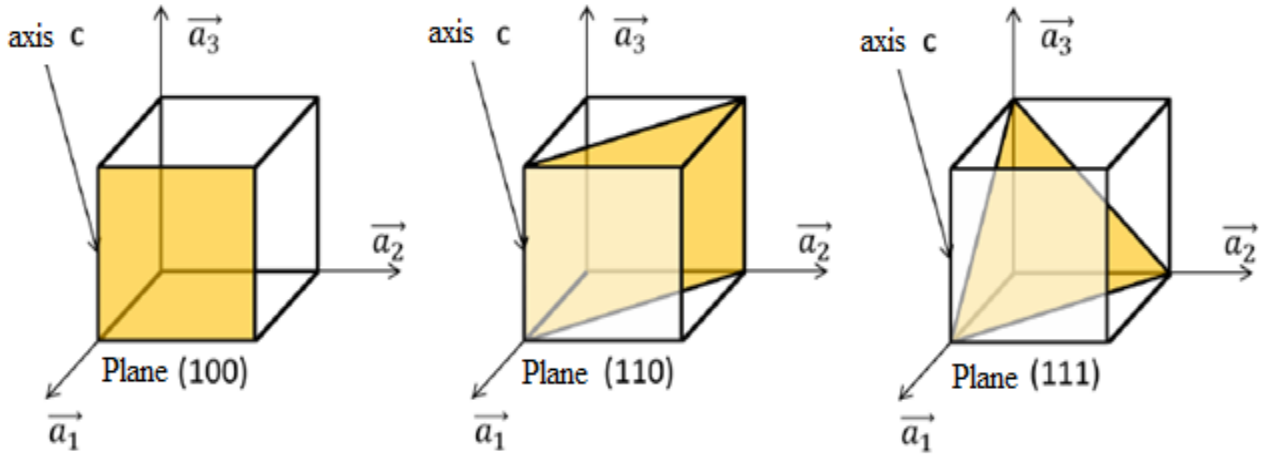

Fig. 17: Drawings of (100), (110) and (111) plains [8]

When the PZT is grown on a non epitaxial substrate, a polycrystalline phase with different amount of the above planes is obtained. This means that the deposit is formed by mono-crystalline grains orientated toward different crystallographic planes. When a epitaxial substrate like Platinum is used, it's possible to grow crystals epitaxially, obtaining in this way films with crystallographic planes preferentially oriented toward a mono- direction. The mechanism of crystallization is controlled by the nucleation of piezoelectric grains. It means that the energy required for the nucleation of a grain must be higher than the energy required for its growth. This balance of energy defines the way it grows, and therefore also the preferential orientation (texture) the lattice is going to assume. The (111) is usually stiffer than the (100) direction and it has lower piezoelectric coupling coefficients. Moreover, the (100)-oriented PZT shows a weaker non-linearity. This is probably due to the different role that the lattice boundaries play for the two configurations. Recent studies show that the domain-wall contributions to the piezoelectric properties for the (100) PZT are much less significant than for the (111). The growth of (100) or

(111) plane depends essentially on kinematics and thermodynamics of grains growth. The thermodynamics of the phenomenon promotes the growth of PZT (100), because it is the more stable phase. On the other hand the kinetics tends to minimize the interfacial energy which depends on the substrate properties and composition. For this reason, if a substrate which lattice constants matches the (111) PZT phase, the growing layer will tend to be oriented according to that direction. It is clear now that the under- layers play a fundamental role in the definition of the final PZT -silicon stack [3].

4.1.2 DOPED PZT

The electrical property of a PZT film can be modified by the introduction of dopants. According to the defect chemistry of the perovskite structure, introduction of charged impurities can change the degree of oxygen vacancy. If trivalent acceptors are substituted in the B site of PZT films, oxygen vacancies are generated in the PZT structure. On the other hand, donor doping is considered to be one of the suitable way to compensate the oxygen vacancies. When the pentavalent donors are introduced into the PZT structure, the amount of oxygen vacancies will be decreased. Additionally, the introduced foreign elements can influence the structure and lattice energy of PZT, since the ionic sizes and charges of dopants are different from those of Ti(IV) or Zr(IV). In order to modify the ferroelectric property of PZT, pentavalent Nb(V) as a donor element and trivalent Sc(III) as an acceptor element, are generally used. It is considered that these elements can substitute the B site of perovskite structure in the PZT film, since their ionic size are similar to those of Ti(IV) or Zr(IV). Donor-doped PZT ceramics show much higher levels of domain wall motion than do acceptor-doped PZT, which increases the piezoelectric coefficients. Donor dopants like Nb and La induce Lead vacancies into PZT for compensation, and simultaneously reduce the oxygen vacancy concentration. The exact mechanism by which donor doping induces softening is still in question. It is possible that the doping produces defect dipoles such as $Nb^{\circ}_{Ti} - V^{''}_{Pb}$. If such defects form, they should be immobile, since both species are immobile near room temperature. It is postulated that such immobile defect dipoles will produce random fields that locally destabilize the domain structure. They then attribute the increased mobility of domain walls in the donor-doped PZT to the lowered stability of the domain structure against external mechanical or electrical fields. This is consistent with recent observations where disorder in defect dipoles in soft PZT was reported to be correlated with high domain wall mobility. Alternatively, it is possible that the softening occurs in response to the associated decrease in the oxygen vacancy concentration. Substitution of La3+ for Pb2+ or of

Nb^{5+} for $(Ti, Zr)^{4+}$ should produce defect concentrations dominated by the dopant, i.e. $[Nb^{\circ}_{Ti}] \approx 2[V^{''}_{Pb}]$ This reduces the hole concentration, and hence the hole conductivity. In addition, it also reduces the oxygen vacancy concentration. This can be understood by considering the Schottky defect reaction: nil <----> $V^{''}_{Pb} + V^{''''}_{Ti,Zr} + 3V^{\circ\circ}_{O}$. The equilibrium constant for this reaction is $K_{Vo^{\circ\circ}} = [V^{''}_{Pb}][V^{''''}_{Ti,Zr}][V^{\circ\circ}_{O}]^3$. As the concentration of Lead vacancies is driven up by the dopant, the concentration of oxygen vacancies falls commensurately, so that the equilibrium constant is unchanged. In the case of $BaTiO_3$, high concentrations of oxygen vacancies did not significantly change the mobility of domain walls, while defect dipoles involving oxygen vacancies did. Oxygen vacancies are mobile at room temperature. Defect dipoles with oxygen vacancies (e.g. $Fe^{'}_{Ti} - V^{\circ\circ}_{O}$ or $V^{''}_{Pb} - V^{\circ\circ}_{O}$) can provide an internal bias which reduces domain wall mobility. Finally, Gerson has suggested that the key role of donor doping is simply to increase the concentration of Lead vacancies. The Lead vacancies were hypothesized to minimize local stresses in the lattice, which in turn facilitated domain wall motion. [29]

4.2 DEPOSITION METHODS

Although many applications of electrical ceramic materials are found in the form of bulk or thick films, an increasing need for thin film ceramics to meet the needs of new devices has been apparent in recent years. The process of depositing PZT as a thin film involves many common practices adopted from bulk and thin film production techniques. Commonly, precursors are used in either in gaseous (CVD), solid (PVD), or liquid (solution deposition) form to react or combine to produce a thin film on a substrate.

The main approaches for thin film PZT processing can be categorized into the following categories

1- Physical vapor deposition (PVD)

2- Chemical solution deposition (CSD)

PVD techniques require medium vacuum, usually between 10^{-2} and 10^{-6} torr, to increase the mean free path of the atoms ejected from the target in order to obtain a sufficient flux of ions capable of depositing onto a substrate. Sputtering, evaporation and laser ablation are examples of well-established PVD techniques. Among the advantages of the PVD techniques there are high purity, cleanliness, potential compatibility with semiconductor integrated circuit processing and

epitaxial/single crystal film growth is possible. However, these are certain drawbacks as slow deposition rates, and difficult stoichiometry control in multi-component systems where evaporation or sputtering rates differ considerably, moreover high temperature post deposition annealing is often required and high capital equipment acquisition and maintenance costs are necessary. Ion-beam assisted evaporation and sputtering are potentially capable of increasing film uniformity and increasing deposition rates. In general, laser ablation, a technique which is similar in concept to flash evaporation, and is based on the creation of jet of atoms from the target material using an ultra high-energy laser beam seems advantageous for congruent transfer of target material on the final substrate, however, the control of the final composition and morphology is not that easy due to the different reaction rate of the elements to be deposited. The CVD techniques are usually characterized by higher deposition rates, good stoichiometry control, large area pinhole free films and lower initial equipment costs. However, the limited availability, stability, and toxicity of the precursors for the ferroelectric compositions has posed a serious, technical challenge. Another method that has been quite extensively employed for producing ferroelectric thin films is chemical solution deposition. Chemical solution deposition has the advantages of precise composition and thickness control in multicomponent system, as Lead zirconate titanate, ease of process integration with standard semiconductor manufacturing, process simplicity, and much cheaper equipment costs [4].

4.2.1 PHYSICAL VAPOR DEPOSITION

By using a solid source and heat, plasma, ion-beam, or laser to vaporize the solid target, a thin film can be deposited onto a substrate. Although this technique has been used often in the production of metal films, a growing number of processes are being modified and developed to deposit ceramics, especially stoichiometric multicomponent films like PZT. Physical vapor deposition (PVD) techniques used in ceramic processing include ion-beam, magnetron, and RF-diode sputtering; thermal, electron beam, and flash evaporation; and pulsed laser ablation. Sputtering is an ablative plasma assisted method operated in high vacuum. It utilizes a inert gas ion bombardment, very often Ar+ ions. The Ar+ ions are generated by cold plasma. The sputtering relies on the transfer of physical momentum and kinetic energy from the incident particle (ions) to the surface target atoms. The ion bombardment leads to structural changes in the near surface atoms and/or clusters of atoms by breaking the bonds and dislodging the surface atoms. Due to a considerable kinetic energy of some eV the sputtered atoms and ions move away from the target and condense on a substrate, located opposite to the target at small distances.

Plasma discharge can be realized by DC or RF electrical field. The advantage of RF sputter sources is the possible deposition of non-conducting and semiconducting materials. The deposition rate is reduced significantly and cannot be compensated by higher electrical power supply. DC power supplies are able to provide more plasma energy [30]. Plasma sputtering deposition (PSD) is practical for both commercial and research environments, but often problems of thickness and compositional uniformity from using bulk targets alter the process. Also, extreme sensitivity to deposition conditions and geometry result from the nature of the physical configuration. Depending on the process conditions a high amount of defects like grain boundaries, pores and dislocations, vacancies, impurities and significant residual stress can be generated in the deposited thin films. As is the case for general PZT processing, the formation of the perovskite phase is greatly influenced by the incorporation of Pb. With PSD, the type of system can influence the transport of Pb to the surface depending on the gas pressure. Another PVD method, ion-beam sputtering deposition (IBSD) uses multiple ion beams directed a single elemental target, for example Pb, Zr, and Ti for PZT, to counteract preferential sputtering of multi-component oxides. Thus, control of the film stoichiometry stands out as this is an often a drawback for many vapor-based deposition processes. Although IBSD has lower deposition rates than PSD, some advantages include lower pressure during deposition and the production of smoother films. This technique is on the other hand quite difficult to control and quite expensive. Thermal evaporation is also a vacuum-based PVD deposition technique in which a metal is heated to generate a metal vapor that can condense onto a substrate surface inside a vacuum chamber. For fabrication of high quality thin films a collision-less flight of particles has to take place from the vapor source to the substrate, so a vacuum of better than 10-5 Pa is required. The temperature needed is a function of vapor pressure of the material [31]. Primarily yet under research, pulsed laser ablation deposition (PLAD) is good for rapid exploration of novel chemistries and has been shown to produce single phase PZT at temperatures from 600-700°C. It is most widely used for its ability to deposit a variety of ceramic films [22]. Exposing targets to an high intensity laser beam creates a plume of material from the target, providing an evaporation source and transferring the target atoms to a heated substrate where these atoms can be incorporated in the substrate forming a thin film with a composition similar to the target. This method is good for multicomponent system like PZT due to the accurate transfer of the target stoichiometry to the film in the case of oxides. Complexity arises in the spatial and time dynamic evolution of the ablated plume, and there are problems of conformal and large-scale uniform coverage. For PZT, the presence of Pb may cause contamination problems during fabrication

[21]. It is a very quick and expensive method due to equipment like laser and geometry-dependent chambers, and hence limited to research laboratories and not suitable for industry [30]

4.2.2 CHEMICAL VAPOR DEPOSITION

Chemical vapor deposition (CVD) processes differ from PVD in a way that the deposition is due to chemical reactions of the precursor gases which react on the surface of the substrate. Typically, this is a thermally driven process because of the use of heat energy to activate the reactions. In the case of depositing PZT, a specific kind of CVD employed is metallorganic CVD (MOCVD) distinguished by the generally high volatility of the precursors permitting lower temperature processing. Unlike PVD processes, stoichiometry in MOCVD is not such an issue due to the ability to precisely control the flows of the gaseous precursors and so the amount of precursor reacted. This make it a suitable candidate for the preparation of PZT and other ferroelectric oxides films [22]. In many cases of CVD processing, the modification of using glow-discharge plasmas enables low temperature deposition of films. Some drawbacks include complex metal precursor selection, (typically metal alkoxides) and lower deposition temperatures. Further complexities arise from the precursor delivery technique. A proposed option called liquid-source injection produces a viable, but expensive, alternative technique for multicomponent systems. Even with the decrease in processing temperature, the high costs override as a major drawback to use such methods.

4.2.3 CHEMICAL SOLUTION DEPOSITION

CSD processes, mainly including metallo-organic deposition (MOD) and sol-gel process, have been the subjects of considerable research interest relative to the deposition of thin ceramic films like PZT. Fukushima et al. in 1984 published their work on metallo-organic deposition (MOD) processing of thin films of PZT and right after that, Budd et al [31] published their work on the sol-gel processing of thin films of PZT. These pioneers works demonstrated that it is possible to obtain the desirable properties of bulk perovskite materials in thin-film form. The early work by these investigators and others led to a rapid expansion of research in this area [32]. MOD and sol-gel process differ in the chemistry of the solution. They allow the potential to control both chemical composition and microstructure to the levels required in electronic materials processing applications. In addition, experimental evidence indicates that temperature-time requirements for the subsequent crystallization/densification processing can often be minimized due to the high degree of chemical homogeneity in the polymeric ceramic precursor systems. The general

principle of CSD involved in the solution deposition of ceramic films is to prepare a homogeneous solution of the necessary precursors dissolved in an appropriate solvent, and later to spread the solution onto a substrate using spin coating or dip coating. The homogeneity of solution is one of the most important parameter in assuring a high quality thin film, because it prevents the formation of nano-island or nano-clusters. Other important parameters that will define the solution precursor properties are the precursor size, structure, shape and rate of reaction. The starting reagents are dissolved in a common solvent. The selection of the starting reagents, depending on the solution routes, is dictated by solubility, accessibility and reactivity considerations of solution precursor species desired. Similar consideration have to be done for the choice of the solvent. For depositing the solutions onto substrates, the basic process involves substrate dipping or spin coating followed by some baking or pyrolysis, conducted at relatively low temperature (100-300°C), and crystallization, carried out at high temperature (550-700°C for PZT) in either a standard conventional furnace or better in a rapid thermal annealer (RTA). The use of the latter increases the final films quality and reduces the possibility of film cracking, as discussed hereafter. Among the processing methods available to produce thin PZT films, solution deposition stands out as the most adaptable and versatile as it can be used in the production of thin and thick films, tailoring such parameters as chemistry and thickness fairly simply and covering large surfaces easily and with a low cost. The deposition is divided into two parts, the solution synthesis and the film deposition. Prepared solutions can be easily made in-house or commercially purchased.

CHAPTER V

5 EXPERIMENTAL PROCEDURES

The experimental procedures were divided in seven different step.

1. Sol-gel preparation and Characterization of the solution with an XRF procedures
2. Preparation of Pt substrate
3. Deposition of the solution on a substrate
4. Thermal treatment
5. Characterization of the piezolectric film with XRD and SEM
6. Deposition of the controelectrode
7. Measuring of the ferroelectric property

5.1 SOL-GEL PROCESS

All solutions are prepared with the same sol-gel process, using a carboxylic sol-gel route. 1-propanol are used as solvent, acetic acid are used as chelating agent. Lead(II) acetate trihydrate ($Pb(CH_3CO_2)_2 \cdot 3H_2O$, Niobium(V) ethoxide ($C_{10}H_{25}NbO_5$), Zirconium propoxide $Zr(OCH_2CH_2CH_3)_4$ (70 wt% in propanol) and Titanium isopropoxide [Ti $((CH_3)_2CHO)_4$] are used as precursors material. In order to verify the effect of Niobium as a doping element in the piezoelectric film, four different solution are prepared varying the Nb composition. The first solution was prepared adding 0% of Nb to produce a simple PZT solution, then we add 1% of Nb, in the third solution there was 2% of Nb and 3% of Nb in the last one. A general procedure to prepare the solution is described in the following scheme, later on the exactly composition used in the solution is explained for the different Nb concentration. An hot plate with an oil bath is at 90 C°, in a triple neck round bottom flask (50ml) we put Zirconium propoxide and Niobium ethoxide. The Zirconium must be added in the flask before the Niobium, the inverse operation produce a solidification of the Niobium ethoxide on the glass and we lose part of the molar

concentration. Then we add 5ml of acetic acid and we mix it with a stirrer. Titanium isopropoxide is put in the bottom flask and then we add 5ml of 1-propanol. Lead acetate trihydrate is put in the solution and then we heat the flask for 30minutes on the hot plate. After 30 minutes we leave the solution to rest for 20minutes at 60° C. It ‘s important to leave the solution rest at 60°C to avoid segregation of the precursors. Then we add 8.7ml of acetic acid and 10ml of propanol in order to have a 0.5 molar solution, then we leave the solution at 60°C for 3 hours. Using a pressure filter we filter the solution into a container.

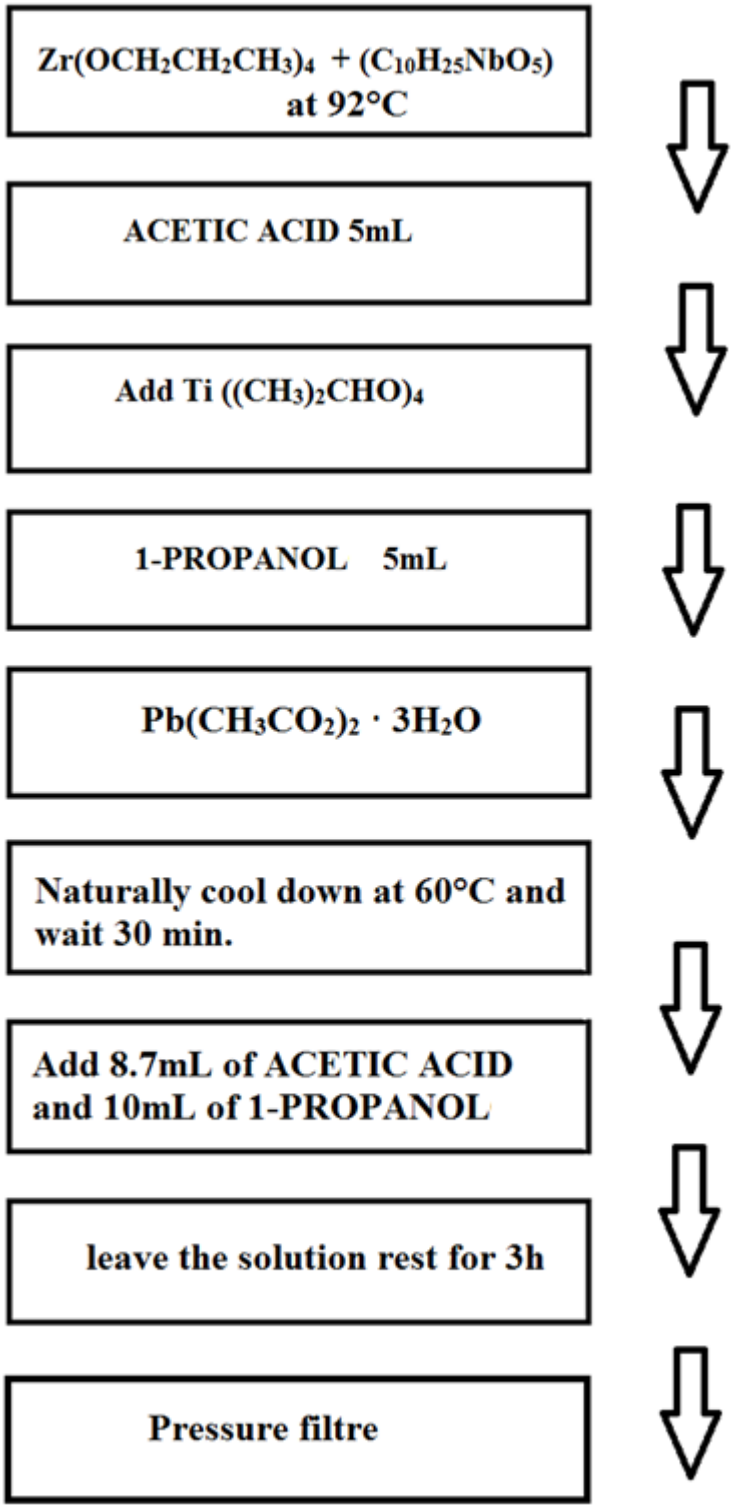

Fig. 18: schematic representation of the sol-gel solution preparation.

5.1.1 PZT

The molar composition of the solution we want to obtain is $\mathbf{Pb_{1.1}Zr_{0.52}\ Ti_{0.48}}$. The molar concentration of Pb is 1.1 because we add a 10% more to avoid an excessive dispersion of Pb during heating. In order to obtain the molar composition desired we have to add

-$Pb(CH_3CO_2)_2 \cdot 3H_2O$ = 0.02moli+ 2% = 8.345g

-$Zr(OCH_2CH_2CH_3)_4$ = 0.0198*0.52= 0.0102moli = 4.867g

-[Ti $((CH_3)_2CHO)_4$] = 0.0198*0.48=9.504*10^-3 moli = 2.784g

-Acetic acid =14,38g

-1-propanol= 16g

5.1.2 PNZT 1%Nb

The molar composition of the solution we want to obtain is $\mathbf{Pb_{1.1}(Zr_{0.52}\ Ti_{0.48})_{0.99}Nb_{0.01}}$.

-$Pb(CH_3CO_2)_2 \cdot 3H_2O$ = 0.02moli+ 2% = 8.345g

-$Zr(OCH_2CH_2CH_3)_4$ = 0.0198*0.52= 0.0102moli = 4.818g

-[Ti $((CH_3)_2CHO)_4$] = 0.0198*0.48=9.504*10^-3 moli = 2.756g

-($C_{10}H_{25}NbO_5$), = 0.01*0.02= 0.0002moli = 0.063g

-Acetic acid =14,38g

-1-propanol= 16g

5.1.3 PNZT 2%Nb

The molar composition of the solution we want to obtain is $\mathbf{Pb_{1.1}(Zr_{0.52}\ Ti_{0.48})_{0.98}Nb_{0.02}}$.

-$Pb(CH_3CO_2)_2 \cdot 3H_2O$ = 0.02moli+ 2% = 8.345g

-$Zr(OCH_2CH_2CH_3)_4$ = 0.0198*0.52= 0.0102moli = 4.725g

-[Ti $((CH_3)_2CHO)_4$] = 0.0198*0.48=9.504*10^-3 moli = 2.72g

-($C_{10}H_{25}NbO_5$), = 0.01*0.02= 0.0002moli = 0.127g

-Acetic acid =14,385g

-1-propanol= 16g

5.1.4 PNZT 3%Nb

The molar composition of the solution we want to obtain is $\mathbf{Pb_{1.1}(Zr_{0.52}\ Ti_{0.48})_{0.97}Nb_{0.03}}$.

-$Pb(CH_3CO_2)_2 \cdot 3H_2O$ = 0.02moli+ 2% = 8.345g

-$Zr(OCH_2CH_2CH_3)_4$ = 0.0198*0.52= 0.0102moli = 4.720g

-[Ti $((CH_3)_2CHO)_4$] = 0.0198*0.48=9.504*10^-3 moli = 2.70g

-$(C_{10}H_{25}NbO_5)$, = 0.01*0.02= 0.0002moli = 0.19g

-Acetic acid =14,385g

-1-propanol= 16g

Every solutions is then analyzed with XRF in order to obtain the exact composition of the container.

5.2 PREPARATION OF THE PT SUBSTRATE AND DEPOSITION

5.2.1 CHOICE OF THE SUBSTRATE

The choice of the substrate for PZT thin film deposition has fundamental relevance both on the morphological and electrical properties of the final deposit, for the presence of cracks, the density of the film and the ferroelectric and piezoelectric features . Contrary to the bulk PZT fabricated using sintering process, which crystals don't possess a preferential orientation and are randomly oriented, for PZT thin films the substrate strongly influences the growth of PZT grains and their final crystalline planes direction. The dielectric, ferroelectric and piezoelectric properties are strongly influenced by the preferential crystallographic plane orientation and by the density of the film, so the relevance of the substrate on the final properties of the deposit is

obviously fundamental. During years different types of substrate have been used to fabricate PZT films. Some of these are summarized in the table below with their behavior:

Tab. 1: different example for PZT substrate

SUBSTRATE MATERIALS	
Stannic oxide	Medium resistance
Indium tin oxide (ITO)	Medium resistance
Ti/Platinum	Good and reproducible
Aluminum	Temperature limited
Silver	High adhesion
Stainless steel	Good at low T°
Ni, Co, Ti, W	Oxidized
Niickel based alloy	Acceptable
Ruthenium Oxide	High conductivity
Yttrium Copper Barium Oxide	Lattice matched
W, Ti, Pt silicides	Some success

As noted earlier, the definition of a good electrode material is not trivial. It has to survive processing in oxygen without degradation or the development of unacceptable interface layers and the thermal expansion difference between the electrode and the film must be lower as possible. The metallization has two roles to play with respect to the film: it must nucleate the required phase and provide adequate conductivity for device purposes [33]. Many metals such as Ni, Co, Ti and W oxidize rapidly under oxygen processing. Aluminum is often acceptable, although an interfacial film can nucleate a non-piezoelectric phase of PZT and care has to be taken to maintain the processing temperature below that of the Al-Si eutectic temperature which is around 480°C . Platinum electrodes with a 0,01 μm thick Titanium adhesion layer are most often reported as having the highest reliability**.** In both cases, the quality of the metallization is of great significance. Low density, porous deposits can lead to irreproducible crystallization conditions and interfacial barriers. This often makes simple evaporation suspect and the deposition of metallic layer by sputtering onto heated substrates has been found to be the most reliable. Stannic oxide and indium tin oxide (ITO) are transparent electronic conductors and remain excellent prototyping electrodes for piezoelectric films. Such substrates are available commercially and provide good results at low frequency. There are two explanations for this. The material remains conducting in an oxygen atmosphere up to temperatures of 400°C, and it

tends to promote crystallization of the required perovskite phase. On ITO coated glass the films usually growth with a (100) preferential orientation and with a less pronounced pyrochlore phase. The main disadvantage of ITO is that its n-type conductivity, associated with oxygen vacancies, reduces when the film is fired in oxygen. This can lead to interfacial diffusion and a limitation of the high frequency response [33]. As for ferroelectric memory applications it's the relatively high sheet resistance of the film which limits the upper frequency response of the device. This is less important at the frequencies normally employed in piezoelectric devices. The most used substrate is Platinum deposited on a SiO2/Si wafer. This material is chemically inert and possess a very low diffusion tendency. Moreover it can form a metallic-ferroelectric interface that promotes the formation of a perovskite phase and doesn't reduce the electric properties of the film. Platinum is usually oriented towards the (111) direction and this can promote the nucleation of PZT with the (100) or (111) planes depending on parameters as the deposition temperature of Platinum and its residual stresses as reported in [8]. To enhance the adhesion of Platinum, often Ti is used as adhesive layer between the Silicon dioxide and the Platinum. The PZT annealing temperature, the diffusion of Titanium into the Pt and PZT layers is probable, but this can be beneficial for PZT grains growth. In any case, to reduce the Ti diffusion, the creation of an oxide layer on the top of Ti, or the direct use of TiO_2 has been proposed. Certain conditions promote the nucleation and growth of grains with the (111) preferential plane direction, even if the most thermodynamically stable orientation is the (100), and one of the key points for this, is the substrate texture. Three main conditions can promote the (111) plane nucleation: the diffusion of Ti towards the surface of the substrate; the formation of an intermetallic phase of Pt-Ti or Pb-Pt; and the Pt residual stresses. It's also possible to use a seeding layer on the top of the substrate to promote the nucleation of only one plane. Such seeding layer aims to promote the kinematics which assures the growing of the preferred orientation of PZT layer. The presence of Ti or TiO_2 layers (even very fine) will assure the growing of (111)-oriented PZT while $PbTiO_3$ (PTO) layer, will promote the growing of (100) planes [3]. The PTO layer can be obtained both via sputtering and sol-gel deposition. Residual stresses in the Pt layer also have a great influence on the final PZT orientation, as mentioned before. When the Pt layer is subjected to a thermal pre-treatment, which consists in an annealing cycle at 500 -600°C before spin coating, residual stresses are created inside the layer. It has been demonstrated by Quin et al. [34] that the residual tension will promote the growth of the (111) PZT and a residual compression will favor the (100) planes growth. When the substrate is annealed before spin coating in a conventional furnace at 500°C the (111) plane growth is preferred. When the Pt layer is annealed in a rapid thermal annealer (RTA) at 500°C the PZT

(100) will preferentially grow. In both cases a residual tension will be present in the Pt layer and it will be stronger in the RTA annealed sample. The residual tension will decrease the mismatch, and consequently the interfacial energy, between the (111) Pt and the (111) PZT and so the latter plane will easily grow. When the residual stresses are more important, as in the case of RTA annealing, the lattice mismatch will be still large and the thermodynamically more stable (100) plane will preferentially grow because of the high interfacial energy between the (111) Pt and the (111) PZT plane. The use of a barrier layer is very important to avoid the diffusion of the substrate elements towards the deposited film. PZT films are usually annealed at temperatures higher than 550°C, temperature at which the perovskite phase begins to form, and at this temperature the risk of Lead diffusion into the Silicon and of Titanium diffusion towards the surface is very high. For this reason, usually, a silicon dioxide layer is thermally fabricated on the top of the Si wafer to prevent elements diffusion.

5.2.2 DEPOSITION

In this work the sol gel precursor solution has been spinned on $Pt/TiO_2/Si$. $Pt/TiO_2/Si$ is given in the form of disk. The disk is cut in the form of little square measuring about 2cm per side. In order to avoid damage of the structure the disk are coated with a TEOS film that has to be removed. The removal of this TEOS film is obtained using hydrofluoric acid 5% in weight. We put our sample in a bath of HF 5% for 7 minutes and then we perform conductivity measures to verify the exactly removal of the polymeric film. The substrate is then put in a spin coater. For thin film fabrication, dip coating and spin coating are typically used to coat sol-gel onto substrates. In this thesis, PZT/PNZT thin films were fabricated exclusively using the spin coating process. Spin coating has been used extensively in the semiconductor industry because of the numerous advantages that it offers as low cost, great control of the precursor chemistry, possibility to cover large surfaces and good thickness on morphology control. This method also assures the highest ferroelectric and piezoelectric properties of the final thin layer. The sol-gel spin coating step can be divided into 4 main stages [35]. In the first stage the sol is dispensed onto the substrate, fig.19a. In the second stage the substrate is accelerated to its final desired rotational speed, fig.19b. This stage is usually characterized by aggressive fluid expulsion from the wafer surface by the rotational motion. Eventually, the fluid is thin enough to be completely co-rotating with the wafer and any evidence of fluid thickness differences has gone. Ultimately, the wafer reaches its desired speed and the fluid is thin enough that the viscous shear drag

exactly balances the rotational accelerations. In the stage three, fig.19c, the substrate is spinning at a constant rate and fluid viscous forces dominate fluid thinning behavior.

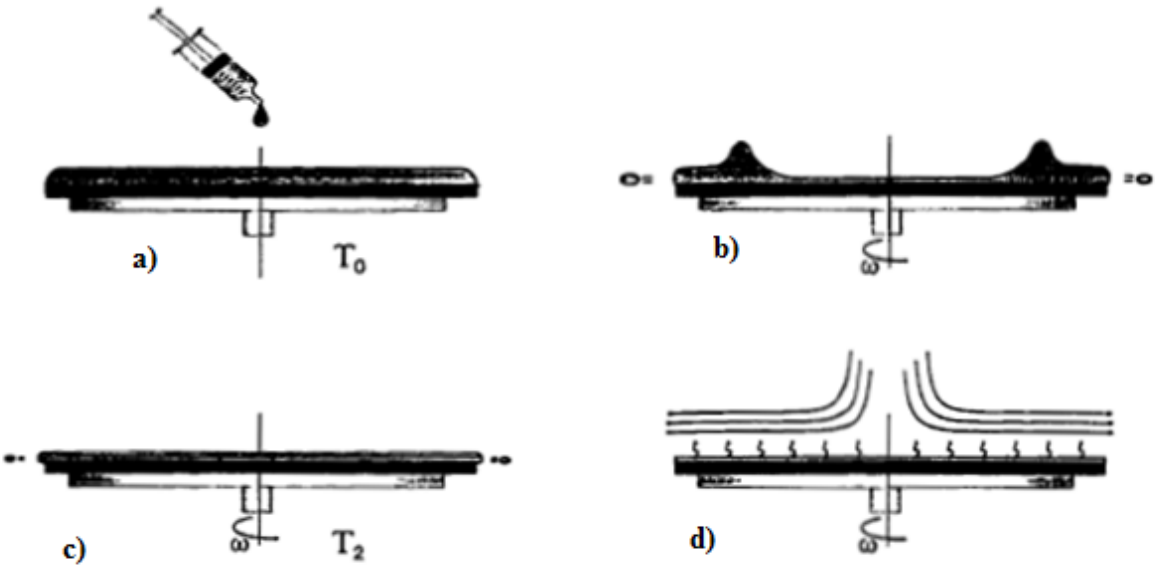

Fig. 19: schematic example of spin coating [26]

This stage is characterized by gradual fluid thinning. Depending on the surface tension, viscosity, rotation rate, there may be a small bead of coating thickness difference around the rim of the final wafer. If the fluid thickness was initially uniform across the wafer, then the fluid thickness profile at any following time will also be uniform, leading to a uniform final coating (under ideal circumstances). In the fourth stage, fig.19d, the substrate is spinning at a constant rate and solvent evaporation dominates the coating thinning behavior. As the prior stage advances, the fluid thickness reaches a point where the viscosity effects yield only rather minor net fluid flow. At this point, the evaporation of any volatile solvent species will become the dominant process occurring in the coating. At this point the coating effectively gels. As these solvents are removed, the viscosity of the remaining solution will rise [35]. The hydrolysis is allowed to occur since the film has been deposited onto the substrate to create a dense film . Moisture in the atmosphere is used to supply water for the reaction. The reaction should proceed at a significant rate implying that gelation will occur in a short period of time. The final coating thickness depends on viscosity, type of substrate, surface tension, spin rate and solvent evaporation rate. In this work the spin coating stage was divided in two steps. Initially the solution was spun for 8 seconds at 500 rpm with an acceleration of 100 rpm/s, then the spin

speed was increased to 3000 rpm with an acceleration of 200 rpm/s and the sample was maintained at this speed for 40 sec. In this way during the first step the solution wets all the substrate slowly, reducing the possibility of striations and increasing the film homogeneity and then, at higher speed, the liquid film becomes thinner and denser along with time and solvent evaporation. When the spinning cycle finished the sample was immediately moved onto an hotplate to start the thermal treatment. With this procedure single films of 0,2-0,3 μm thickness have been successfully deposited onto all the substrate used. To create thicker films, multi-layers have been deposited sequentially after thermal cycle. It is important to underline that the step of spin coating is very critical, many defect can be arisen during the coating as a consequence of some mistake. Defects that can occur during spin coating include comets, striations, cracks and wafer edge effects. Comets occur when relatively large solid particles impede the normal flow of the solution on the spinning wafer. The presence of comets can be reduced or eliminated by working in cleaner environments and by filtering solutions as part of the dispense process (fig 20 a). Striations are radially oriented lines of thickness variation in the as-coated film, fig. 20b. Their occurrence is thought to arise because of evaporation driven surface tension effects. The early evaporation of light solvents can cause an enrichment of water and/or other less volatile species in the surface layer. If the surface tension of this layer is larger than the starting solution, then instability exists where the higher surface tension actually draws material in at regular intervals and the spaces in-between are more able to evaporate, and surface relief develops. Other defects, like concentric circles, can form due to solution contamination with particle during spinning or drying steps fig.20c. The formation of defects during spinning implies the presence of the same kind of irregularities after the heat treatment. This phenomenon decreases the ferroelectric and piezoelectric features of PZT because defects form areas with tampered composition and make impossible the surface area control when other structures, like electrodes, have to be built on it. Cracks instead can arise due to a bad evaporation of the solvent. Solutions haven’t a sufficient molar ratio of solvent due to a rapid evaporation of this one go to a wrong gelation that produce a cracked film, fig. 20d.

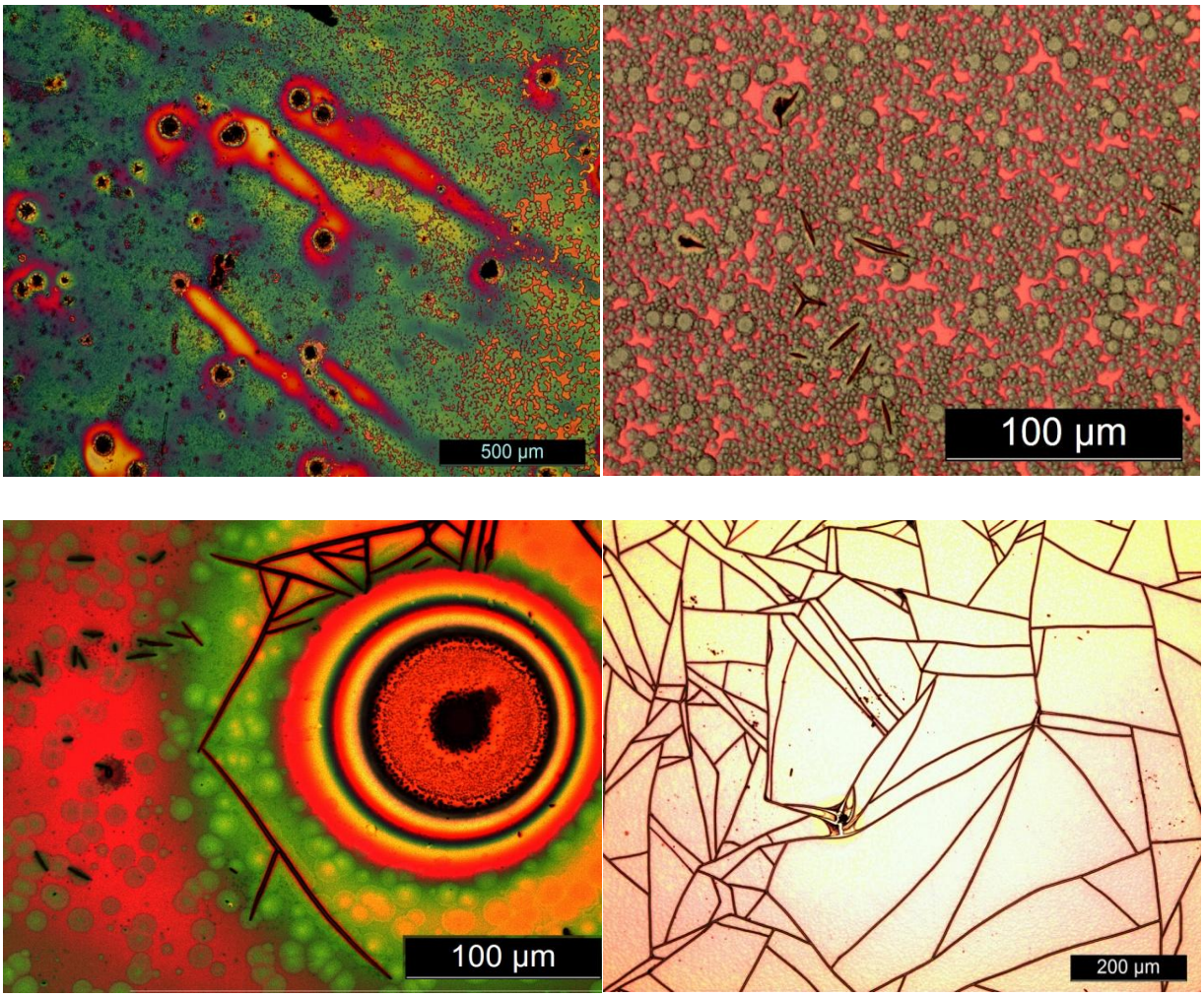

Fig. 20: different kind of defects that can arise during spin coating: a) comets; b) striations; c) concentric circles; d) cracks

5.3 HEATING TREATMENT

It was said before that many and different defect can arise during a sol gel process, in fact even though the sol-gel method seems to be a simple process, it does possess a number of variables and constraints allowing exploitation of its unique features. These are mainly related to the volume of organic content in the solution, that may influence the mechanical film behavior and the formation of cracks during high temperature treatment. The thermal treatment is the fundamental step to transform the PZT precursors solution film into the final crystalline material. There are essentially four steps:

- Deposition of the solution containing the precursors and gelation on the substrate

- Drying of the layer for evaporating the solvents

- Calcination of the layer for eliminating the remaining solvents and the organic components. After this step the material reaches an amorphous phase

- Crystallization for obtaining the Perovskite phase and densification of the material

As can be imagined, significant weight loss and shrinkage occur in the film during thermal stages. Hence, a careful control on these parameters and on processing conditions is required and their influence on the final structure must be understood to minimize the issues.

5.3.1 THERMAL ANALYSIS

It is important to find and justify a correct heating sequence to know the effect of heating the sol-gel precursors solution at different temperature. TGA studies from the literature [26],[8],[36] confirm that the maximum weight loss occurs at 100-200°C and this is justified with the solvent and most volatile species evaporation. At temperature between 200-300 °C the evaporation of the residual solvent held in the sample continue and there are the first traces of CO_2, that prove the beginning of the carbon chains burning into the film. This release will reflect the bonding of the organic species to the inorganic components of the gel. For example, acetic acid, that in solution acts both as chelating ligand and solvent, is evolved from the coating in different temperature regions. The acetic acid that is vaporized in the temperature region from 70°C to 120°C is free in the solution . As water is lost , more acetate groups are bonded to the Titanium and Zirconium ions. The bonded acetate groups are driven off around 175°C. This thing justifies the continuous evaporation of acetic acid until high temperatures. A weight loss peak is present at 285°C and this is attributed to the Lead acetate dissociation and production of PbO. In fact, when the gel films are heated to T=285 °C, Lead acetate melts and starts to decompose to the more stable Lead carbonate. The amount of acetic acid driven off increases drastically, carbon dioxide is evolved, and network movement takes place. At temperature of 300-450 °C the loss of weight continues, even if with a slower rate. In this range of temperature there is still evolution of acetic acid, that comes probably from Lead acetate decomposition, CO, CO_2, and PbO. Upon heating in this range of temperature the organic residuals are burned off, forming an amorphous solid. This step is referred to as firing stage. This solid is transformed into an intermediate pyrochlore phase at pyrolysis temperature between 300 and 470°C. The firing has a great

relevance on the subsequent crystallization step and the temperature at which this occurs strongly influence the crystallization mechanism as reported later on. At temperature of 450-800°C the weight loss is minimal and there are traces of evaporated PbO, CO_2 and CO [36]. The residual organic content in the film is completely burned off during this stage and the film transforms from an amorphous solid to a crystalline perovskite structure. This step is referred to as annealing. The amorphous film transformation begins at different temperature, depending on the type of sol gel used, and it's observed in the TGA as an exothermic peak that indicates phase transformation. Using low carbon content solution it's possible to obtain crystallization at low temperature as 550°C. Usually it is necessary to select an appropriate temperature to obtain the largest amount of perovskite phase and to eliminate the non ferroelectric pyrochlore phase. The temperature usually used varies from 550 °C to 800 °C. It is also important to balance the Lead loss during high temperature heating, since the Pb content decreases monotonically with increasing annealing temperature and the Lead loss may obstruct the formation of the perovskite phase.

5.3.2 CRYSTALLIZATION MECHANISMS

The PZT/PNZT films are built on a substrate and during annealing these films transform from an amorphous state to a crystalline one. This process starts from the substrate and it's principally governed by the nucleation of crystalline grains. This means that the energy needed for the grain's nucleation is bigger than the energy required for their growth. The nucleation is governed by many factors as the texture of the substrate, its residual stresses and composition. All these factors can Lead to crystals growth with different preferential orientations. The grain growth is governed by the competition between the kinetics, that promotes the (111) planes growth when the substrate properties favor it, and the thermodynamic, that promotes the (100) or the (110) planes growth, since it is the most thermodynamically stable. For this reason if the substrate is oriented (111), as in the case of Pt, the PZT will tend to be oriented according to the same direction because the kinetics tends to minimize the interfacial energy between the substrate and the deposit, which depends on the substrate properties and composition. On the other hand the thermodynamic favors the (100) plane growth and so the final PZT orientation will depend on which of the two mechanism prevails. The grains growth process depends also on the number of nucleation sites; if these sites are numerous, the kinetic will govern the process, if there are just few sites the thermodynamic will be predominant [8]. Moreover it has been noted that when the kinetic governs the growing process, as in the case of (111) plane growth, the grains dimension

is smaller compared to the grains of the (100) PZT. This fact demonstrates as the kinetic governed growth is more rapid and is favored by a large amount of nucleation sites, while the thermodynamic controlled growth is slower and favored by a small amount of nucleation sites, that also permits the growing of larger grains. The firing temperature, that influences the stability of the pyrochlore phase, is another parameter that has a certain relevance on the grain growth mechanism because it makes the phase transformation easier or not. In the first case the kinetic will be favored, in the second the process.

5.3.3 HEATING SEQUENCE

The thermal analysis provides guides to choose the different temperatures to process the PZT films. Other considerations such as the film thickness and the specific type of sol-gel need to be considered before selecting a final thermal processing sequence. After spinning a thermal treatment is required to promote gelation, pyrolysis and crystallization of the film. Acetic acid based PZT films require a carefully chosen heating sequence in order to maximize the crystallization and the electrical properties. In addition to the high carbon content, film cracking could be also an issue when using this type of sol-gel [26]. The heat processing in this work has been divided into three steps. During the first step the film is dried in air on a hot plate, at temperature between 100-200 °C. At this range of temperature the most volatile element will evaporate (acetic acid, water and alcohols in our case). Solvent evaporation produce shrinking and densification of the film as it loses liquid. During this process bubbles and in-homogeneities can appear on the film surface when the solvent is not free to evaporate from the film. Moreover, during the drying process, some solvent will flow across the polymeric network present in the film, to compensate for the different solvent evaporation rate through the film. This latter causes a gradient of pressure inside the matrix of the sol gel that can lead to the breaking of the rigid network and defects formation. For this reason an appropriate temperature and time must be chosen to improve the quality of the dried film. After drying, the film is much denser, and any remaining liquid is held in by capillary action. In this work the drying stage has been performed in air on a hot plate at 150 °C for 5 minutes for all the samples. This choice has been done comparing the data from literature about the mass loss rate at different temperature for the kind of solutions used in this work. The data in literature have been gathered using thermo gravimetric analysis (TGA). This process assures the complete evaporation of the solvent without producing any type of defects. After drying, the as-deposited film is an amorphous gel of metallorganic compounds. After drying, the sample is immediately moved on another hot plate at

temperature between 300°C and 450°C. This step is referred to as firing or calcinations. At these temperatures the residual solvent is eliminated and Lead acetate dissociation occurs, producing free acetic acid. The organic fraction in the film is burned off and the gel transforms into an amorphous solid. The firing temperature and time must be chosen in order to assure the burn of the organic component and the amorphous solid phase formation and it must prevent excessive PbO evaporation. Firing at lower temperatures for prolonged periods results in only partial removal of the residual carbon, and contributes to the evaporation of Lead oxide. In order to maximize the removal of the carbon and to minimize the Lead loss, a rapid increase of the temperature from 150°C to the crystallization temperature would be desirable. However, increasing the temperature directly from 150°C to 650°C is not beneficial since stresses in the film due to the sudden volume change can lead to cracking. kinetics. As discussed in the previous section, when the kinetics dominates the growth mechanism, the (111) plane orientation is preferentially obtained on Pt substrates. On the other hand, when the calcinations temperature is high as 420°C, the more stable pyrochlore phase created slows down the crystallization kinetic. Under these conditions the thermodynamic dominates the further crystallization and the (100) phase growth is favored. Many other authors noted that varying the calcination temperature from 200 °C to 500 °C the final PZT orientation varies from the (111) to the (100). In any case, it's difficult to establish a defined temperature at which the growth mechanism change, but it remains a good method to qualitatively control the final grains orientation. The calcinations temperature, the annealing method, the substrate type and its thermal pre-treatment, that induce residual stresses into it and promote the formation of intermetallic species that favor the (111) plane growth, are so far the most important parameters to control the grains growth mechanism and final crystallographic planes orientation. For this reason an intermediate firing step is crucial to improve the film features and an excess of Lead is added in all the solution to compensate the Lead loss. The amorphous solid formed during heating creates an intermediate pyrochlore phase that will evolve in a perovskite structure during high temperature annealing. As reported in the M.Cueff work [8], the stability of the intermediate pyrochlore phase is fundamental for the final properties of the crystalline film, and this depends directly on the calcination temperature. When the temperature of calcinations is high, also the oxygen concentration in the pyrochlore phase increases and this latter thing promotes the stabilization of the pyrochlore phase. When lower firing temperatures are used, as 350°C, the pyrochlore phase obtained is metastable and it will transform easily in perovskite. The fact that the phase transformation is made easier by low calcinations temperature, increases the crystallization kinetics. As discussed in the previous section, when the kinetics dominates the growth

mechanism, the (111) plane orientation is preferentially obtained on Pt substrates. On the other hand, when the calcinations temperature is high as 420°C, the more stable pyrochlore phase created slows down the crystallization kinetic. Under these conditions the thermodynamic dominates the further crystallization and the (100) phase growth is favored. Many other authors noted that varying the calcination temperature from 200 °C to 500 °C the final PZT orientation varies from the (111) to the (100). In any case, it's difficult to establish a defined temperature at which the growth mechanism change, but it remains a good method to qualitatively control the final grains orientation. The calcinations temperature, the annealing method, the substrate type and its thermal pre-treatment, that induce residual stresses into it and promote the formation of intermetallic species that favor the (111) plane growth, are so far the most important parameters to control the grains growth mechanism and final crystallographic planes orientation. In this work, 350°C has been chosen as firing temperature and this step was performed on a pre-heated hot plate, moving the sample onto it immediately after the first drying step. The use of low temperature as 350°C has been done to decrease the possibility of cracking due to thermal mismatch between the substrate and the amorphous film and too rapid densification . A calcinations time of 5 minute assures the burning of the residual solvent and of the organic species present into the film. After calcinations follows the third and last step of the thermal treatment . This is performed at high temperature using a normal furnace or a rapid thermal annealer (RTA), and this step assures the crystallization of the amorphous deposit. The annealing temperatures used in the literature vary from 550°C to 750°C and the heating ramp should be fast enough to prevent the excessive Lead loss from the film. Lack of Lead during thermal processing is a factor inhibiting crystallization of the PZT into the perovskite phase. The choice of a proper annealing temperature and time must be done to guarantee the maximum percent of perovskite phase formation into the film. This depends on many factor as the type of PZT precursors solution used, substrate and firing temperature. Usually high temperatures guarantee complete perovskite phase formation, but the Pb content decreases monotonically with increasing annealing temperature due to PbO evaporation, and similarly to the Pb content, also the oxygen content decreases with increasing annealing temperature. For this reason a right balance between the Lead loss and the necessity of obtaining a total perovskite phase must be found and that is done tuning the annealing temperature and time for the different substrates and solutions used. The PZT crystallization temperature for thin films is in general much lower than that one used in bulk PZT processing, and it depends strongly on the carbon content into the gel film and on the evolution degree of the rigid structure formed by poly-condensation of the metal alkoxides during the first drying processes. The presence of an ordered rigid structure into the film, before

thermal treatment, helps the PZT crystallization and contributes to the enhanced electric properties. For these reasons, it has been possible to crystallize thin films at low temperature as 550°C. Usually PZT film are annealed between 650 - 700°C, which assures the formation of the perovskite phase. In the Cueff work [8] the crystallization temperature is not considered very relevant for the final films properties, since it has to be just high enough to transform the amorphous solid film into a crystalline perovskite structure. Besides the crystallization temperature, the method used to anneal the film has a big relevance on the grains growth mechanism. The two annealing methods, adopted during years, imply the using of a normal furnace, or the crystallization in a rapid thermal annealer (RTA). Using a normal furnace the kinetic of crystallization is slow and for this reason the most thermodynamically stable phase, in our case the (100) for PZT, will tend to form. On the other hand, using a RTA, the increase of temperature in the furnace is very quick and the kinetic will be dominant in the growing mechanism, promoting the formation of the phase that will be kinetically favored, as the (111) for PZT on Pt substrate. Another time, it can be shown how the PZT crystallization mechanism depends on the balance between the kinetic and the thermodynamic of grains growth. In this work different annealing temperature are used. The presence of Niobium as we said stabilize the pyrochlore phase, higher the content of Niobium higher the temperature needed to obtain a full ferroelectric film. We set the temperature at 650°C, 700°C, 750°C and 800°C and the annealing time has been optimized for each one of the different composition used to obtain a complete perovskite phase formation and to avoid any presence of non-ferroelectric pyrochlore phase.

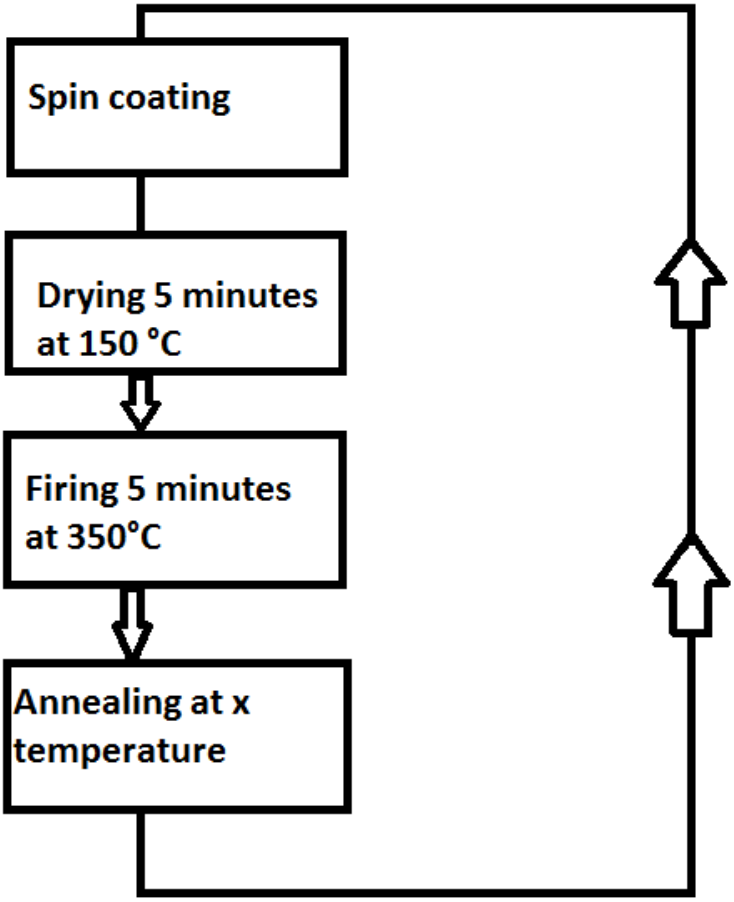

Fig. 21: schematic process of the thermal treatment.

5.3.4 EFFECT OF NIOBIUM ON HEATING TEMPERATURE

Niobium plays an important role in the heating sequence. It is well known in the literature that the addition of Nb in the PZT matrix leads to an increase in the crystallization temperature. Considering that the perovskite phase is formed from the pyrochlore phase, this inhibition of crystallization in the Nb doped PZT is the main cause of the appearing of pyrochlore containing matrix. An estimate of lattice parameters confirmed PNZT solid solution formation[37]. Furthermore it was found that with increasing Niobium content, the lattice parameter a increased slightly, with a greater decrease in c. The net result was an approximately linear decrease in the c/a ratio as a function of increasing substitution of the smaller Nb^{5+} ion onto the B site Films generally exhibited (111) preferred orientation consistent with nucleation and growth at low temperatures from the bottom (111) oriented polycrystalline Pt electrode and a (111) $PbPt_3$ interfacial phase that is well documented in the literature [38]. It is also found that the grain size of PNZT films changes between 100 and 200 nm. The use of Pt as a substrate allows for easy nucleation of the perovskite phase because of the approximate lattice parameters of $PbTiO_3$ and

Pt. Since Ti makes nucleation easier and Nb^{5+} substitutes for Zr^{4+} in some proportion, the surface number density of nuclei increases in PNZT thin films leading to a fine grained perovskite structure.For the undoped PZT films, grain size of 85±1.1 nm is achieved and 5% Nb doping, grain sizes of 104±1.4 nm and 69±1.2 nm, respectively, were obtained. Grain size decreases with increasing Nb content starting from 1% Nb addition. This can be explained with previous studies that, Nb is an effective grain growth inhibitor [39]

5.3.5 STRESSES EVOLUTION DURING HEATING

Gel films are converted into ceramic films by thermal treatment, and this latter is divided into three steps as discussed in the previous section. Drying and firing causes densification, pyrolysis and the release of volatile compounds from the film. These changes in volume combined with a mismatch between the thermal expansion coefficient of PZT and substrate, produce internal stresses in the film, which may lead to cracking. Stress that generates during firing is the origin of the cracks in gel-derived films, and can also provide substrate bending. Properties of the films like Curie point and crystallographic plane orientation could also be affected by stress into the film. Therefore, scientific understanding is quite important on stress evolution in gel-derived films. When fired, gel films experience: heating-up, isothermal heating (annealing), cooling-down stages. In the heating-up and isothermal heating stages, gel films undergo changes in structure and chemistry, which results in evolution of stress. The stress thus generated at any occasion during heating-up or isothermal heating stage is called intrinsic stress. In the heating-up and isothermal heating stages, gel films become more dense with several 10% in volume reduction due to capillary pressure on solvent vaporization and polycondensation reaction between PZT metals precursors. Densification leads to in-plane tensile stress because the films are constrained on the substrates. Thermal stress could also be generated in the heating up stage when the films and substrates have difference in thermal expansion coefficient. In the range of temperature from 200°C t o 300°C, gel films crack readily . As the volatile components vaporize, the films must shrink . However, because it is constrained by the substrate and by internal parts of the network, the surface cannot shrink freely and internal tensile stress will be created. If these cannot be relaxed the film will crack when the internal tensile stress achieves a critical value. For this reason fresh films are generally dried at lower temperature to reduce the rate of solvent evaporation and consequentially to allow the stress release, and only after drying, treated at higher temperature. This reduces the thermal shock at which the film is exposed. The film densification during the heating up stage is the main source of stresses. In fact, because the

difference in thermal expansion coefficient Δα and the change in temperature ΔT , would be in the order of 10-7/10-5 K-1and 102 K respectively, and the resulting strain, ΔT Δα, would be 10-5 10-3 in order, which is much smaller than those occurring via densification. [40] Therefore, stress due to densification would be dominating in the heating-up (and isothermal heating) stage. In the cooling down stage, on the other hand, no major changes are expected in structure and chemistry. Therefore, it would be thermal stress that is expected to be generated in the cooling stage. The intrinsic stress at the end of the isothermal heating stage and the thermal stress generating in the cooling stage are accumulated in films, giving rise to residual stress, which can be measured at room temperature after firing. In our case Pt acting as bottom electrodes, have a larger thermal coefficient of expansion than the PZT. This mismatch leads to stresses build up during the subsequent heat treatments. On application of PZT, the stress prevalent in the annealed substrate decreases as the film is initially stretched and then shrinks following the heat treatment for the PZT layer. The pictures below illustrate cracked PZT using an optical microscope and a Scanning Electron Microscope . These are very long and interconnected cracks that arise in few seconds when the sample is put on the hotplate at 350°C for the firing steps, and they can be seen by naked eye. They are caused by sudden film densification and thermal mismatch between the substrate and the PZT layer as discussed previously. It's possible to prevent the formation of these cracks depositing thinner film or adding into the sol gel solution some plasticizer as glycerol.

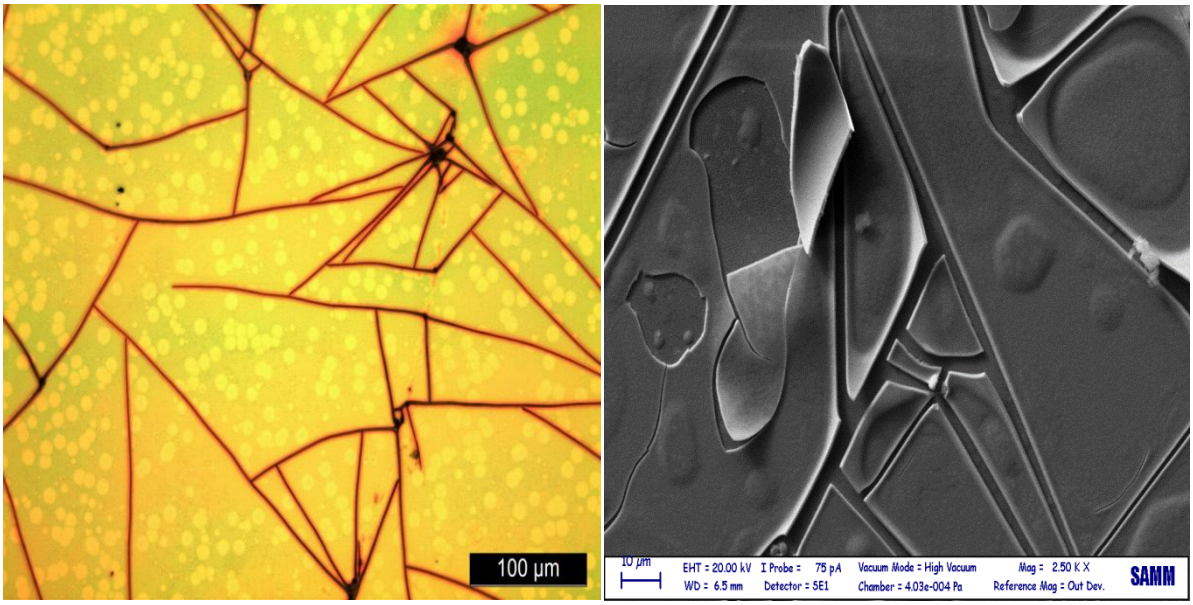

Fig. 22: optical microscope image of a cracked PZT Nb-doped film onto Pt substrate.

5.4 TOP ELECTRODES DEPOSITION

After PZT film deposition, top electrodes must be patterned onto the film to check the electrical properties of the PZT ferroelectric ceramic film deposited. Pattering top electrodes with the use of an appropriate shadow mask, a matrix of capacitors is obtained and this structure is suitable for electrical measurement, fig.23a. More exactly, a matrix of circular gold electrodes has been deposited using Argon ions cold sputtering technique. With the appropriate time of exposure, a gold layer of 80 nm thickness has been deposited on the top of the mask. To create the pattern onto the film, a shadow mask has been fabricated making a (9x9) matrix of holes of the desired dimension, into brass foil of 0,45 mm thickness. The mask is placed on the sample that has to be patterned and removed at the end of the sputtering process to create the desired circular gold electrodes.

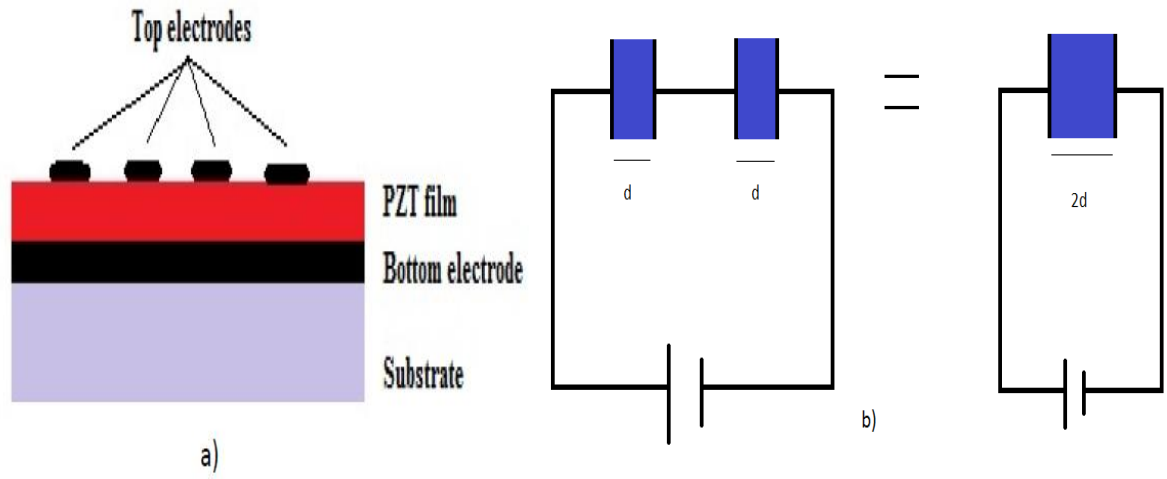

Fig. 23: **a)** PZT capacitors stack structure b):electric scheme of two capacitors in series

The electrical characterization will be performed connecting in series two capacitors and checking the final capacitance and polarization of the system. The total capacitance will be equal to that one of a capacitor with a double dielectric thickness, considering that the area of all the electrodes is the same. A scheme of the final system that has been tested is reported in fig. 23b

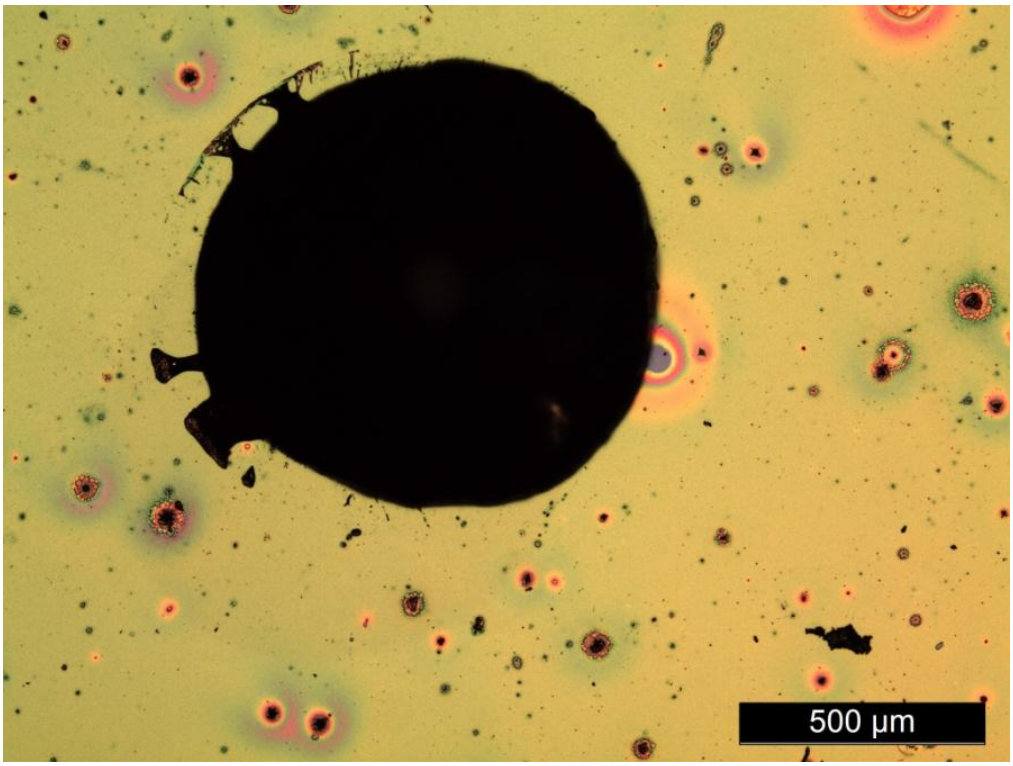

Fig. 24: electrode deposited ont PNZT film

CHAPTER VI

6 RESULTS AND DISCUSSION

The final PNZT and PZT ceramics films morphology, crystal structure, composition and electrical features have been analyzed and discussed after thermal treatment for all the different concentration of Nb added in the solution. The film morphology has been checked using optical microscope and scanning electron microscope (SEM) and the detection of the crystallographic phase of the films, has been performed using grazing incident X-ray diffraction to increase the signal from the films and eliminate the substrate interference. The final film morphology and crystal structure display great differences depending on the annealing time chosen, on the thickness of the film, on the concentration of Nb, this factor obviously impacts on the electrical characteristics of the final device. For all the different doped solution used, it has been possible to deposit uniform and dense films that showed a fully crystallization into a perovskite phase. However the increase of the concentration of Niobium can lead to a film crack. It will be discussed that increasing the doping it is necessary to increase the annealing temperature in order to obtain a full perovskite phase without pyrochlore phase. Higher temperature reduces the probability to have a crack free film and as a consequence the probability to have good electrical device. The annealing times has been optimized for the different samples, to obtain a fully crystallization of the films and to reduce all the problems that arise when long annealing time are chosen. The electrical features of the films which possess good morphology, uniformity and a proper XRD pattern have been checked through measuring the C-V curves and extrapolating the dielectric constant and the coercitive field values. As will be discussed, all the C-V curves derived from the films have a butterfly-like shape and this fact confirms that the deposited films have a ferroelectric behavior. In fact, the non linearity between the applied field and the capacitance of the dielectric is a proof of the presence of remanent polarization and coercitive field of the ferroelectric film. Due to large differences in crystallization behavior and films morphology shown by the various types of sample used, this chapter will be divided into four

sections, where the results of every single type of concentration of Nb will be presented and discussed. Finally the electrical characterization of those samples that displays the best qualities will be presented and discussed.

6.1 PZT

Platinum is the most used material as bottom electrode when depositing PZT thin films, thanks to its high stability, low reactivity, high conductivity and lattice constant matching with the PZT crystallographic structure. With this kind of sample we use a propanol based 0,5M precursors solution, without Nb. These films showed very good adhesion on platinum, and the final deposits demonstrated good morphology after thermal treatment. All the deposited films were free either from macro and micro cracks, even when long annealing times were adopted. Thanks to the using of TiO_2 as platinum adhesion layer, it has been possible to reduce the Titanium diffusion towards the PZT film, and this opens helps performing long annealing times during thermal treatment to obtain a complete films crystallization. As it will be demonstrated by XRD analysis, there was no evidence of Ti diffusion towards the PZT film or Ti-Pt and Ti-Pb intermetallic phases formation, even when long annealing times as 30 minutes was performed. Also the cracking problems related to the use of long annealing times and the consequent high Titanium diffusion, has been eliminated using TiO_2 as adhesion layer. Moreover, the platinum layer shows low reaction tendency with the PZT film and it's stable at the temperature used in the annealing steps.

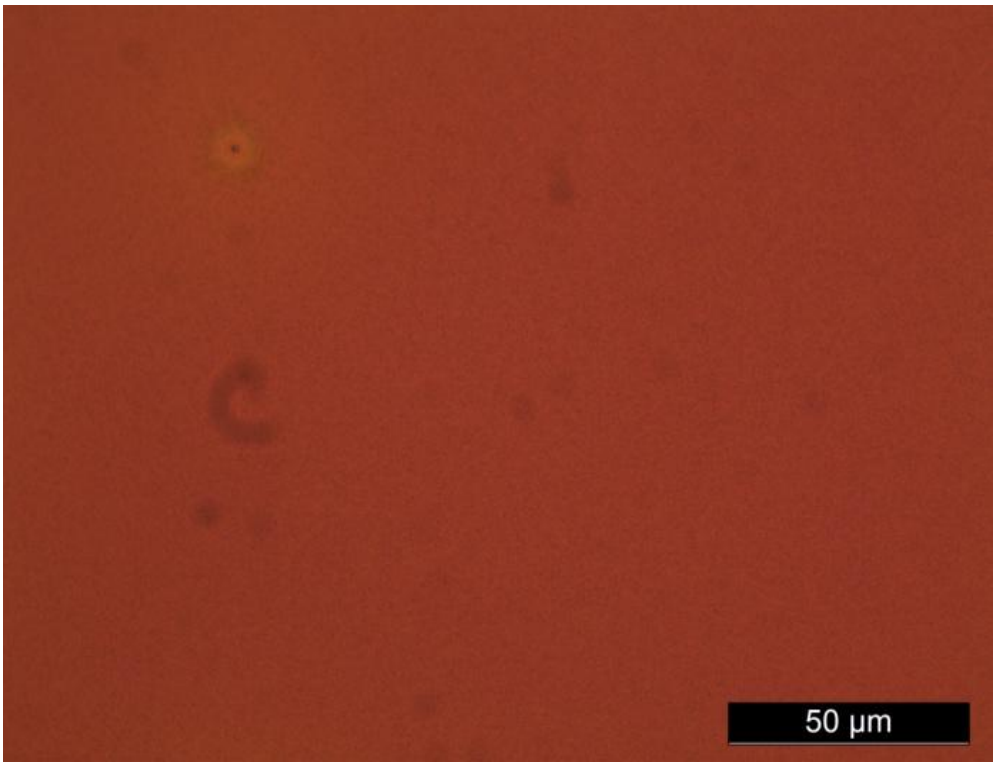

Fig. 25: Optical microscope images of double layer PZT films deposited on Pt/TiO2/Si substrate and annealed for 30 min at 650°C

Fig. 25 shows optical microscope images of PZT double layers films deposited on platinum and annealed for 30 minutes. Both samples show good density and homogeneity and the films are free from cracks and present only few punctual defects. PZT films possess good morphology even when long annealing times as 30 minutes were performed, thanks to the beneficial effects of the reduced diffusion tendency of TiO_2, and the high stability of the Pt bottom layer. Figure 26 shows a SEM image of a PZT single layer deposited on Pt substrate and annealed for 30 minutes. As can be seen there are no evidences of macro or micro-cracking.

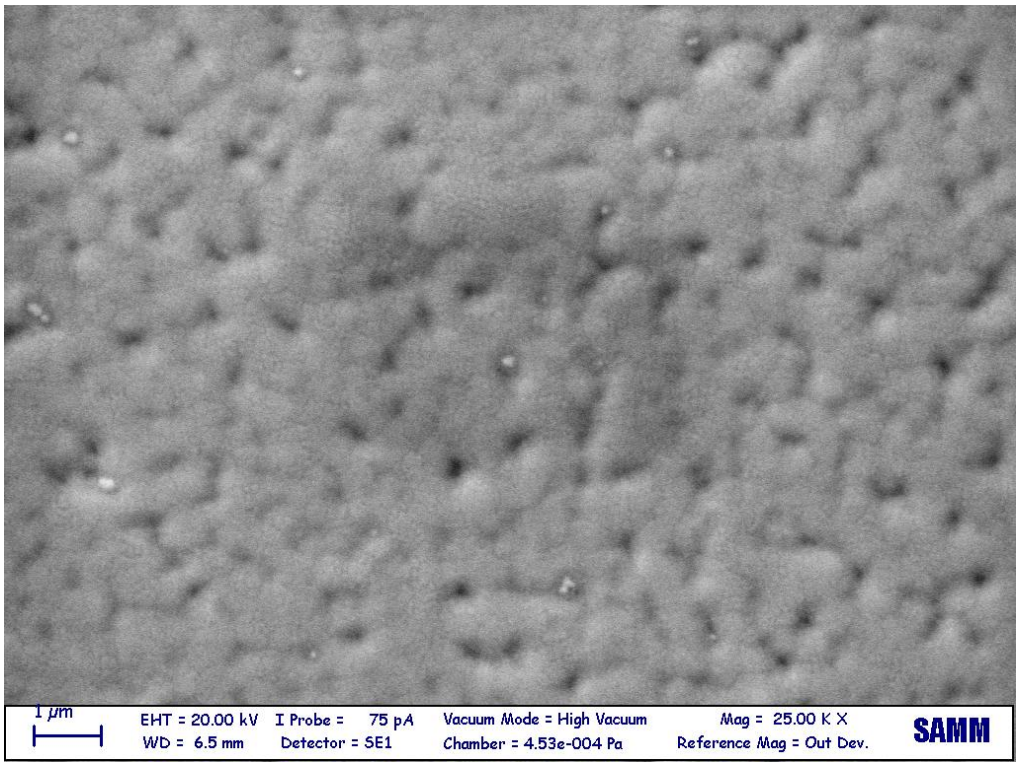

Fig. 26: SEM of PZT single layer deposited on Pt/TiO_2/Si substrate and annealed at 650°C for 30 min

Using the Scanning Electron Microscope it is also possible to verified the thickness of the layer, fig. 27 shows the section of a double layer film and thanks to the image it is possible to calculate the real thickness of the PNZT that is about 500nm, 250nm for each layer.

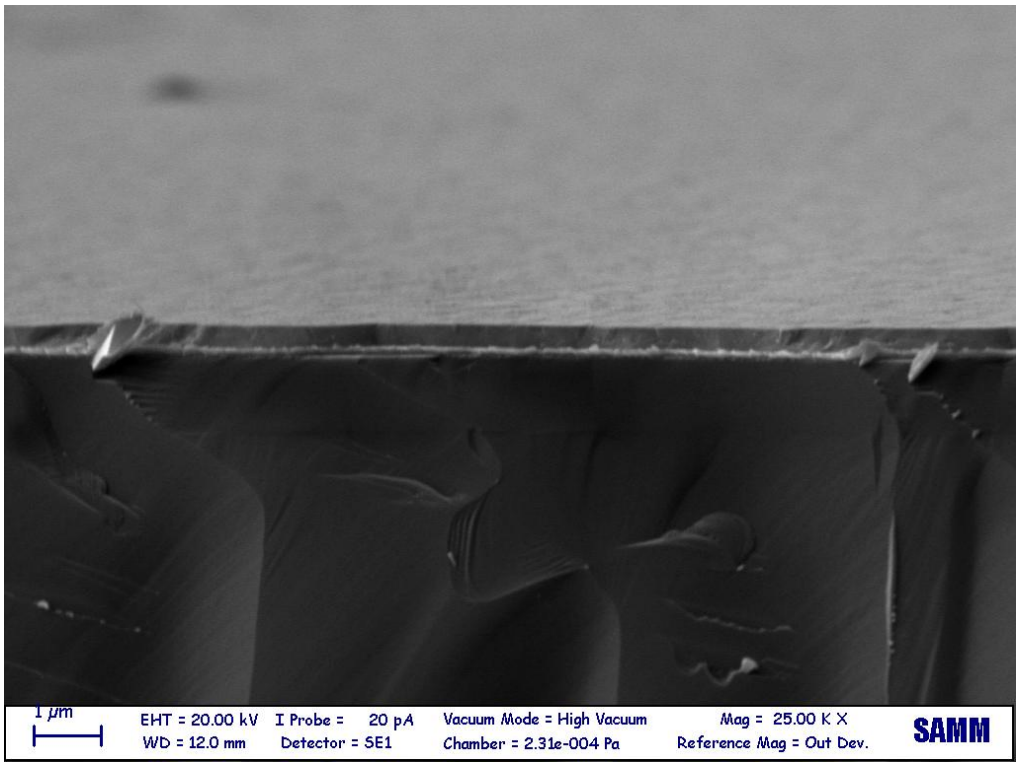

Fig. 27: cross section of a PZT thin film annealed at 650°C for 30minutes

It can be concluded that PZT deposited on $Pt/TiO_2/Si$ substrate matches all the requirements needed to assure good final films morphology. With the solutions used the film appearance and morphology were good, independently from the annealing time chosen. As X-ray diffraction analysis will confirm, the film crystallize into a complete perovskite phase within less than 30 minutes of annealing. Therefore dense, uniform and cracks free PZT thin films can be deposited in this kind of substrate using the required crystallographic structure.

6.1.1 DIFFRACTION ANALYSIS FOR PZT FILMS

The crystallographic structure of all the films deposited on $Pt/TiO_2/Si$ electrode, has been studied using grazing incident X-ray diffraction to increase the thin film signal and to reduce the interference of the substrate. As discussed previously, the annealing time has a great relevance on the final PZT crystallographic structure, and the development of a complete perovskite phase into the film depend strongly on the annealing time and temperature. The latter has been set at 650°C for all the samples and the annealing time has been changed from 5 to 30 minutes. PZT films solutions have been deposited on $Pt/TiO_2/Si$ substrates and annealed for different times to check their crystallization behavior. As discussed in the previous paragraph, using TiO_2 as Pt

adhesion layer strongly reduces the Ti diffusion towards the surface and leaves the platinum electrode chemically unchanged after thermal treatment. Consequently, all the problems related to high Ti diffusion can be avoided and long annealing times can be performed on PZT films deposited on this kind of substrate. Fig 28, 29 and 30 illustrate the XRD results of PZT films derived from propanol based precursors solution and annealed for different times, from 5 to 30 minutes.

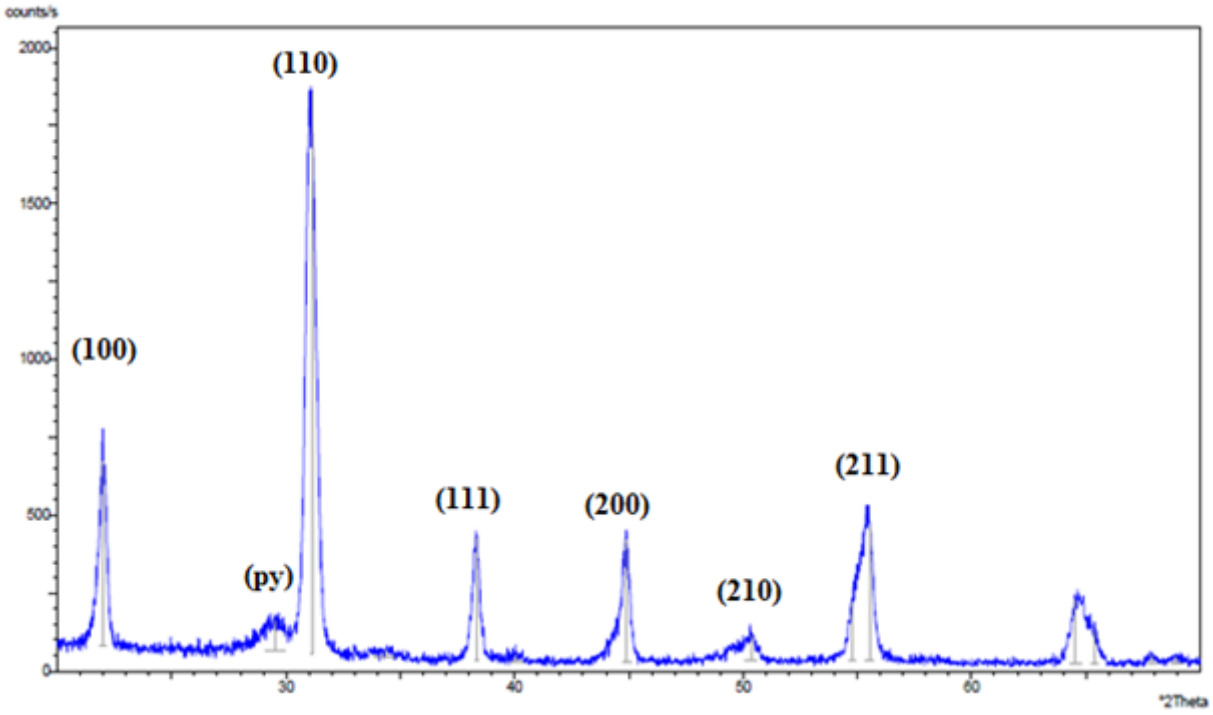

Fig. 28: XRD of PZT films deposited on Pt/TiO2/Si substrate annealed at 650°C for 5 min

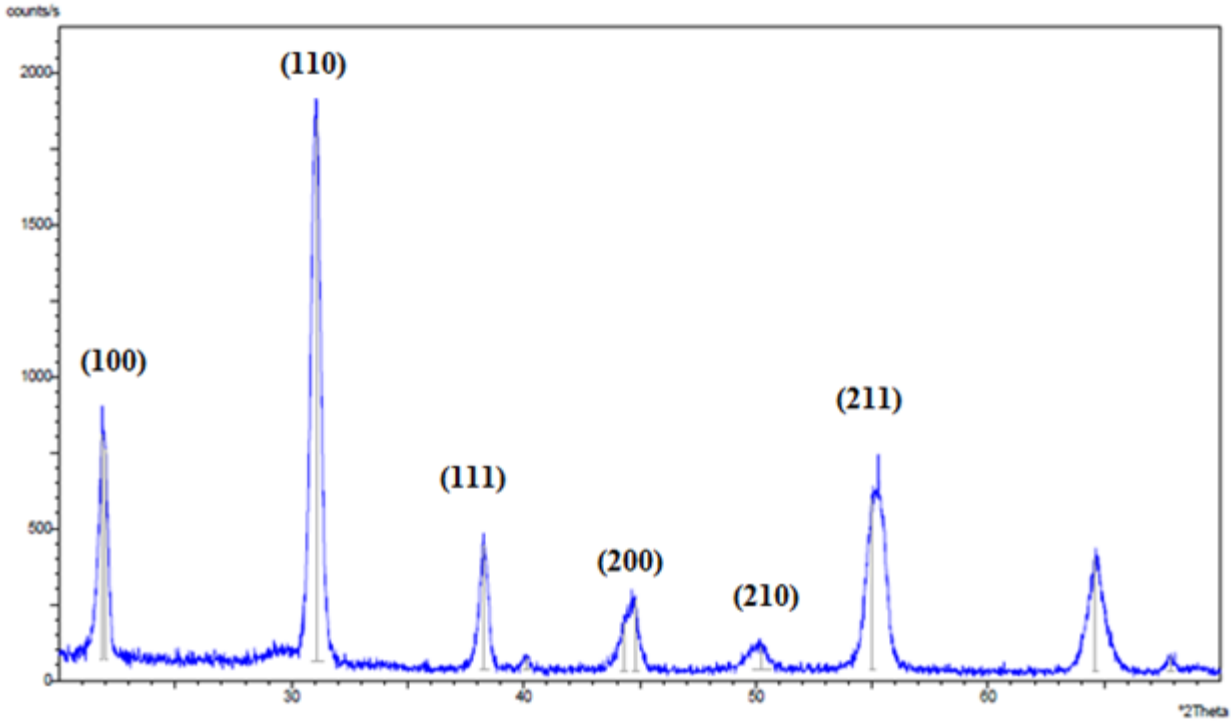

Fig. 29: XRD of PZT films deposited on Pt/TiO2/Si substrate annealed at 650°C for 10 min

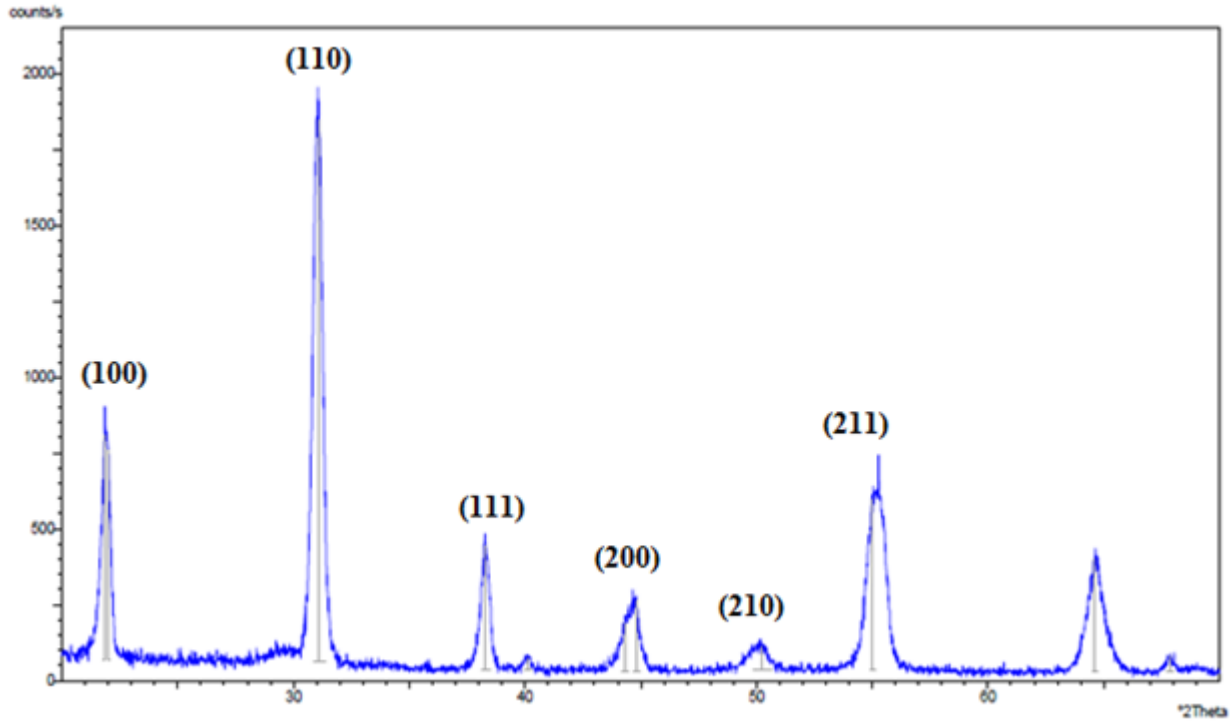

Fig. 30: XRD of PZT films deposited on Pt/TiO2/Si substrate annealed at 650°C for 30 min

It can be seen how, after only 5 minutes annealing the PZT film crystallizes almost completely into a perovskite phase and display a low peak of the pyrochlore at 2θ =29.6°, fig.28 and marked

by the symbol (py). Increasing the annealing time, and maintaining always the annealing temperature at 650°C , the intensity of the pyrochlore peak decreases, until it completely disappears when 30 minutes annealing has been reached, fig.28. The films crystallized with a strong (110) preferential orientation, 2θ =31.1°. The growth of the (111) PZT preferential orientation, should be also promoted by the presence of the (111) oriented platinum bottom electrode, which should favor the kinetics of crystallization promoting the PZT crystals growth along the (111) direction. However its influence is weaker than that one of the Titanium diffusion, and it is the thermodynamics that leads the growing process during crystallization. That is why PZT films oriented toward the (110) plane direction have always been obtained, regardless of the annealing time chosen and of the type of solution used. Usually these films show a polycrystalline structure. The (100) peak is collocated at 2θ =21.9° for PZT films derived from propanol based solution and annealed for 5 and 30 minutes. The peak at 2θ =21.9° is associated with the (100) plane of the rhombohedral PZT structure and it defines a lattice constant a = 4.04Å, while the two peaks at 2θ =21.8° and 2θ =22° probably refer to the (100) and (001) planes of the tetragonal PZT phase and they define the two lattice constants a= 4.036Å and c = 4.07Å with tetragonality (c/a) = 1.008. The peak at 2θ =38.3° represents for all the samples the (111) plane, while the low peak at 2θ =40.11° comes from the (111) plane of Pt and is due to substrate signal noise. The peak at 2θ = 44.8° refers to the (200) plane. The other typical PZT peaks at 2θ =50° , 2θ =55° and 2θ = 64.8° are present. To sum up, films derived from 0.5M propanol based solutions crystallize quickly and within only 5 minutes annealing an almost complete perovskite phase can be obtained. The increase of the annealing time leads to a fully transformation into a perovskite phase and to a better definition of the characteristics peaks. These peaks point out the formation of a polycrystalline structure but with a strong (110) preferential orientation in which the tetragonal and rhombohedral PZT phases coexist because of the film stoichiometry, which is close to the PZT morphotropic phase boundary. In summary, PZT films deposited on Pt electrode crystallize with a (110) preferential orientation. PZT films derived from propanol based precursors solution fully crystallize within only 30 minutes annealing at 650°C. The films deposited are always polycrystalline, with a major presence of crystals orientated towards the (110) direction, and the XRD results show, for both the types of samples, a coexistence between the rhombohedral and the tetragonal PZT phases.

6.2 PNZT 1% Nb

The film obtained adding 1%mol of Niobium shows a morphology and a structure close to the one shown by the PZT not doped. However the annealing temperature has to be changed in order to obtain a complete transformation from the pyrochlore phase to the perovskite one. This difference is due to the presence of Niobium in the solution and this effect is more remarkable when the concentration of Niobium increase. The annealing temperature and time used for the PZT was insufficient in this case, therefore it was necessary to bring the temperature from 650°C to 700°C in order to obtain a complete perovskite film. The temperature was raised to 700°C and the sample was annealed for 30minutes. In this condition the film shows the same characteristics of the PZT film. It displays good density and homogeneity and the films are free from cracks and have only few punctual defects, fig. 31.

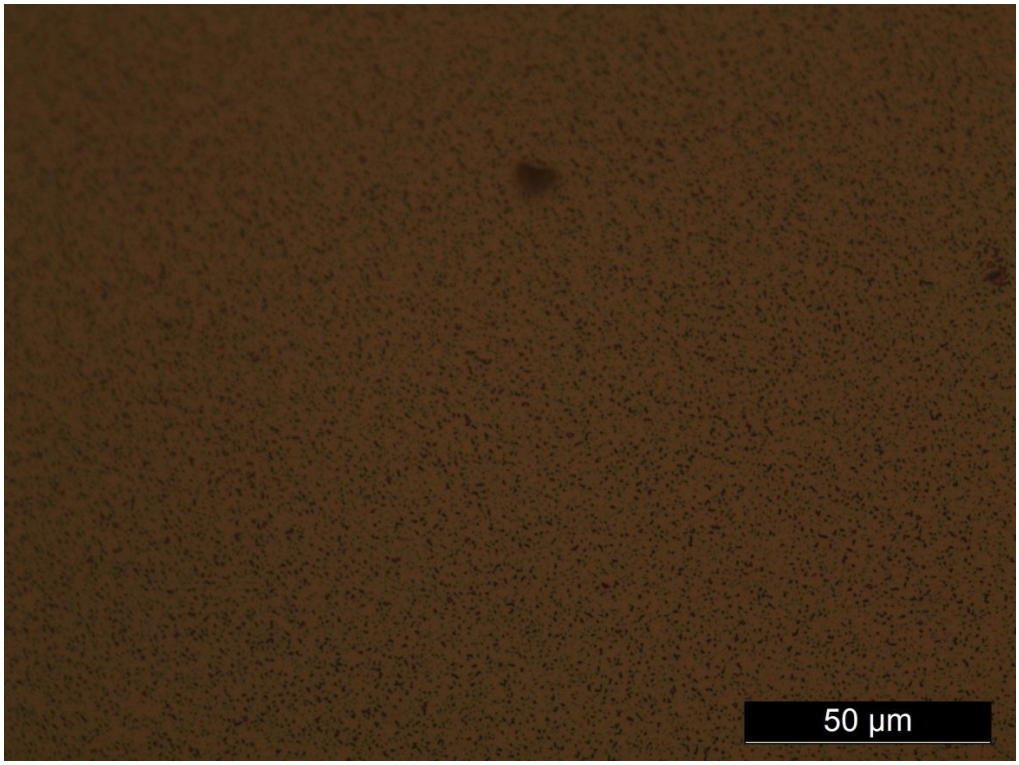

Fig. 31: PNZT 1%Nb double layer annealed at 700°C for 30 minutes.

The good density and homogeneity of the structure were also proved by SEM analysis. Fig.32 shows a scanning electron microscope image of a double layer film of PNZT 1%Nb derived from propanol based precursors solution. The annealing time was set at 30 minutes and both

macro and micro-cracking were avoided, as can be seen. The film shows a good density and an homogeneous grains growth. The film is completely crystallized and, as will be showed by the XRD analysis, the PZT film has a complete perovskite structure with no remaining pyrochlore phase.

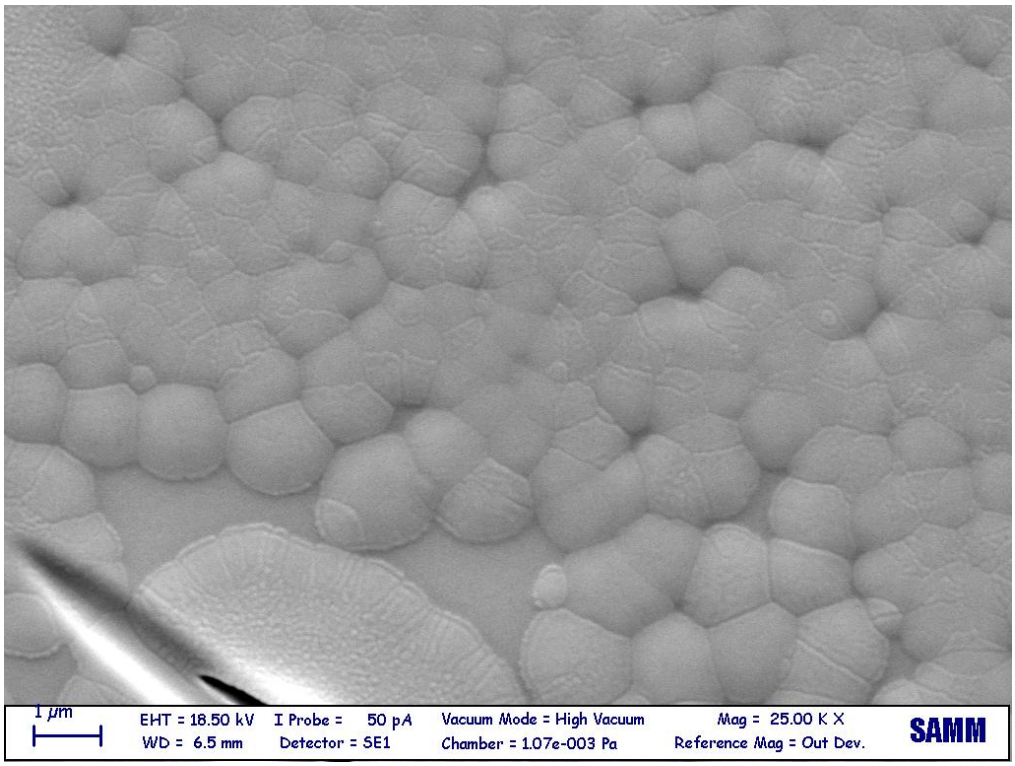

Fig. 32: SEM images of double PNZT1%Nb layer derived from propanol based solution annealed at 700°C for 30min

SEM analysis are also used to measure the thickness of the PNZT film. Fig.33 shows the section of a double layer film and thanks to the image it is possible to calculate the real thickness of the PNZT that is about 500nm, 250nm for each layer.

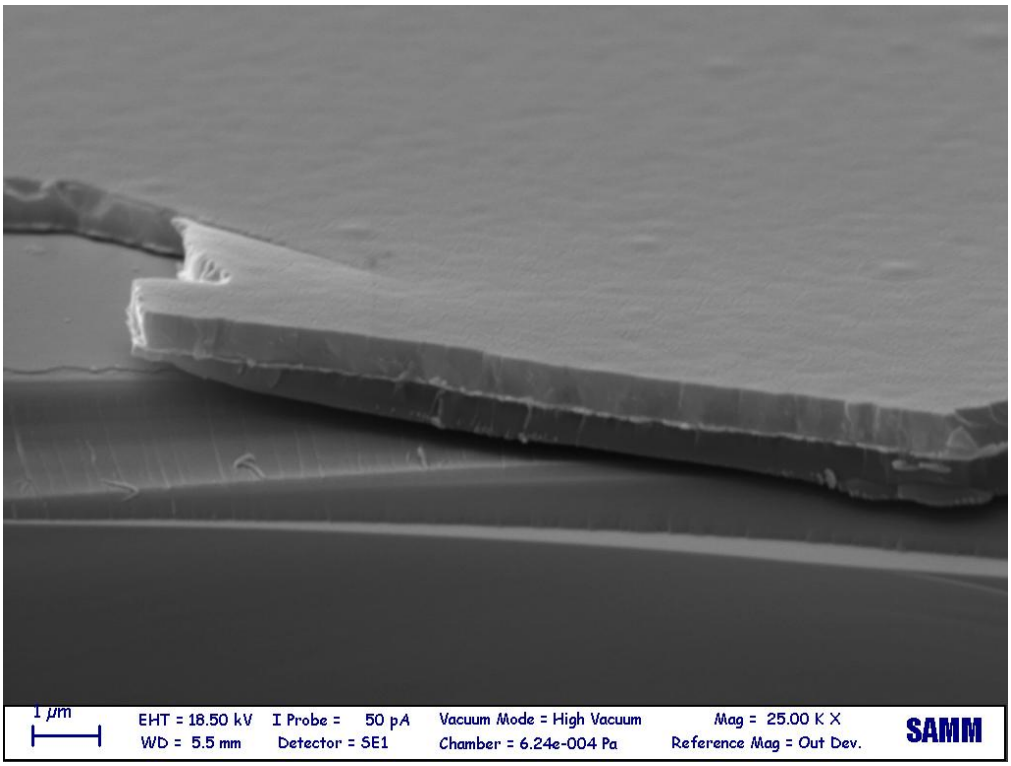

Fig. 33: cross section of single PNZT1%Nb film

In conclusion the PNZT 1%Nb thin films with good morphology, density and free from cracks can be deposited choosing an annealing time of 30 minutes and a temperature of 700°C. The doping effect is related to the time of annealing and doesn't affect too much the structure and the morphology of the sample

6.2.1 DIFFRACTION ANALYSIS FOR PNZT 1%Nb

As discussed in the previous paragraph the annealing time required for the complete transformation from pervskite phase to pyrochlore phase changes as a function of the presence of Niobium. Starting from 650°C different time and temperature of annealing were used to find the best annealing process. Then X-ray diffraction analysis were then used to verify the presence of the pyrchlore phase. Fig. 34, 35, 36 and 37 shows the X-ray diffraction analysis for the sample annealed at 650°C for 5min 10min, 20min and 30min respectively.

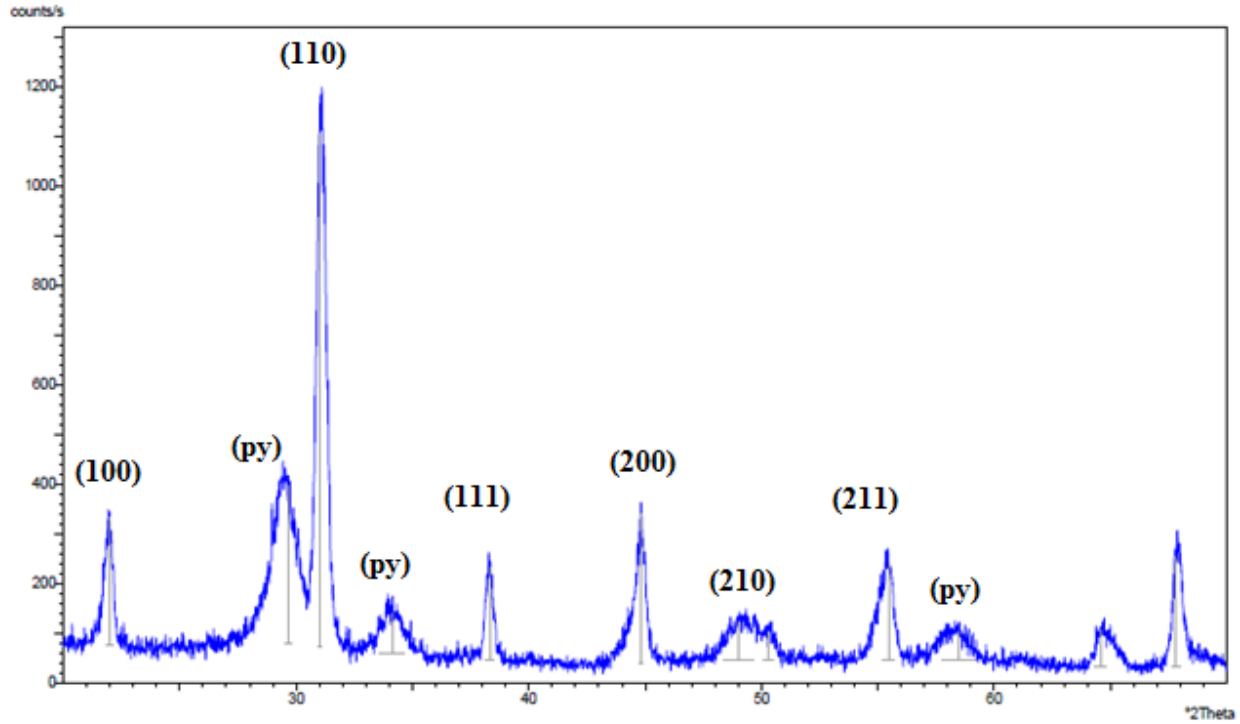

Fig. 34: XRD of PNZT 1%Nb films deposited on Pt/TiO2/Si substrate annealed at 650°C for 5 min

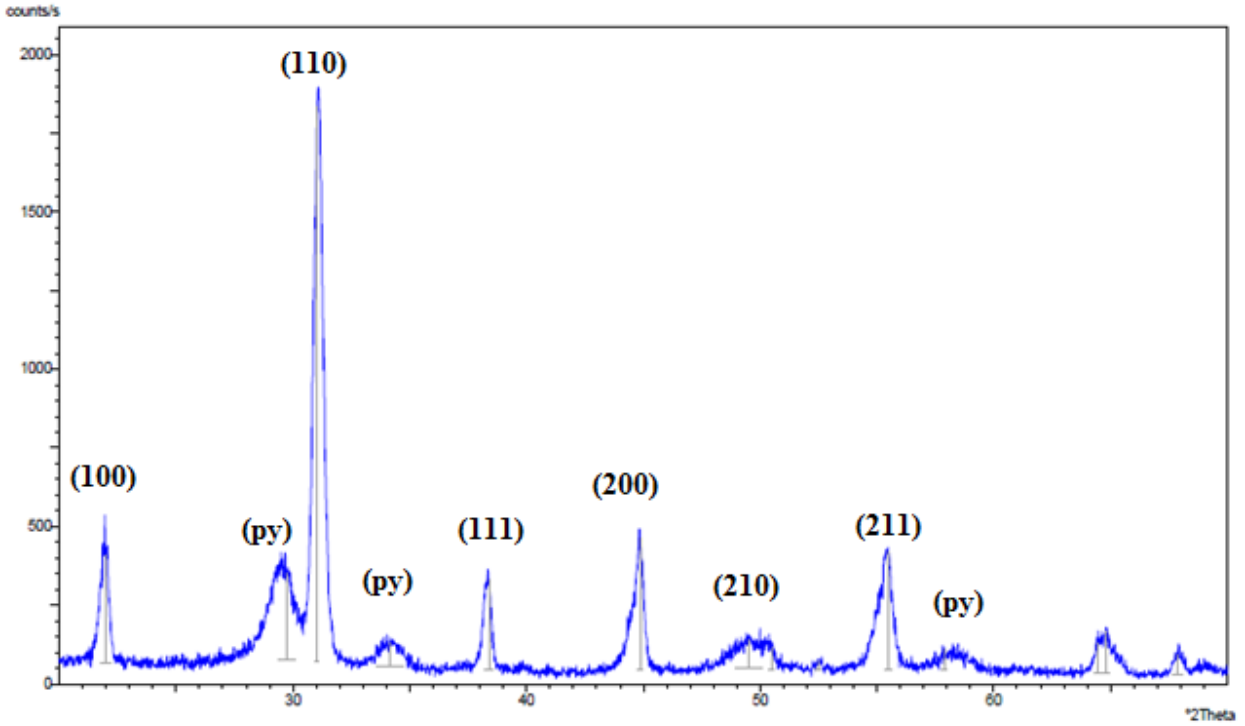

Fig. 35: XRD of PNZT 1%Nb films deposited on Pt/TiO2/Si substrate annealed at 650°C for 10 min

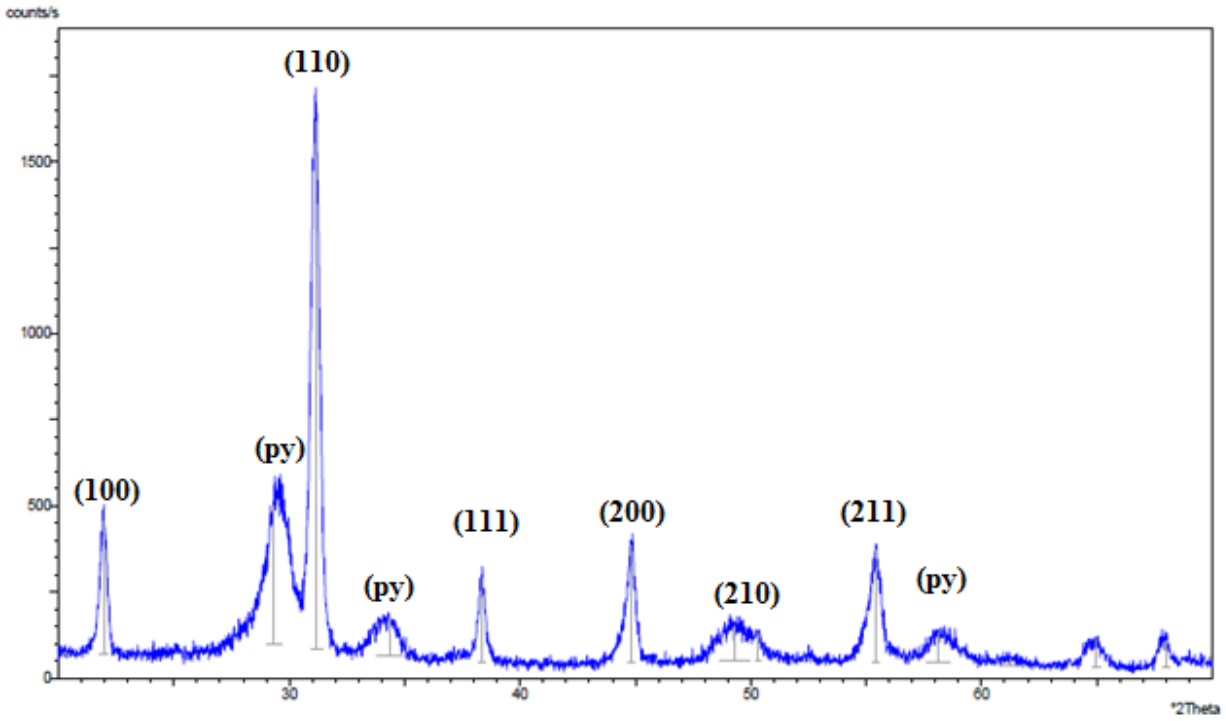

Fig. 36: XRD of PNZT 1%Nb films deposited on Pt/TiO2/Si substrate annealed at 650°C for 20 min

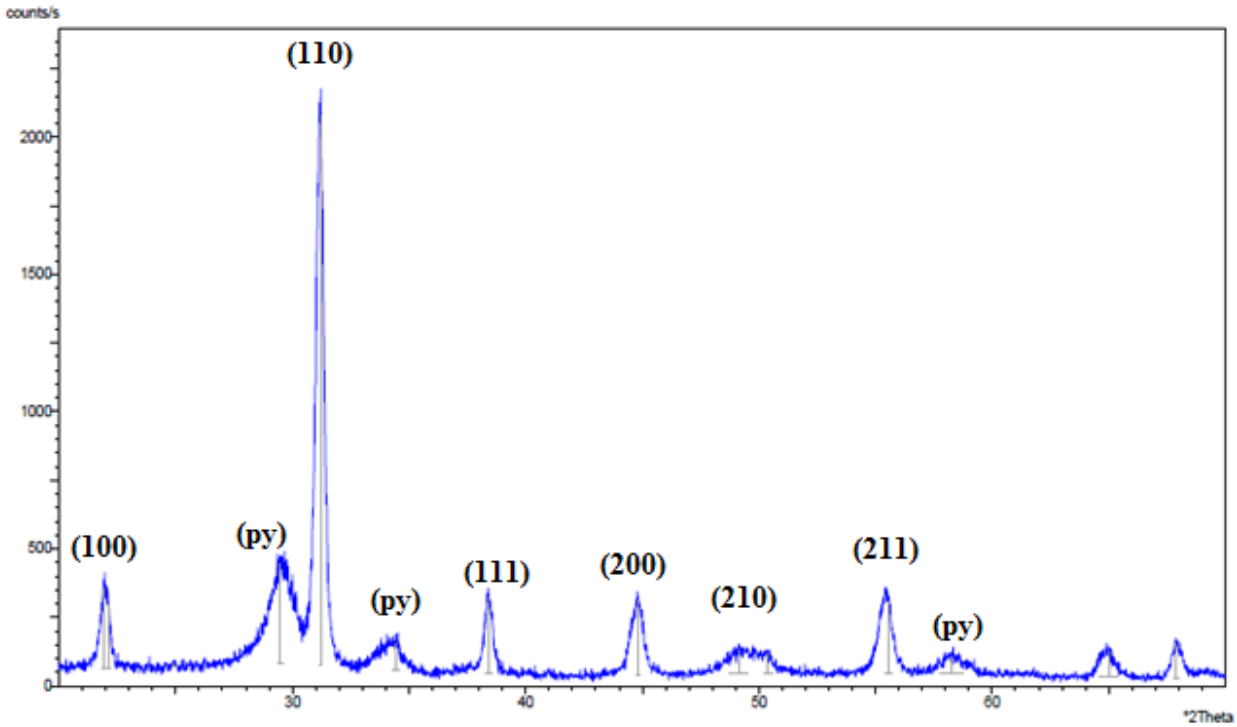

Fig. 37: XRD of PNZT 1%Nb films deposited on Pt/TiO2/Si substrate annealed at 650°C for 30 min

A first important difference between the PNZT 1%Nb and the PZT without Nb is pointed out by the fact that in the previous case the pyrochlore phase at 29.6° decreases when the annealing time is increased while in this case the peak remains almost constant. As a consequence at this temperature for every time of annealing the pyrochlore phase can't be transformed into perovskite phase. Another important difference is that with the doped solution new pyrochlore phases appear in the graph while in the PZT graph they don't. This new pyrochlore phase are pointed out by the peak at 34.5° and at 56.5° and 58.5. This considerable difference is probably related to the presence of Niobium that makes the pyrochlore phase more stable and resistant against the perovskite transformation as well. In order to obtain a complete perovskite phase the temperature was raised to 700°C. Fig. 38, 39, 40 shows the XRD of the PNZT 1%Nb films annealed at 700°C for respectively 10, 20 and 30minutes.

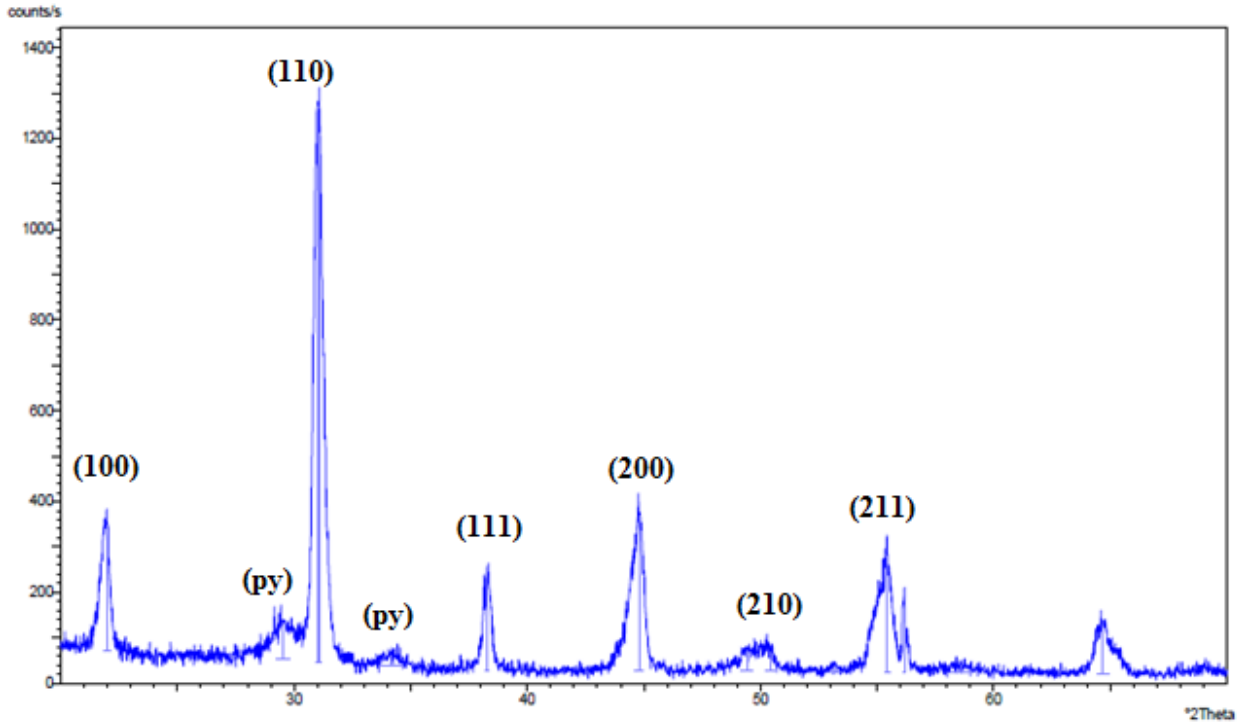

Fig. 38: XRD of PNZT 1%Nb films deposited on Pt/TiO2/Si substrate annealed at 700°C for 10 min

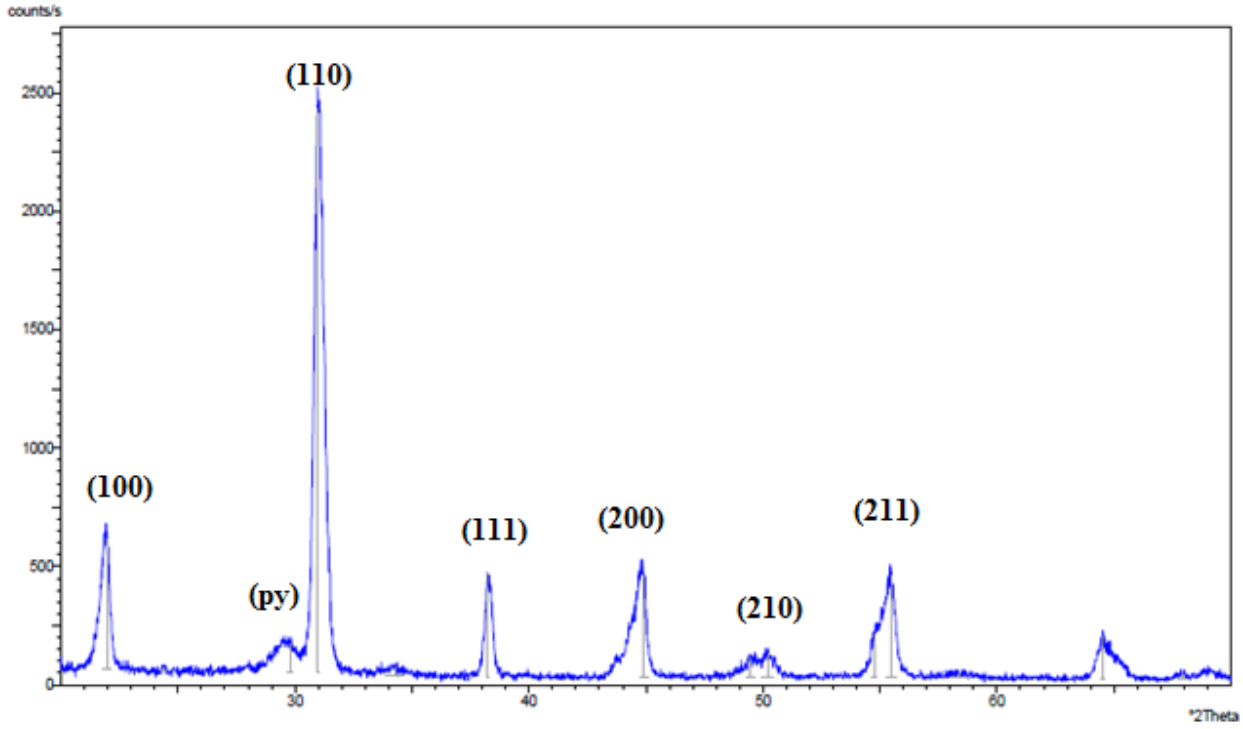

Fig. 39: XRD of PNZT 1%Nb films deposited on Pt/TiO2/Si substrate annealed at 700°C for 20 min

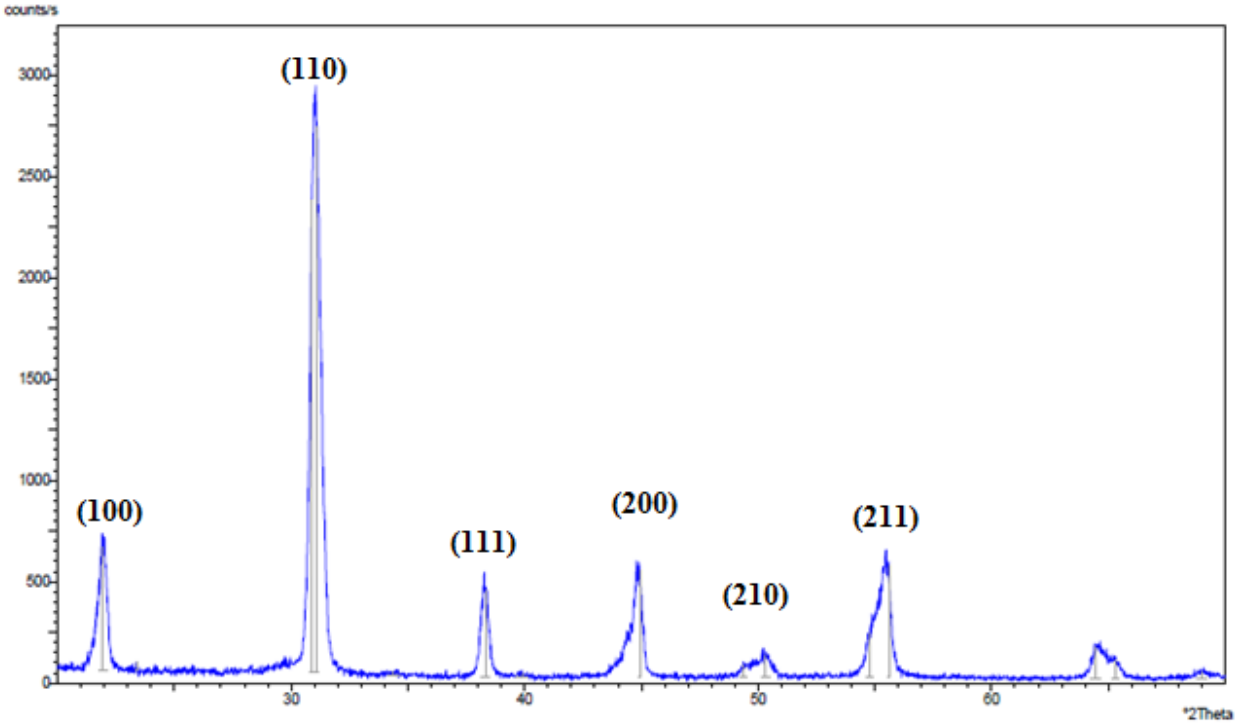

Fig. 40: XRD of PNZT 1%Nb films deposited on Pt/TiO2/Si substrate annealed at 700°C for 30 min

The percentage of the film transformed into a perovskite phase rises through the increase of the annealing time, as showed in fig.40. Within 30 minutes annealing the films fully crystallize into

a perovskite phase and pyrochlore phase disappears. All the films always crystallize with a polycrystalline structure but with a strong (110) preferential orientation independently from the annealing. On the other hand, the percentage of pyrochlore phase into the film decreases when the annealing time is increased, until it disappears when 30 minutes annealing have been reached. This is demonstrated by the vanishing of the peaks that identify the pyrochlore phase at $2\theta = 29.6°$ and $2\theta = 34.4°$. The peak that identifies the (110) plane direction is at $2\theta = 31.1°$, as for PZT film, and the other typical peaks of the PZT perovskite phase at $2\theta = 21.8°$, 38.3°, 44.6°, 55° and 64.8° are still present, indicating a polycrystalline structure. Both for this kind of films and for those ones on PZT electrodes, there is a coexistence between the tetragonal and rhombohedral PZT structures because of the stoichiometry of the PZT precursors solutions, which is close to the morphotropic phase boundary. Within 30 minutes annealing the PZT films fully transform into a perovskite phase with a strong (110) preferential orientation and no remaining pyrochlore phase was detected. These results match with the SEM and optical microscope observations. Also in the case of the double layer films, a polycrystalline structure take shape during crystallization. This structure is a mix between the rhombohedral and tetragonal PZT phase. In conclusion, PNZT 1% Nb films have shown good crystallization behavior and the XRD peaks were always defined properly and the values matched with the literature. Either single and double layers films crystallized completely into a perovskite phase with a strong (110) preferential orientation with 30 minutes annealing and no remaining pyrochlore phase was detected. With shorter annealing time and lower temperature, the films didn’t crystallized completely and a certain amount of pyrochlore phase was always detected and the other peaks worse defined. All deposited films showed good morphology were smooth, and free from cracks and defects. For all these reasons, doping with 1% of Niobium seems to be a suitable procedure to obtain well defined and crystallized PNZT thin films with a strong (110) preferential orientation and with a good morphology.

6.3 PNZT 2% Nb

As anticipated in the last paragraph the increased concentration of Niobium produces important changes in the morphology, in the structure and in the annealing time of the ceramic film. If for the PNZT doped with 1% of Niobium this differences are related only to the annealing time and temperature, for the sample containing 2% and more of Niobium this differences are visible also in the morphology and in the structure of the film. The sample were first annealed at 700°C for 20 minutes, 30 minutes, 40 minutes 50 minutes and 1 hour, but the pyrochlore phase still remained in the structure. The presence of the this metastable phase was detected by optical measure. Fig 41 points out how the incomplete transformation from pyrochlore to pervskite phase can modify the morphology of the sample, as a result we can see different islands related to a different morphology of the PNZT film, these islands are the pyrochlore phase still present in the film after the annealing operation.

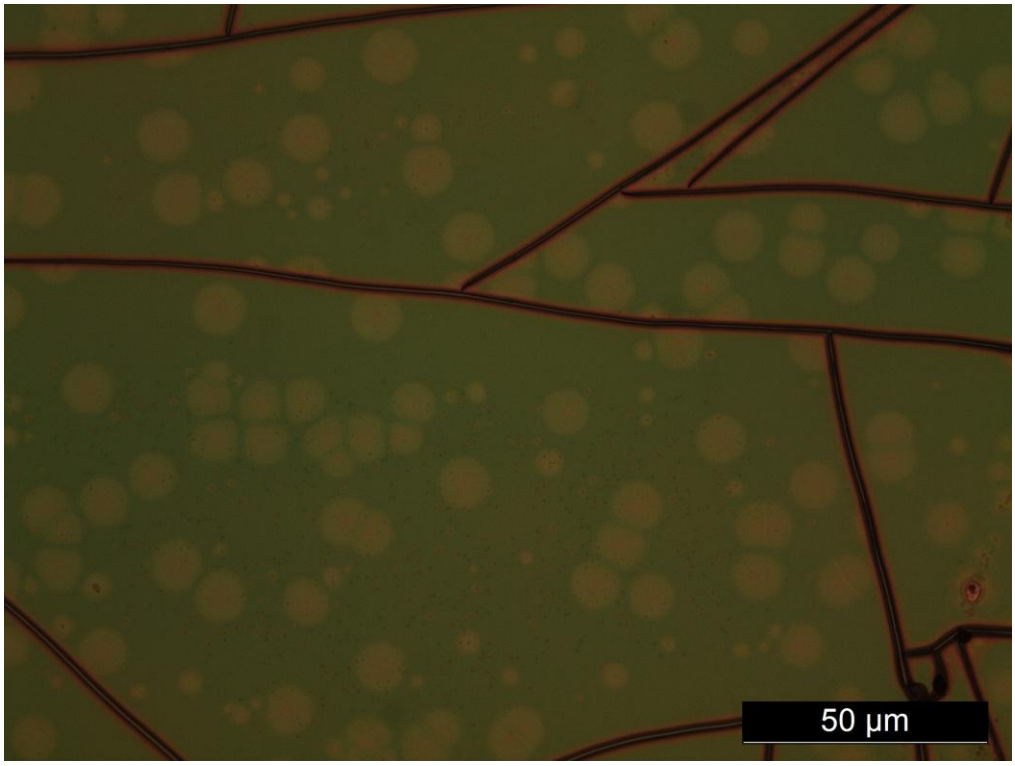

Fig. 41: island of different morphology into PNZT film annealed at 700°C for 30 minutes.

It was necessary raise the temperature from 700°C to 750°C and anneal the sample for 30 minutes. In this condition it is difficult to get a free crack film because of the high temperature reached by the annealing process. In fact every mistake made by either by the operator or the

working conditions can cause damage of the film and the consequently lack of piezoelectric property. Fig 42 shows the cracking of the film probably caused by the presence of dust in the spin coater.

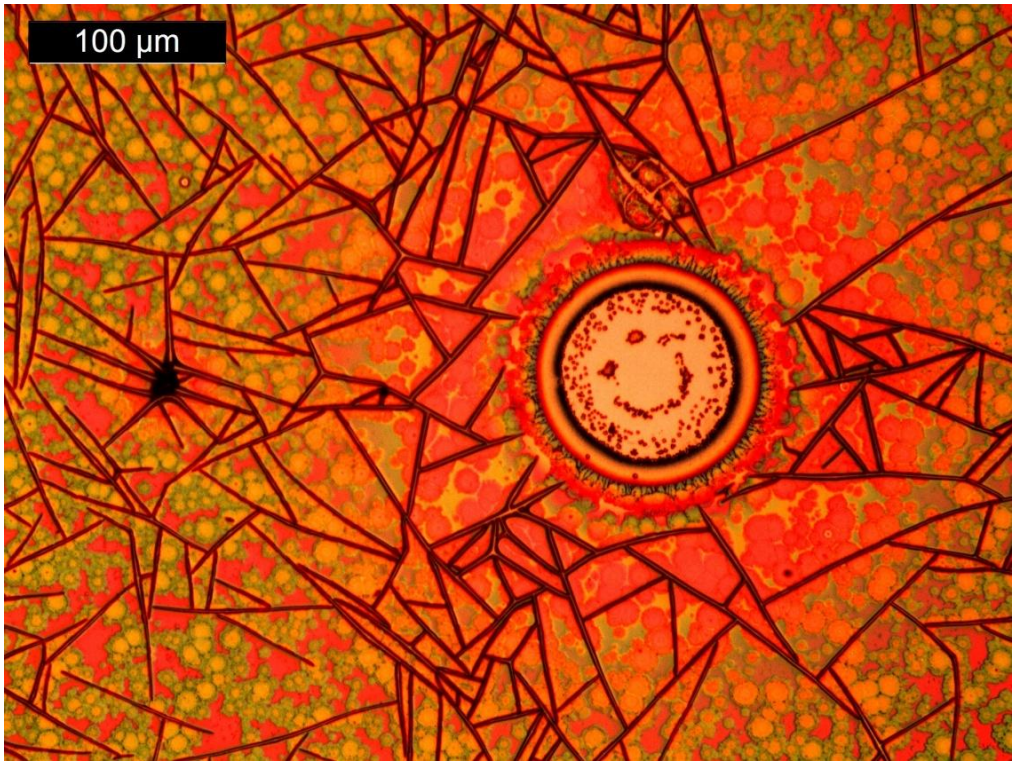

Fig. 42:: crack into PNZT 2%Nb annealed at 750°C for 30min.

With the right procedure it's possible to obtain films that shows good density and homogeneity and films that are free from cracks and have only few punctual defects. Fig 43 displays a double layer film with this very good property.

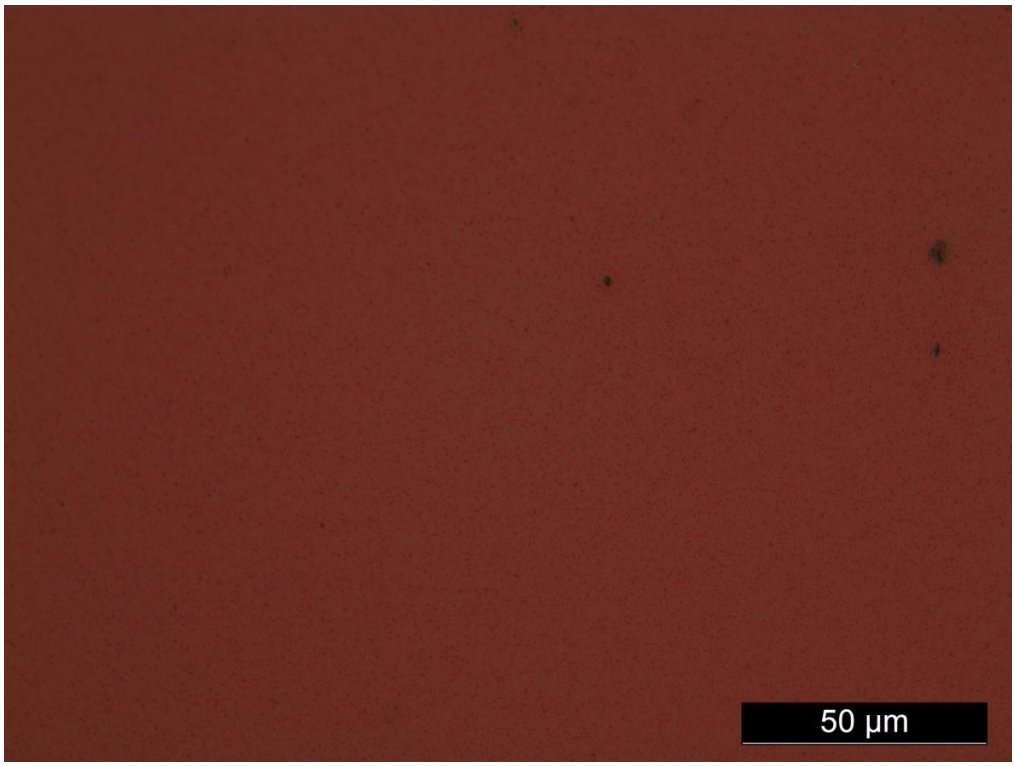

Fig. 43: PNZT 2%Nb double layer annealed at 750°C for 30 minutes.

Good density and homogeneity of the structure were also proved by SEM analysis. Fig.44 shows a scanning electron microscope image of a double layer film of PNZT derived from propanol based precursors solution. The annealing time was set at 30 minutes and both macro and micro-cracking were avoided. The film shows a good density and a homogeneous grains growth. The film is completely crystallized and, as will be showed by the XRD analysis, the PZT film has a complete perovskite structure with no remaining pyrochlore phase.

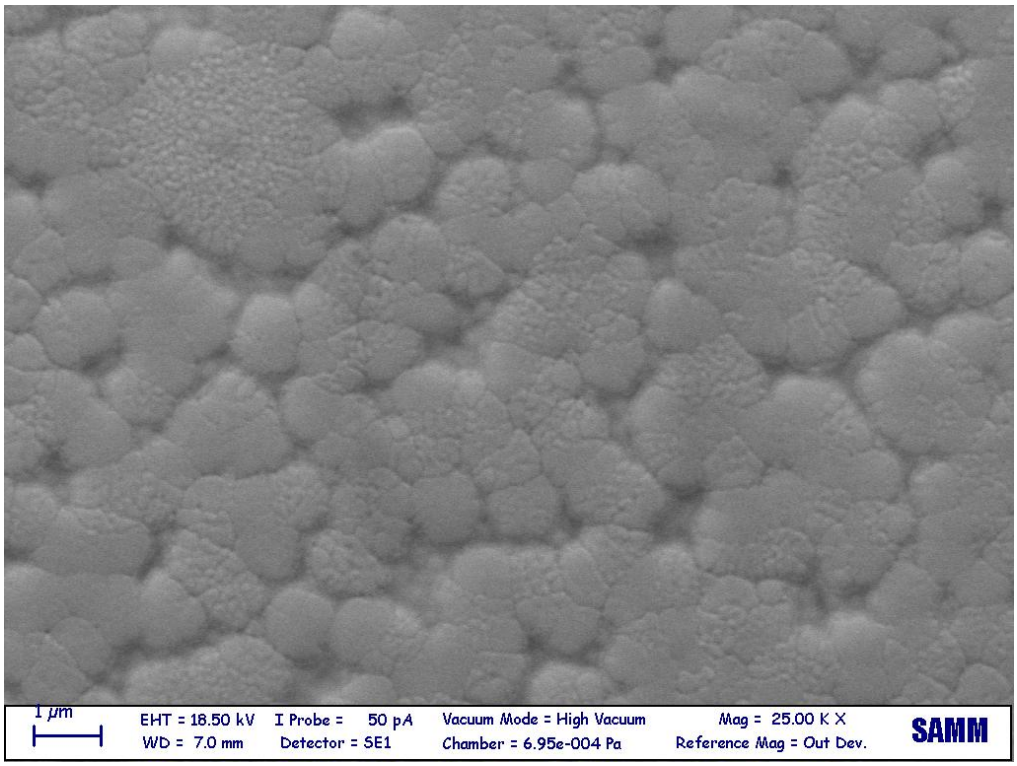

Fig. 44: SEM images of double PNZT2%Nb layer derived from propanol based solution annealed at 750°C for 30 min

With SEM analysis it's also possible to measure the thickness of the sample, also in this case the thickness is about 500nm for a double layers film, that means 250nm for each layer, fig.45

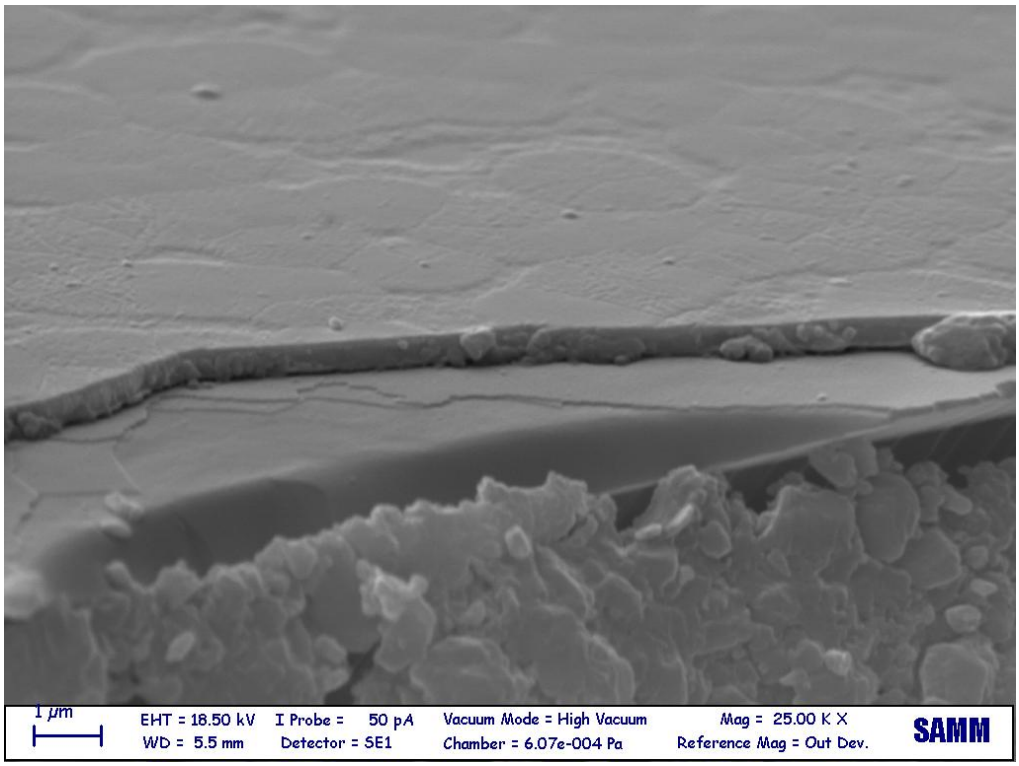

Fig. 45: cross section of single PZT film

In conclusion it can be stated that PNZT 2%Nb thin films with good morphology, dense and crack free can be deposited choosing a 30 minutes annealing time at 750°C. The doping effect is related to the time of annealing and to the probability of cracking the film.

6.3.1 DIFFRACTION ANALYSIS FOR PNZT 2%Nb

XRD analysis confirm that to obtain a complete perovskite ceramic film without pyrochlore phase an annealing temperature of 750°C for 30 minutes is needed. At the beginning we chose to use a temperature of 700°C as in the PNZT 1%Nb and to maintain the sample in the oven from 20 minutes to 1 hour. Also for this long time period the pyrochlore phase doesn't disappear as we can see in fig 45, 47, 48, 49 this graph represent the XRD for sample annealed at 700°C for respectively 20 minutes 40 minutes 50 minutes and 1 hour

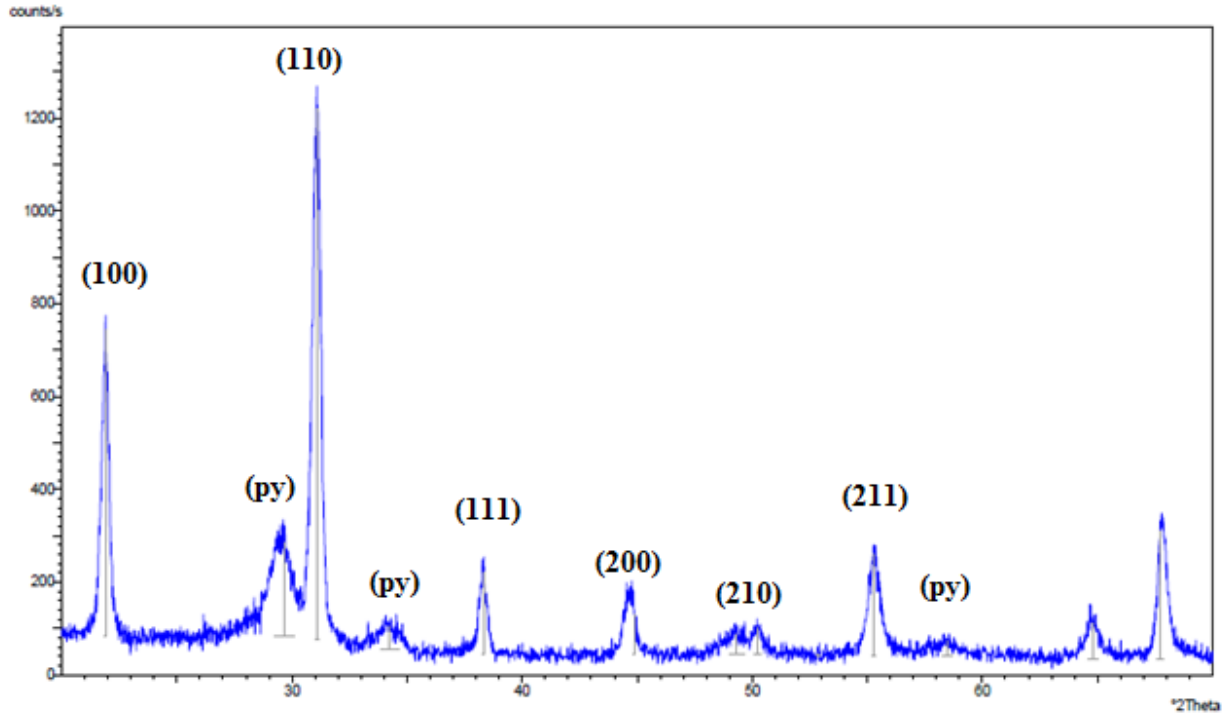

Fig. 46: XRD of PNZT 2%Nb films deposited on Pt/TiO2/Si substrate annealed at 700°C for 20 min

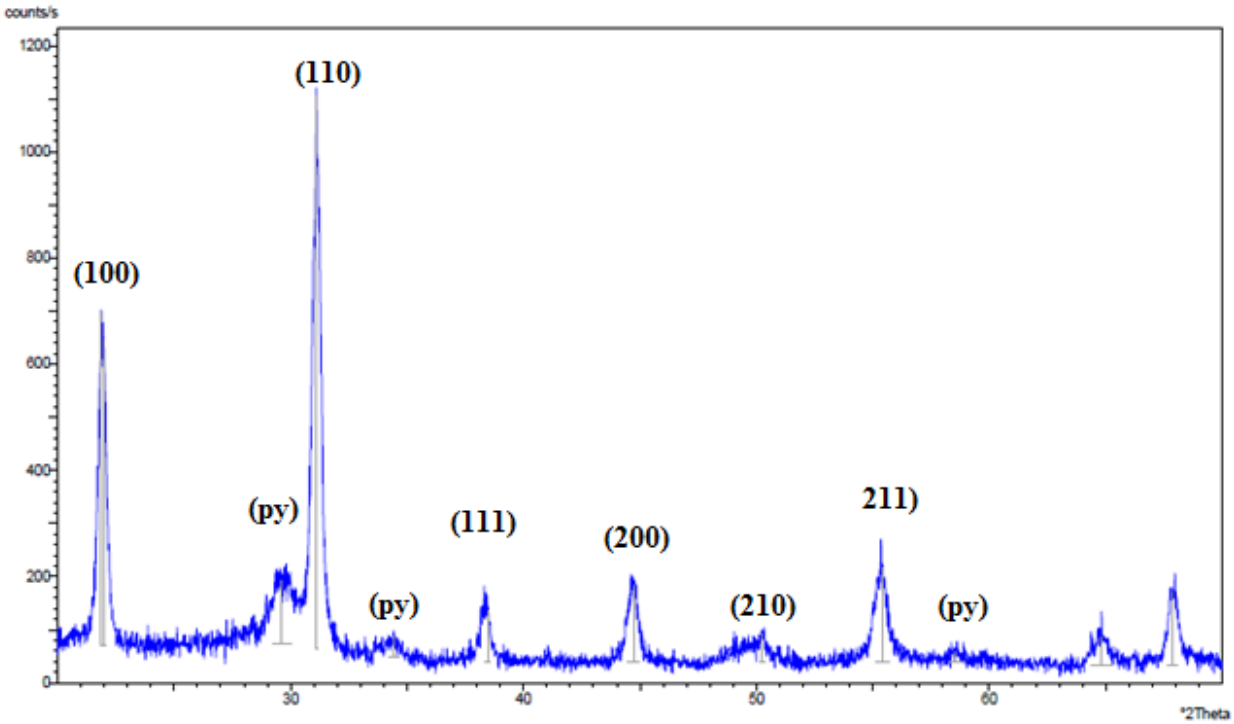

Fig. 47: XRD of PNZT 2%Nb films deposited on Pt/TiO2/Si substrate annealed at 700°C for 40 min

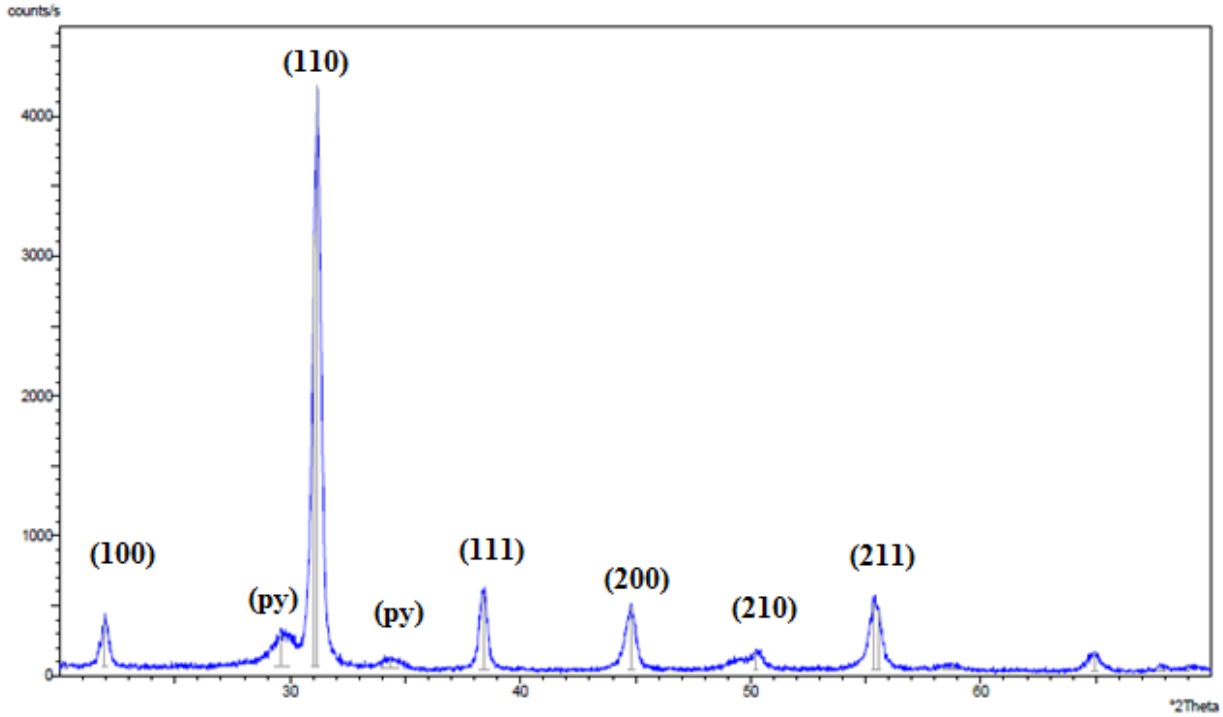

Fig. 48: XRD of PNZT 2%Nb films deposited on Pt/TiO2/Si substrate annealed at 700°C for 50 min

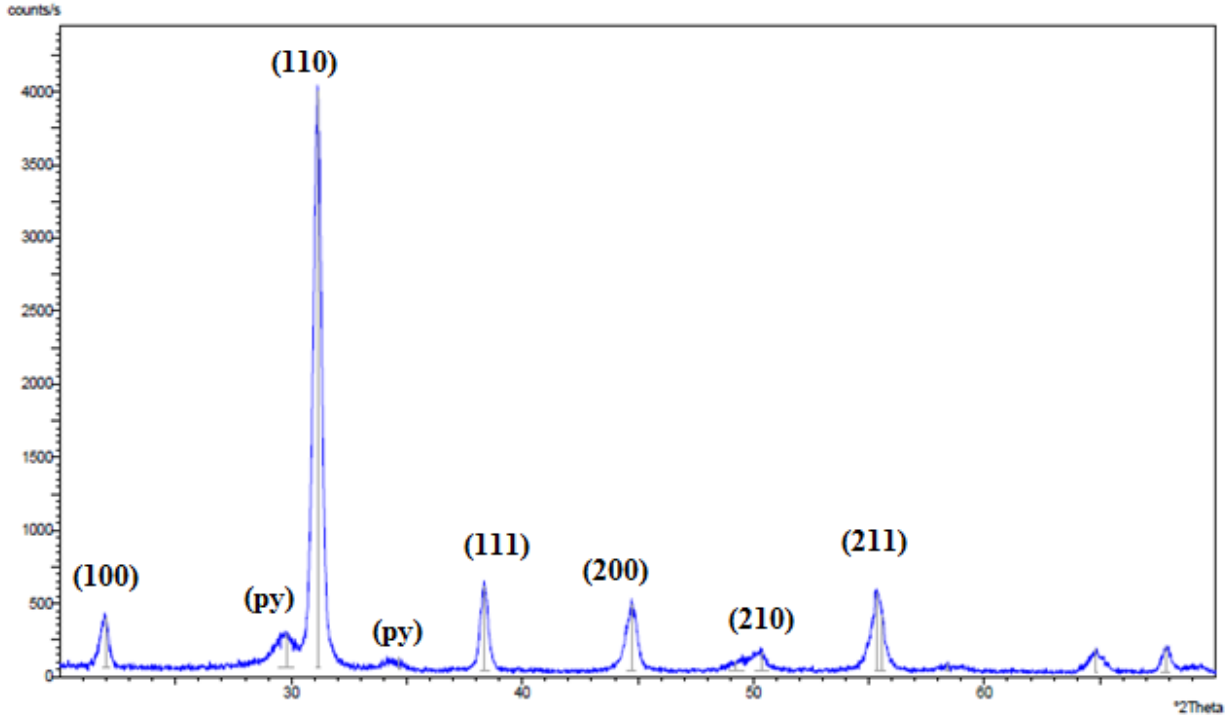

Fig. 49: XRD of PNZT 2%Nb films deposited on Pt/TiO2/Si substrate annealed at 700°C for 1 hour

We can see that the pyrochlore phase is still present in the films and this is confirm by the presence of the peaks at 29.6 at 34.5°and at 58.5°. This fact is a further proof that the Niobium

changes the property of the PZT materials. It is clear that increasing the concentration of Nb it is necessary to raise the temperature of annealing so as to obtain the same structure. We decided to rise up the temperature until 750°C and anneal the sample for 10 minutes 20 minutes and 30 minutes, fig 50, 51, 52.

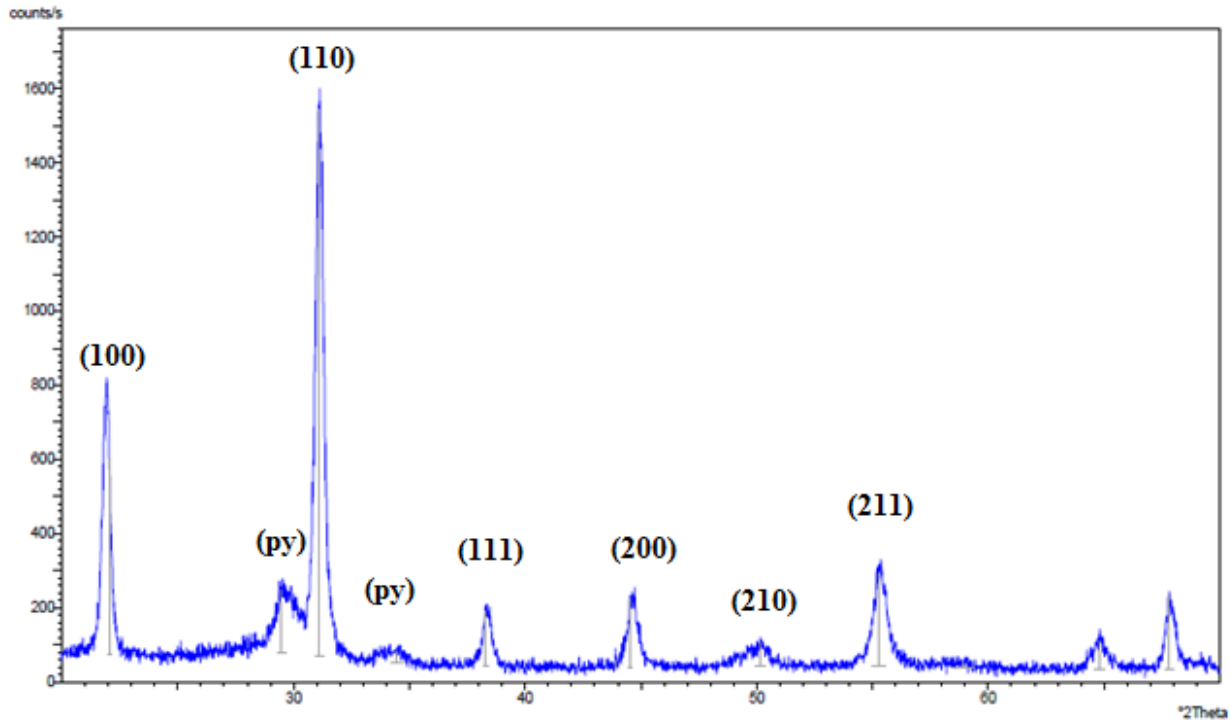

Fig. 50: XRD of PNZT 2%Nb films deposited on Pt/TiO2/Si substrate annealed at 750°C for 10 min

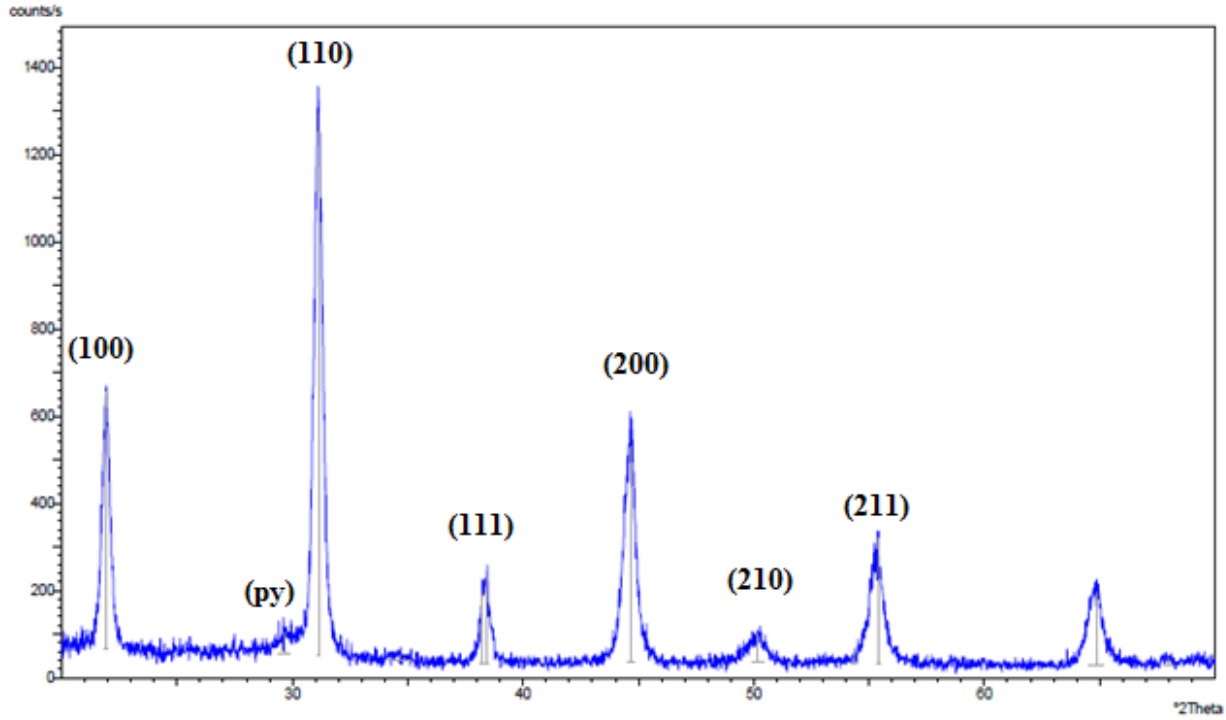

Fig. 51: XRD of PNZT 2%Nb films deposited on Pt/TiO2/Si substrate annealed at 750°C for 20min

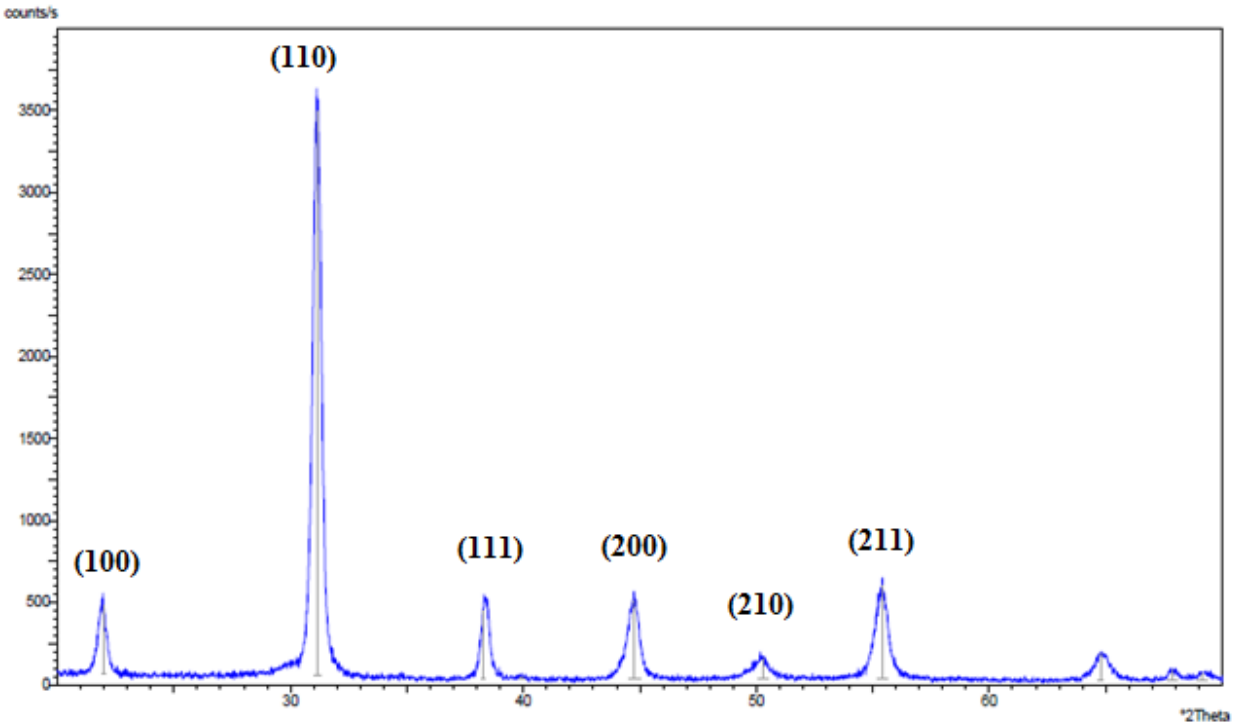

Fig. 52: XRD of PNZT 2%Nb films deposited on Pt/TiO2/Si substrate annealed at 750°C for 30min

Looking at the fig.52 we can find the same peaks obtained from the PZT annealed at 650°C for 30 minutes and from the PNZT 1%Nb annealed at 700°C for 30 minutes (fig.30, 40). In the

previous paragraph it was said that increasing the annealing time the intensity of the pyrochlore peak decreases, until it completely disappears when 30 minutes annealing is reached, fig.51. The films crystallized with a strong (110) preferential orientation, 2θ =31.1°. The growth of the (111) PZT preferential orientation, should be also promoted by the presence of the (111) oriented platinum bottom electrode, which should favor the kinetics of crystallization promoting the PZT crystals growth along the (111) direction. These films always show a polycrystalline structure. The peak at 2θ =21.9° is associated with the (100) plane of the rhombohedral PZT. The peak at 2θ =38.3° represents for all the samples the (111) plane, while the low peak at 2θ =40.11° comes from the (111) plane of Pt and it is the result of the substrate signal noise. The peak at 2θ = 44.8° refers to the (200) plan.. The other typical PZT peaks at 2θ =50° , 2θ =55° and 2θ = 64.8° are present. Increasing the annealing time leads to a full transformation into a perovskite phase and to a better definition of the characteristics peaks. These peaks identify the formation of a polycrystalline structure with a strong (110) preferential orientation in which the tetragonal and rhombohedral PZT phases coexist because of the film stoichiometry, that is close to the PZT morphotropic phase boundary. To sum up, PZT films deposited on Pt electrode crystallize with a (110) preferential orientation. PNZT 2%Nb fully crystallize with only 30 minutes annealing at 750°C. The deposited films are always polycrystalline, with a major presence of crystals orientated towards the (110) direction, and the XRD results show, for both type of samples, a coexistence between the rhombohedral and the tetragonal PZT phases. Also in this case the structure of the film with a good density and homogeneity suggests that PNZT 2%Nb is a good candidate as a piezoelectric material, however it is important to underline that the high temperature reduces the stability of the process and brings to an increase in the probability of failure of the sample, this is more common in the PNZT 3%Nb as we can see later.

6.4 PNZT 3%Nb

The last group of samples analyzed was the one produced using a solution which containing 3% mol of Niobium. Also in this case it was verified that the increase of the amount of Niobium led to important changes in the PNZT film structure and to the annealing temperature. The sample was initially annealed at 700°C for 30 min, 40 min, 50min and 1 hour. The large amount of Niobium in the solution stabilized the pyrochlore phase. If with the PNZT 2%Nb only a few island of this metastable phase was detected using an optical microscope, in the 3%Nb they

seems to be the predominant phase of the film, fig 53. This is a further proof of the effect of the doping element which is able to slow down the transformation into a perovskite phase.

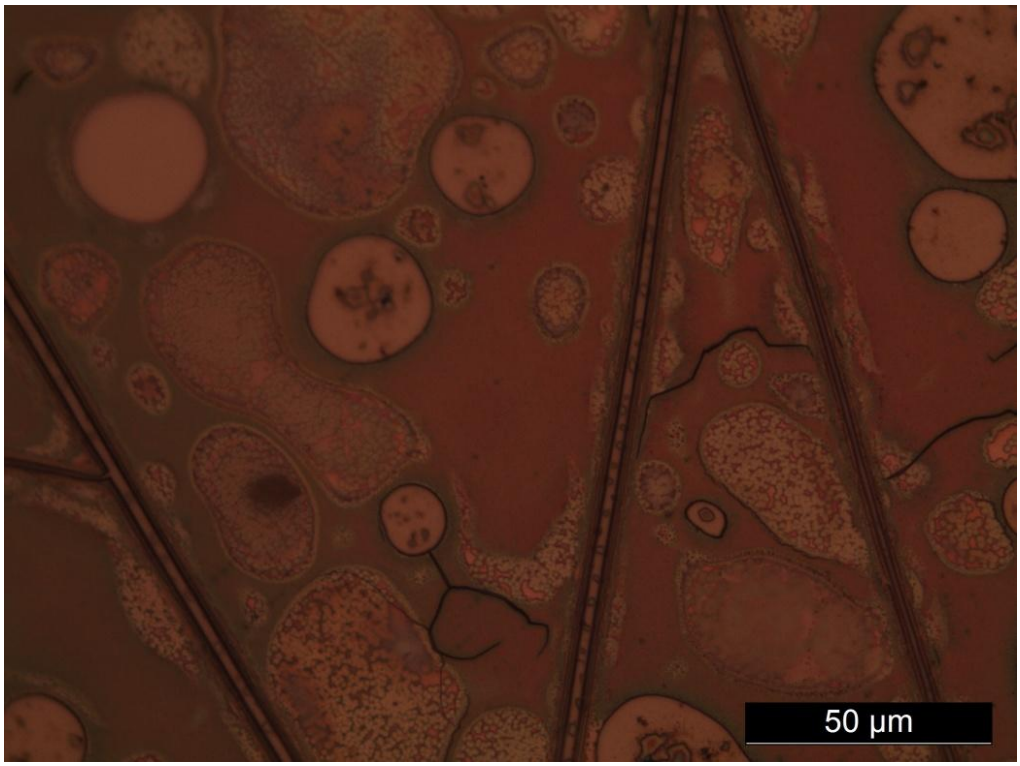

Fig. 53: island of different morphology into PNZT 3%Nb film annealed at 700°C for 30 minutes.

The temperature was raised to 825°C. At this temperature it is very unlikely to obtain a free crack film, fig.53. Working at this temperature is a problem also because it lets the formation of microcracks increase exponentially, fig.55.

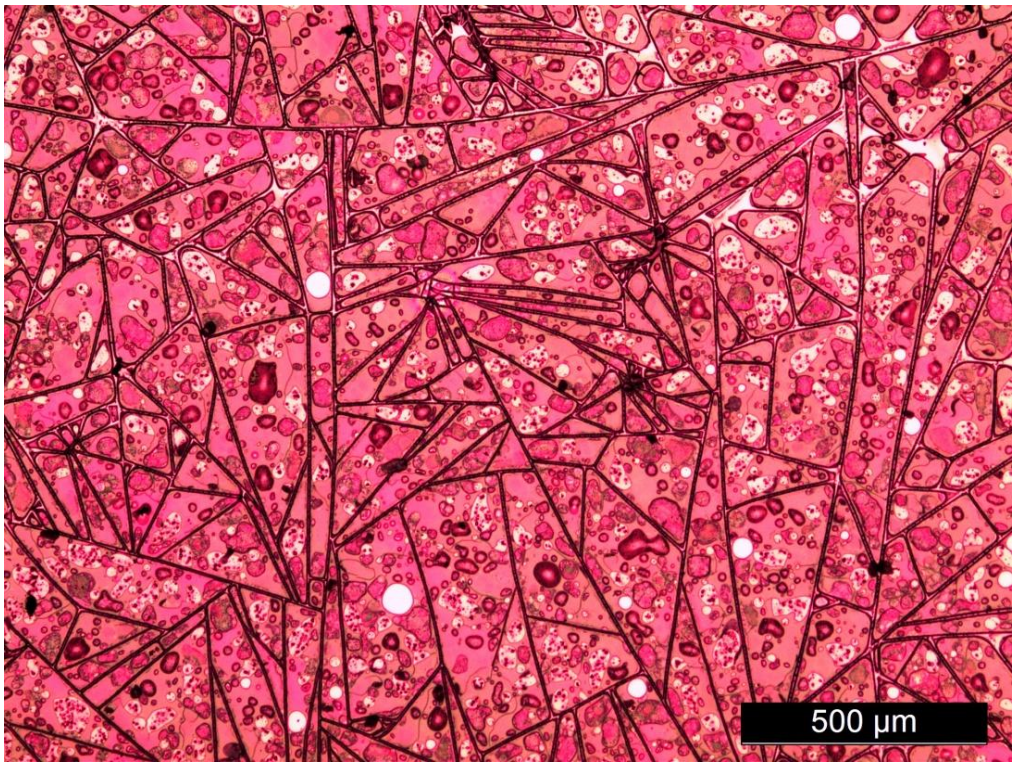

Fig. 54: cracks in a film of PNZT3%Nb

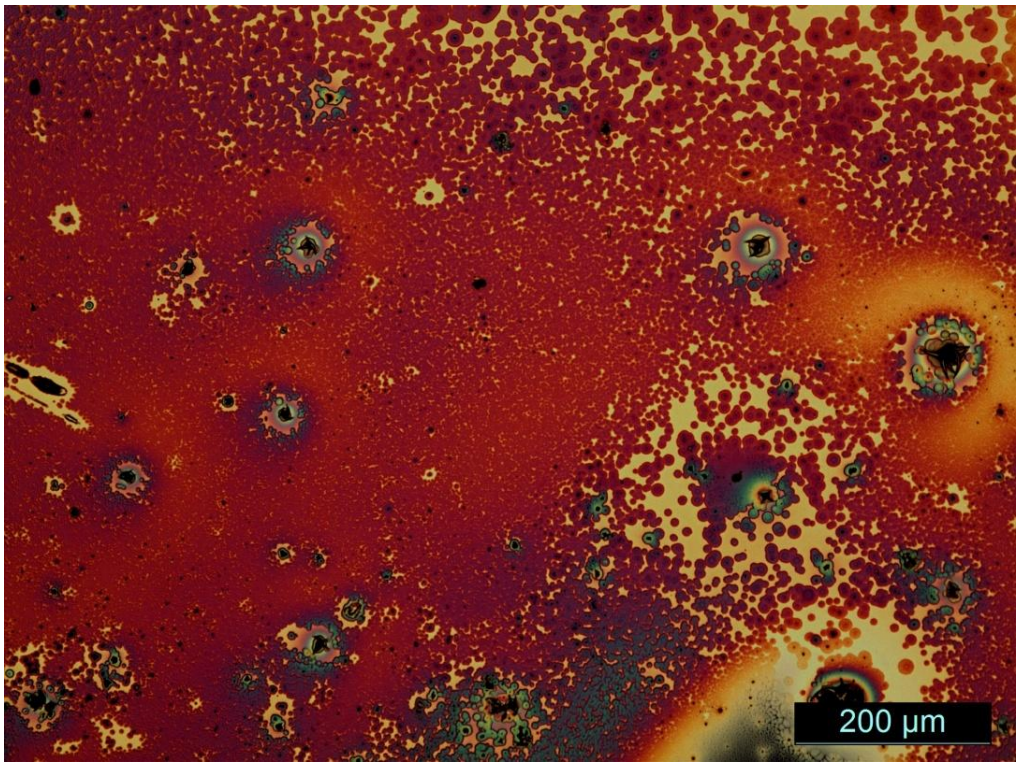

Fig. 55: microcracks in a film of PNZT3%Nb

However when the sample is not cracked it exhibits very good density and homogeneity. This is supported by optical and SEM images, fig. 56, 57.

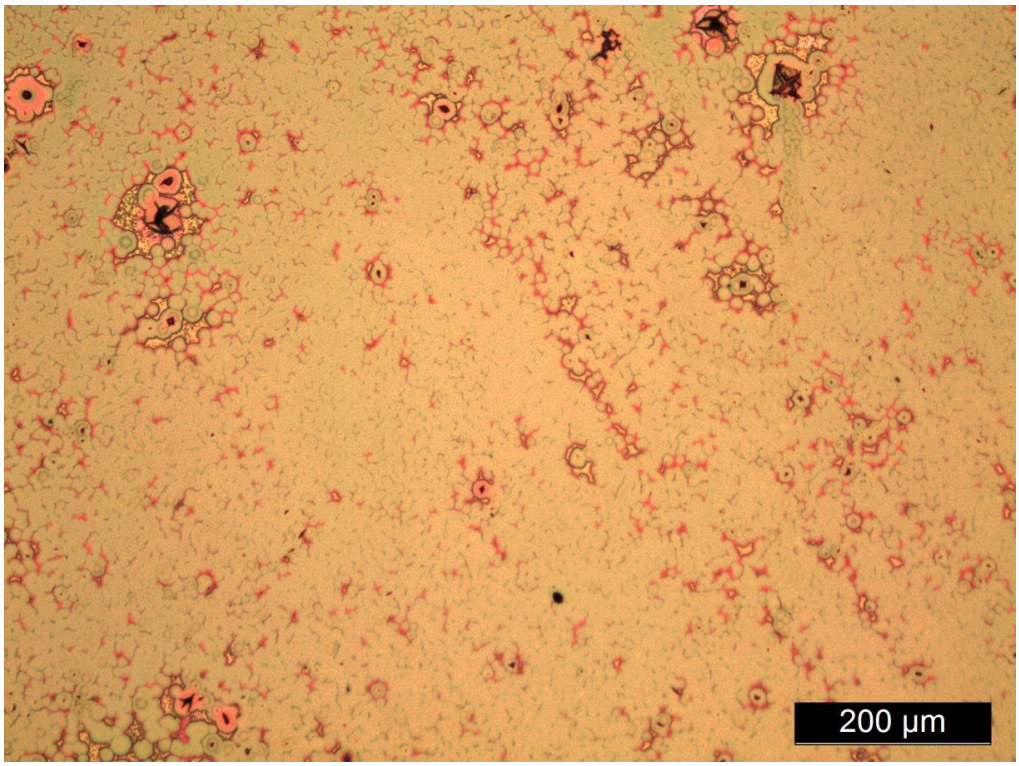

Fig. 56: PNZT 3%Nb double layer annealed at 825°C for 30 minutes

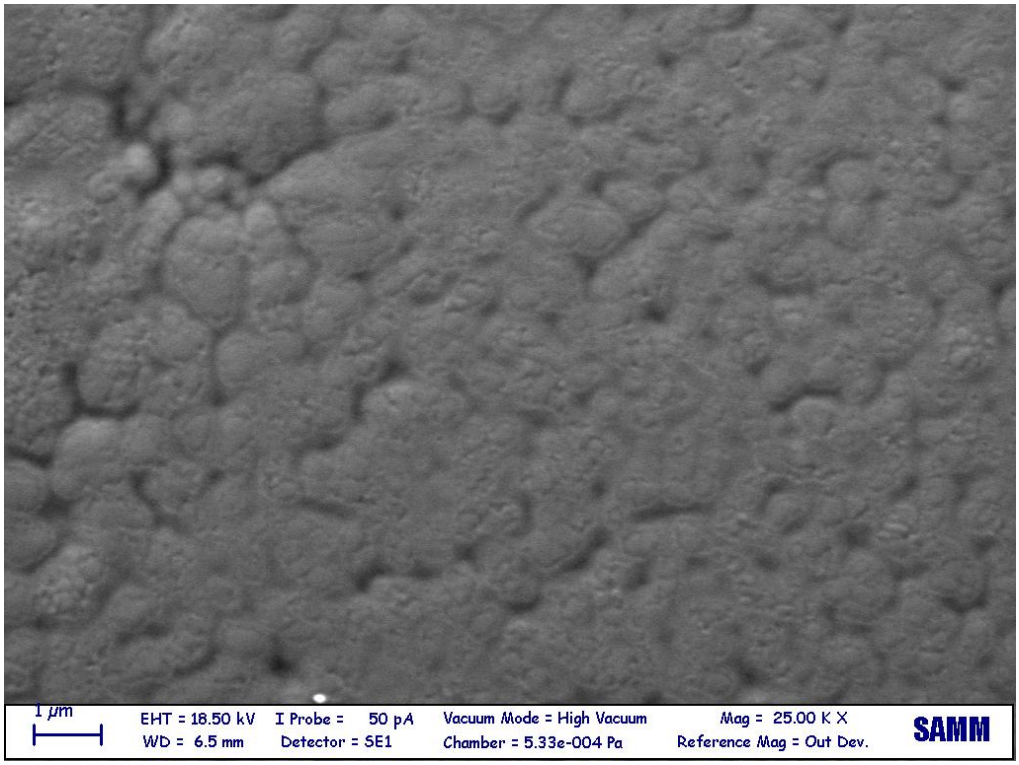

Fig. 57: SEM image of double PNZT3%Nb layer derived from propanol based solution annealed at 825°C for 30 min.

A last observation have to be done about the thickness of the film. Also in this case we measure it using SEM image. We can see a double layer film where each layer display a thickness around 250nm fig.58

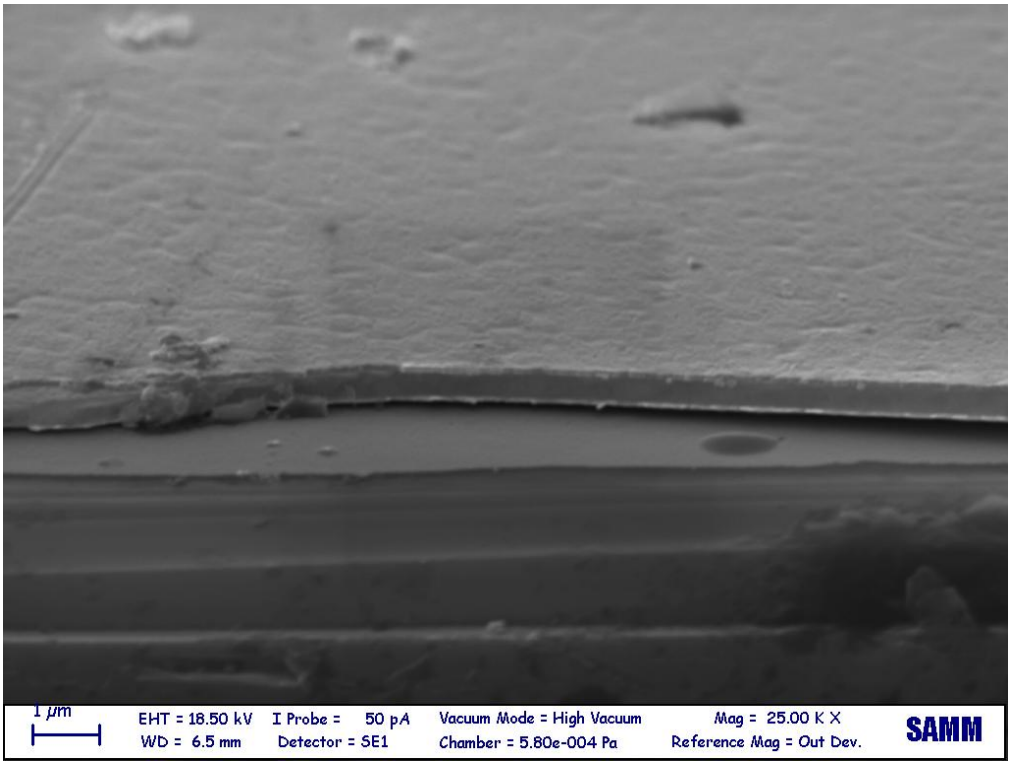

Fig. 58: cross section of single PNZT3%Nb film

6.4.1 DIFFRACTION ANALYSIS FOR PNZT 3%Nb

XRD analysis were made on the sample annealed at 700°C and at 825°C. Analysis confirm that the pyrochlore phase is present until we reach 825°C and an annealing time of 30 minutes. The samples at 700°C are annealed for 30 min, 40 min, 50 min and 1 hour, fig. 59, 60, 61, 62.

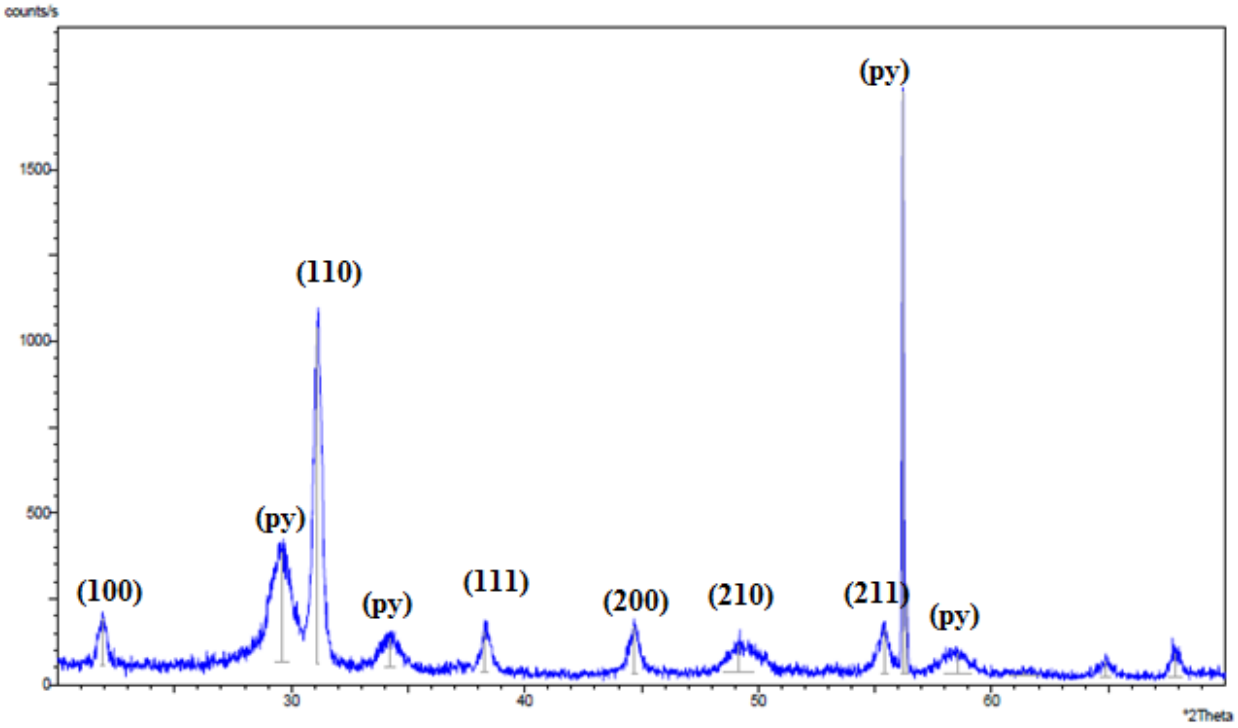

Fig. 59: XRD of PNZT 3%Nb films deposited on Pt/TiO2/Si substrate annealed at 700°C for 30min

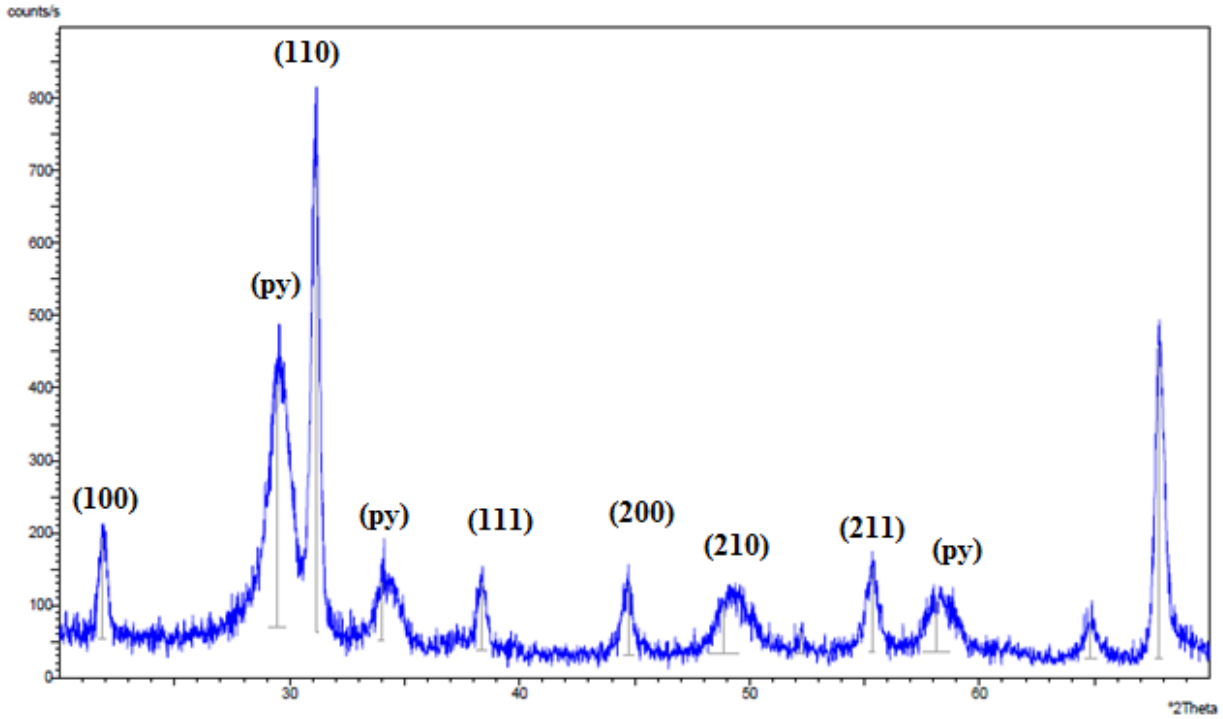

Fig. 60: XRD of PNZT 3%Nb films deposited on Pt/TiO2/Si substrate annealed at 700°C for 40min

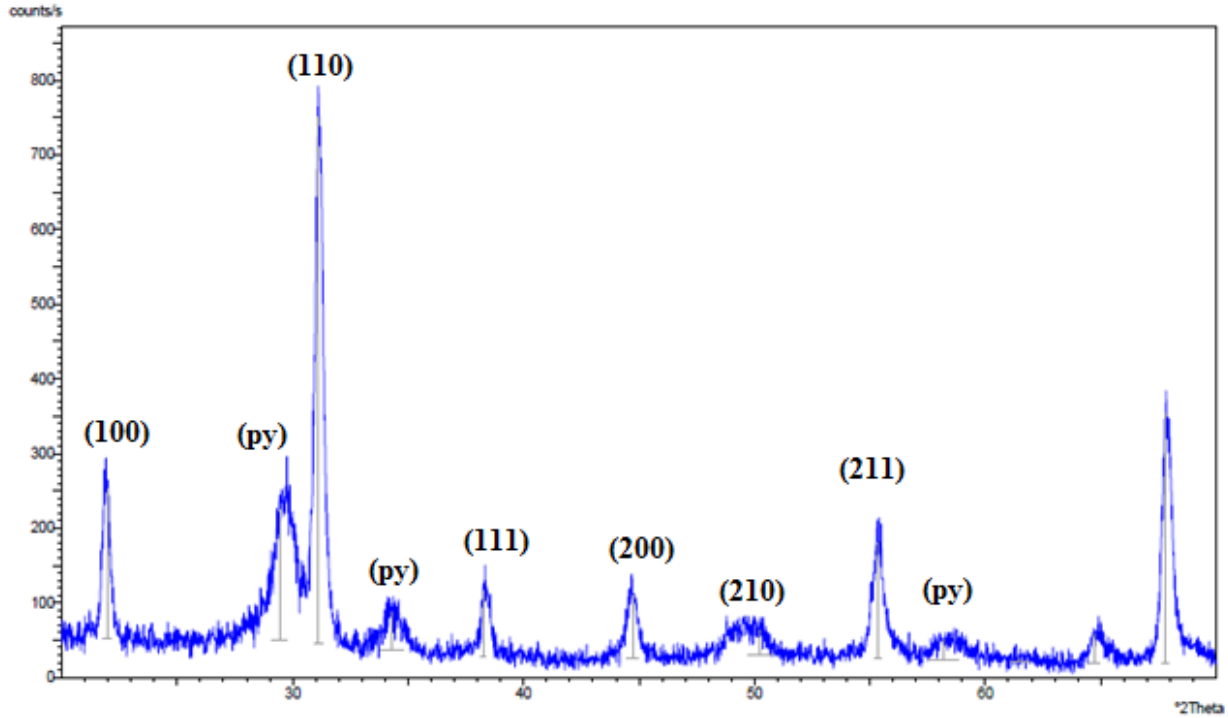

Fig. 61: XRD of PNZT 3%Nb films deposited on Pt/TiO2/Si substrate annealed at 700°C for 50min

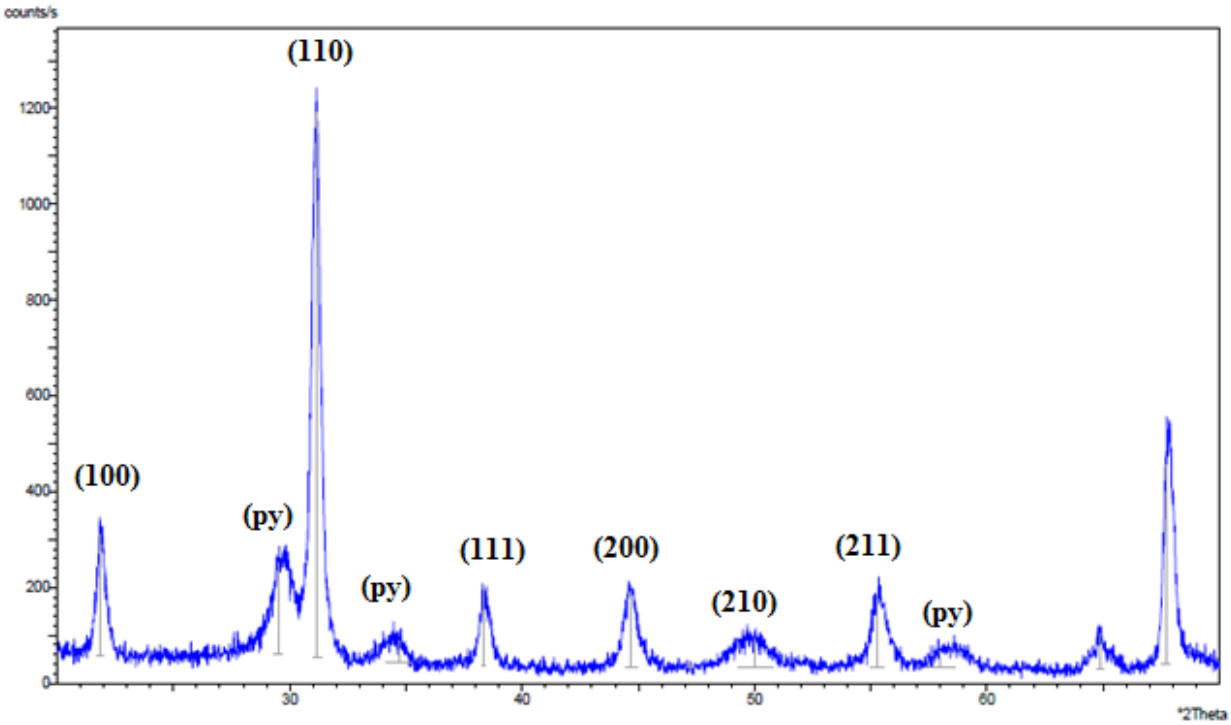

Fig. 62: XRD of PNZT 3%Nb films deposited on Pt/TiO2/Si substrate annealed at 700°C for 1h

The pyrochlore phase is still present after 1 hour of annealing, especially we can see a very high peak at 56.5° in fig.62. This peak never appears in the other sample, which is a consequence of

the high value of Niobium present inside the solution. The other pyrochlore peaks are at 29.6° 34.5°, 56.5° and 58.5°. We decided to bring the temperature at 825°C and anneal for 10min, 20min and 30min fig 63, 64 and 65

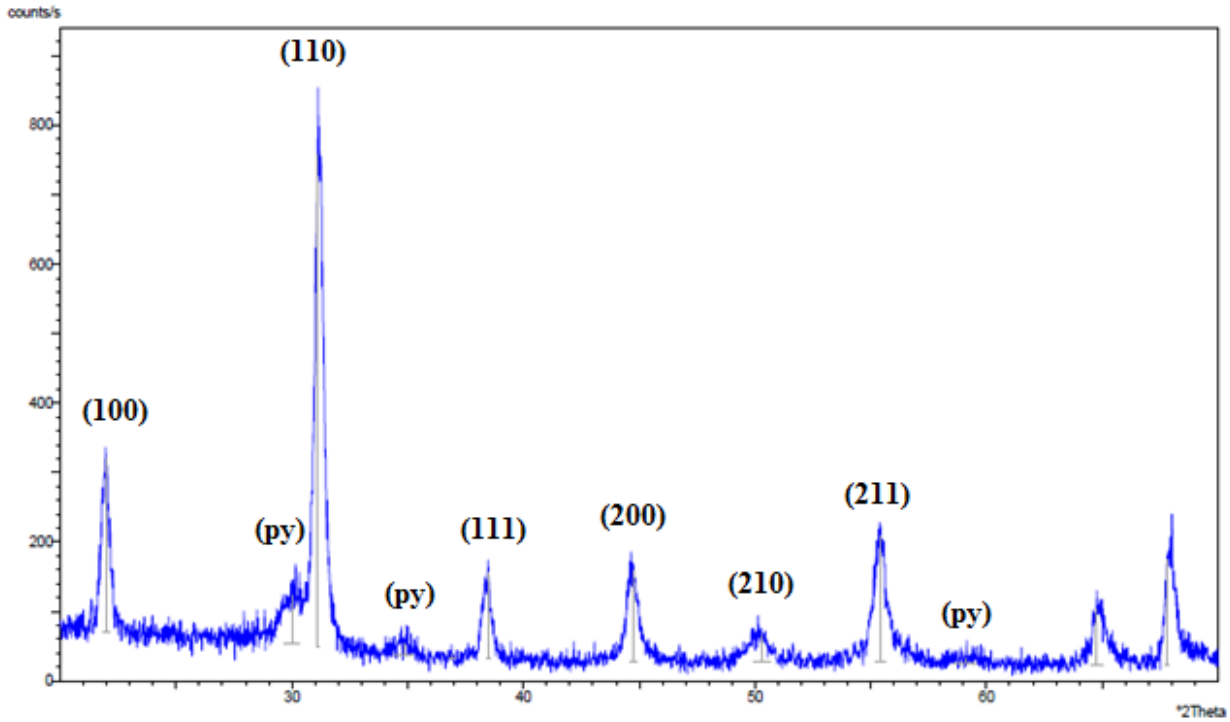

Fig. 63: XRD of PNZT 3%Nb films deposited on Pt/TiO2/Si substrate annealed at 825°C for 10min

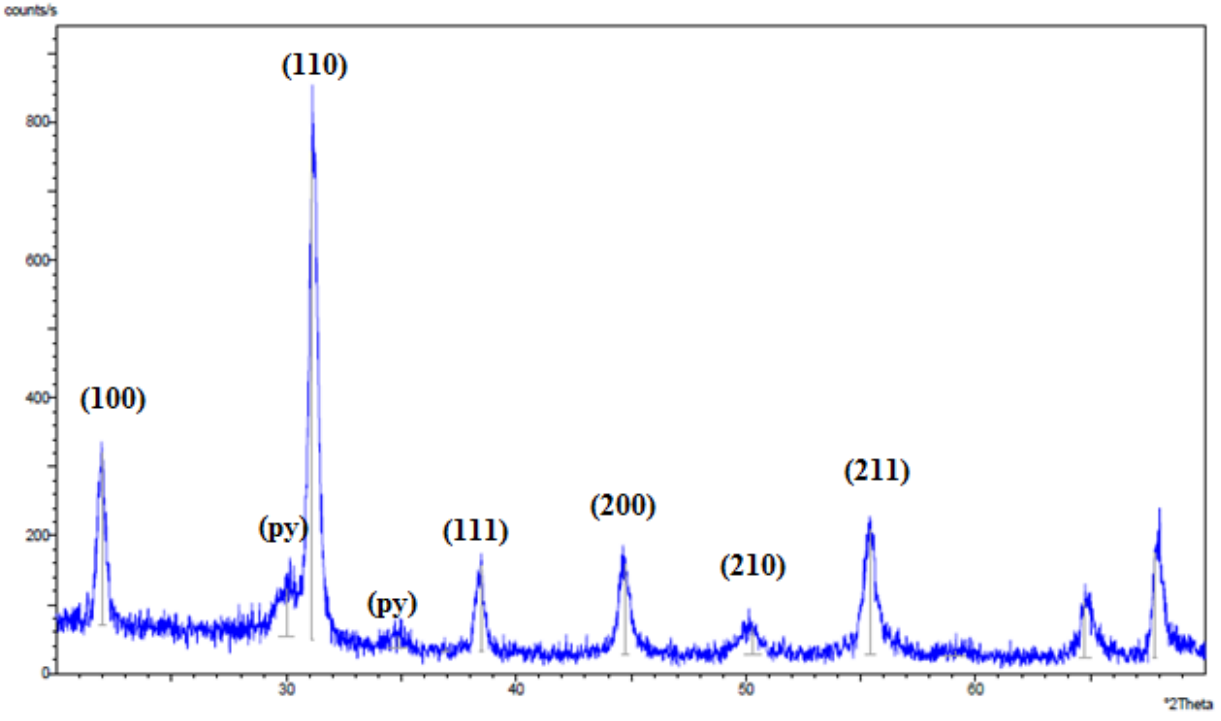

Fig. 64: XRD of PNZT 3%Nb films deposited on Pt/TiO2/Si substrate annealed at 825°C for 20min

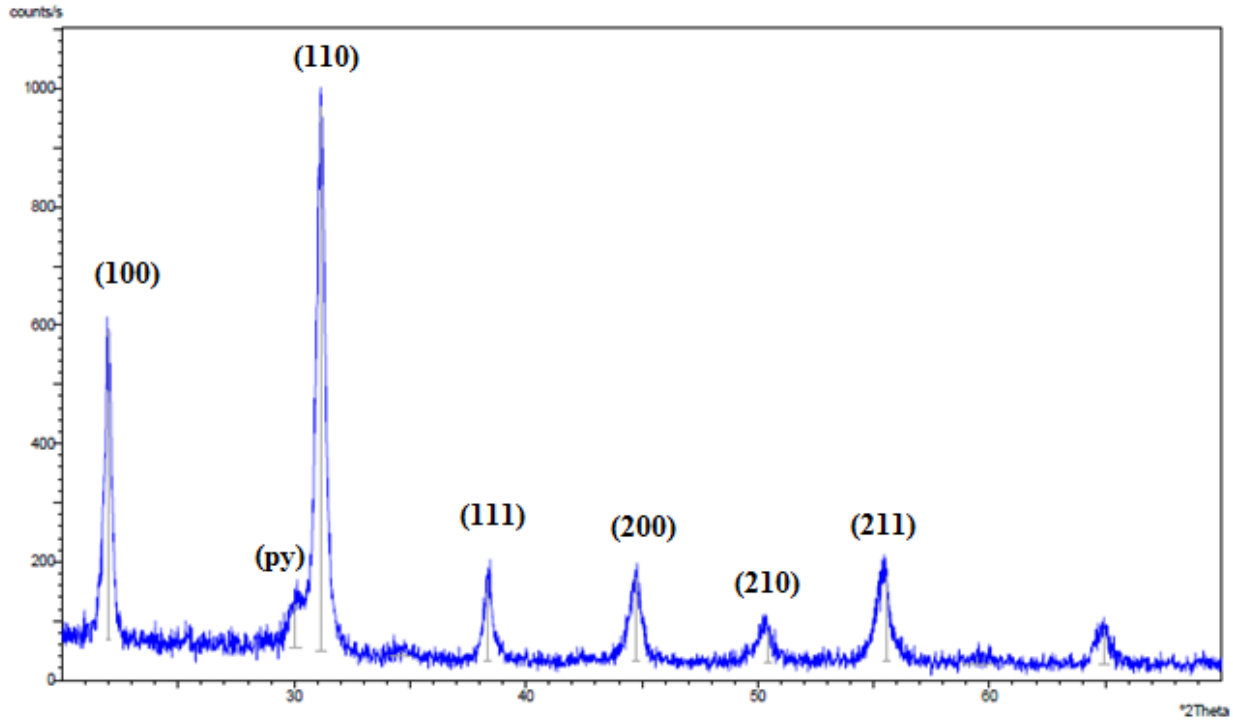

Fig. 65: XRD of PNZT 3%Nb films deposited on Pt/TiO2/Si substrate annealed at 825°C for 30min

The XRD shows that the pyrochlore phase has almost disappeared except for a little amount of metastable phase at 29.6°. The results show that the phase obtained are the same of the film of PZT, PNZT 1%Nb, PNZT 2%Nb. However in this last case it was very hard to obtain a film with good density and homogeneity due to the high temperature used for the annealing process. There is a good chance of obtaining cracked film, for this reason a doping using 1% and 2% of Niobium are preferred.

6.5 COMPOSITION ANALYSIS

The use of the Scanning Electron Microscope equipped with EDX allows us to obtain a composition analysis of our sample. This kind of measures can't show us the real value of the stoichiometry of the sample even if they are very important to reveal if the PZT thin film crystallize properly. The values obtained are slightly different from the ideal one but some assumption must be made. Tab.2 and fig.66 display the composition analysis of the PZT sample without Niobium. We can see that the composition measured is related to the desired composition, $Pb_1(Zr_{0.52}Ti_{0.48})O_{3,}$ but only with a certain allowance. However the analysis shows

that there are too much Oxygen and Titanium in the film. This is probably due to the fact that the results give us also indication about the substrate, made of TiO_2 and SiO_2.

Tab. 2: Composition of a single layer of PZT anneal at 650°C for 30min.

	Pb(%at)	**Zr(%at)**	**Ti(%at)**	**O(%at)**
PZT	14,96	7,70	7,36	60,85

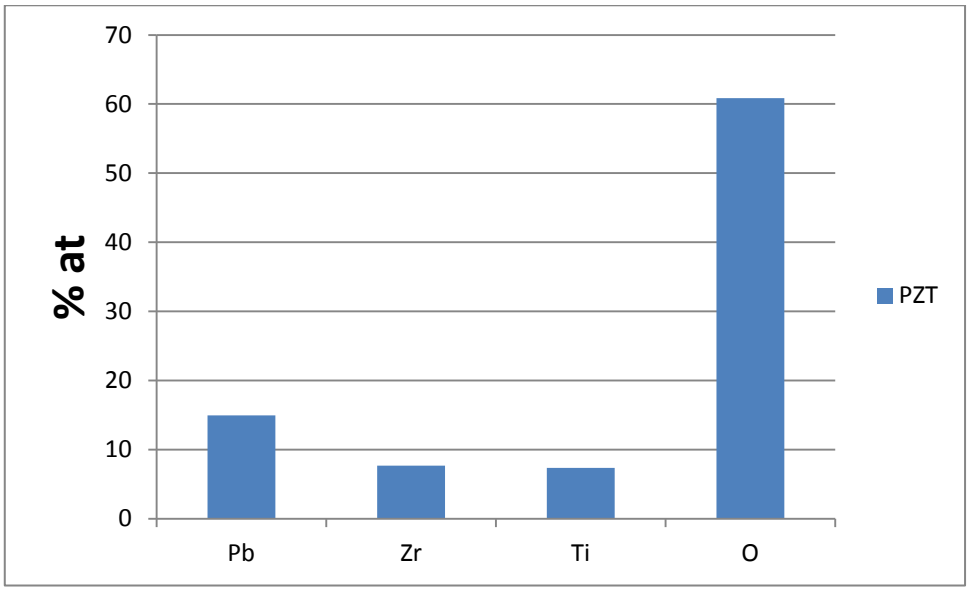

Fig. 66: Composition of a single layer of PZT anneal at 650°C for 30min.

Tab.3 and fig.67 shows the compositional analysis of the PNZT doped Niobium. The analysis shows that we move away from the ideal composition, $Pb_1(Zr_{0.52}Ti_{0.48})_{1-x}Nb_xO_3$.

Tab. 3: composition of three double layer of PNZT (1%,2%,3%)Nb anneal respectively at 700°C, 750°C, 825°C for 30min

	Pb(%at)	Zr(%at)	Ti(%at)	Nb(%at)	O(%at)
PNZT1%Nn	17,06	4,95	9,2	8,08	49,25
PNZT2%Nb	17,43	6,2	8,8	9,78	46,28
PNZT3%Nb	17,77	2,79	9,03	10,59	47,19

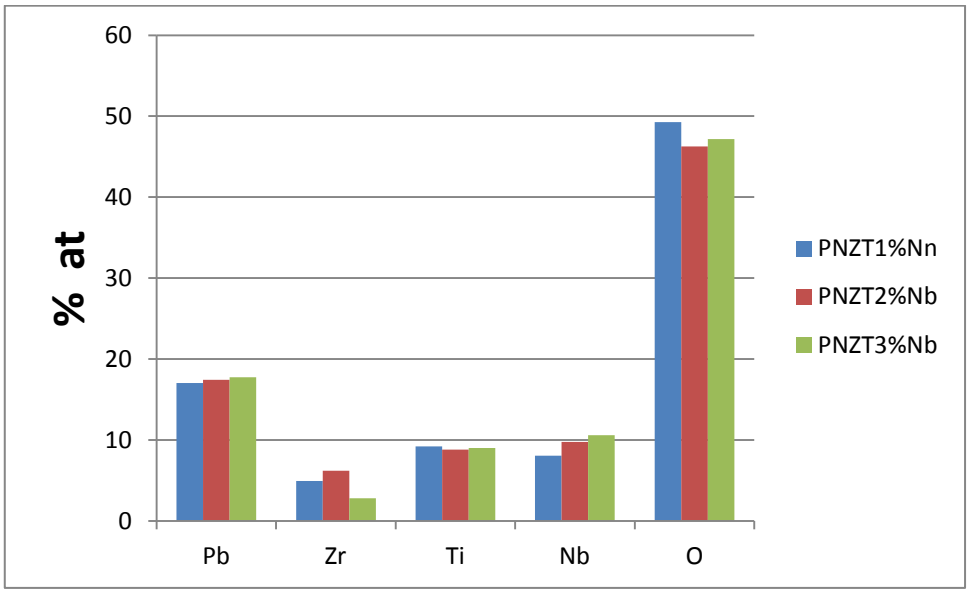

Fig. 67: composition of three double layer of PNZT (1%,2%,3%)Nb anneal respectively at 700°C, 750°C, 825°C for 30min

At this point different considerations can be done. We have a double layer so the great contribution of the SiO_2 for the oxygen that we had in the last case, now is negligible. Other thing to take into consideration are the low amount of Zirconium and the large amount of Niobium with regards to the ideal composition. It is possible that in addition to the Niobium with a doping effect, this element may replace the Zirconium in the crystallographic configuration, this fact could explain the low amount of Zirconium. Moreover some Niobium oxides can be generated during the firing step and they could be found on the surface of the sample. Therefore a large amount of Niobium is detected by the EDX analysis.

6.6 ELECTRICAL CHARACTERIZATION

After the analysis of the morphology and of the crystallographic structure of the deposited films, a matrix of top gold electrodes has been patterned onto those samples which have shown good morphology and that are fully crystallized into a perovskite phase, following the procedures described in the previous chapter. In this way, a metal/PZT/metal structure has been obtained and this is suitable for electrical measurements that in this work have been performed analyzing the C-V curves. Such characteristics as the absence of cracks, good density, good uniformity and a fully crystallization into a perovskite phase, are fundamental to fabricate performing devices. Using a capacimeter, measurements of C-V or ε-V curves have been made by applying simultaneously on the measured sample a DC field which changes as a step-like function and an AC voltage of relatively high frequency of small amplitude. In this case the frequency has been set at 100kHz and the oscillation level at 100mV for all the measurements. The AC voltage is used to measure the capacitance which is then plotted as a function of the DC bias field, resulting in a C-V graph. The C-V curves show a non-linear behavior for ferroelectric material, due to the existence of a remaining polarization and a coercitive field of the ferroelectric that alter the linearity between the capacitance of the dielectric and the applied voltage. The C-V curve for ferroelectric materials usually displays a butterfly shape, whose maximum values of capacitance are obtained near the 0V DC bias. The initial rise in the permittivity values of capacitance near the 0 DC bias is probably due to increased movement of the domain walls which becomes ’free’ from defects and will lock them at zero DC field. This phenomenon is due to partial switching of some domains whose coercive field happens to be small enough and can be switched by the DC and AC field combination. The re-orientation of domains increases the polarization of the ferroelectric and thus rises the overall capacitance measured. The maximum in the C - V curve is supposed to appear close to the coercive field for the P-E hysteresis when most of the domains switch and the material appears to be dielectrically very ’soft’. In fact, when the applied field is next to the value of the ferroelectric coercitive field (Ec), very small changes in the external field could induce wide changes in the polarization status of the ferroelectric. That is due to domain switching. At high DC fields, the permittivity decreases, as a cause of two processes: the decrease in the number of domains as they become more and more aligned with the field (ideally the sample becomes a single domain and only lattice contributions are present) and inhibition of the movement of residual domain walls by the DC field. In this work the top and bottom

electrodes were not made of the same material and this can affect the symmetry of the C-V curves creating a mismatch between the measures performed at positive and negative DC bias.

6.6.1 ELECTRICAL CHARACTERIZATION OF PZT FILMS

PZT films deposited on Pt electrodes have shown good density, uniformity, a fully crystallization into a perovskite structures with a preferential (110) orientation and absence of both macro and micro-cracks. The films derived from the solution have demonstrated good behavior on Pt electrodes. The capacitance of the sample has been tested using a capacimeter and the C-V and ε-V curves plotted, fig.68 and 69. For this kind of capacitors, the thickness of the dielectric between the electrodes, has been considered to be 0,5 µm, since each dielectric film is made by two PZT layers of 0,25µm each. When we calculate the dielectric constant using the capacitance values, the capacitor thickness is considered to be 1 µm, since the capacitance is calculated for two equal capacitors in series. The electrodes area is 197.000µm^2

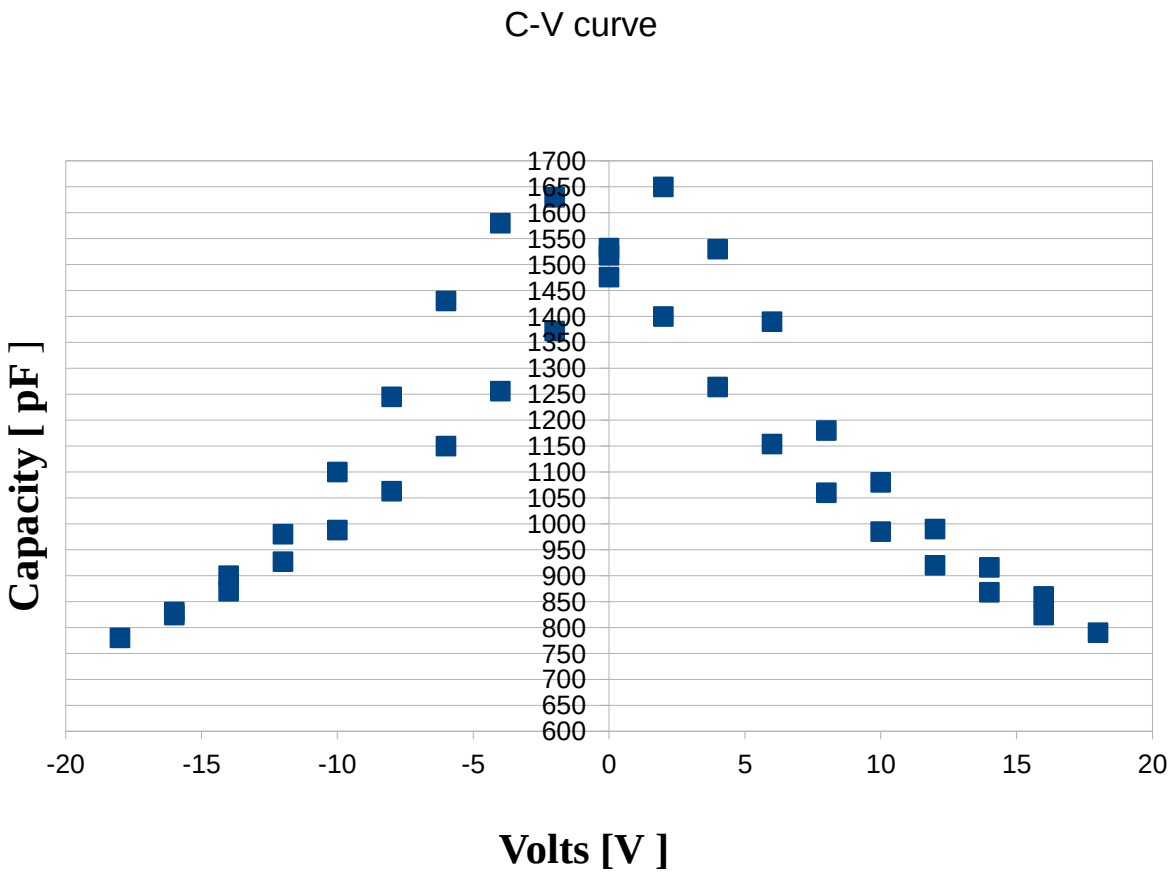

Fig. 68: C-V curve for 1µm PZT substrate annealed at 650°C for 30min

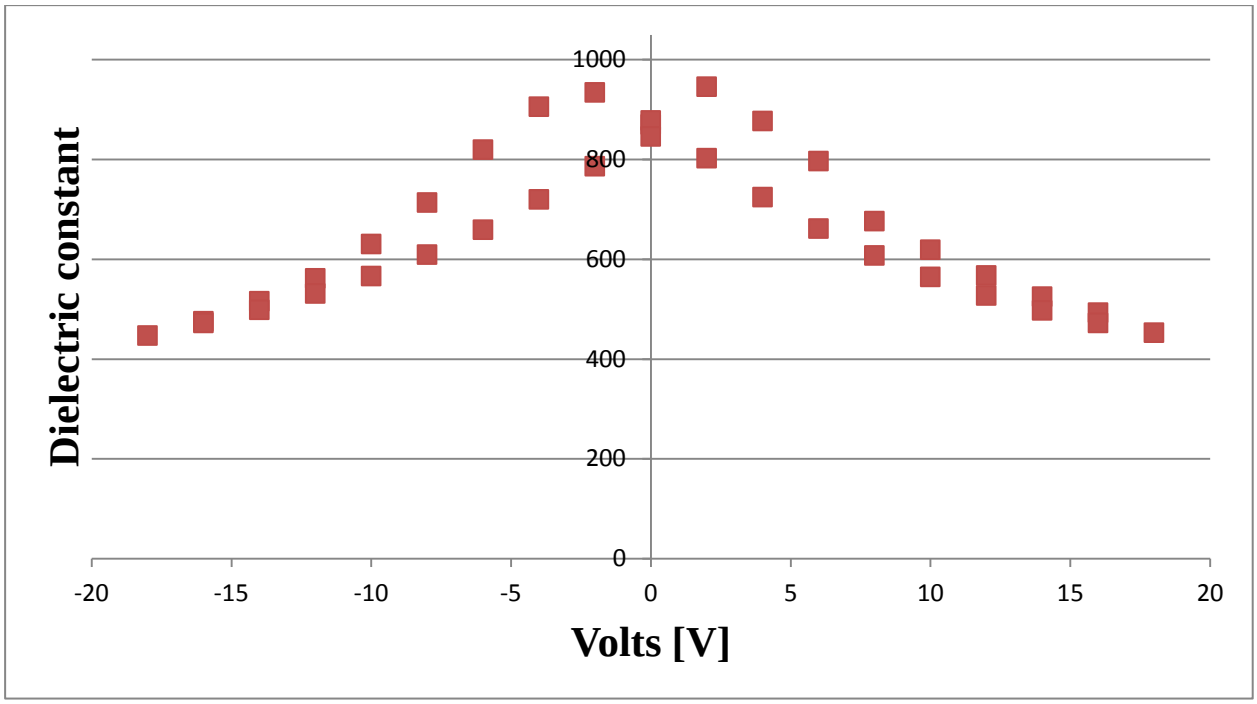

Fig. 69: ε-V curve for 1µm PZT substrate annealed at 650°C for 30min

These curves have a typical butterfly shape that has been already obtained in other works [41,42] and this proves the ferroelectricity of these films. The curve is nearly symmetric, the positive wing is narrower than the negative ones. The value of the dielectric constant at 0 V is approximately 870, which is an acceptable value for this kind of capacitor. Therefore, the PZT films deposited onto Pt electrodes possess the higher values of dielectric constant obtained in this work. The higher value of capacitance are obtained around 2 V for positive bias and it is 946.

6.6.2 ELECTRICAL CHARACTERIZATION OF PNZT 1%Nb FILMS

PNZT 1%Nb films deposited on Pt electrodes have shown very good morphology, good adhesion and it has been possible to obtain a full crystallization without problems of cracking or inter-diffusion elements between the different layers. The sample was annealed for 30 minutes at 700°C. The XRD and optical microscope analysis have shown that the crystallization behavior of these films is very similar to the one of the PZT. The films crystallized with a strong (110) preferential orientation. The capacitance of the capacitors, fabricated pattering a matrix of top gold electrodes onto the films has been measured and the C-V curve has been plotted, fig.70. Moreover, knowing the area of the patterned electrodes and the thickness of the deposited films is possible to find out the value of the dielectric constant and the ε-V curves, fig.71. The electrodes area is 785.000µm^2 and the thickness is around 1µm, considering that the capacitance

is measured for two equals capacitors in series. Each capacitor is made by a PZT film formed by two layers of approximately 250 nm each, as demonstrated by SEM analysis.

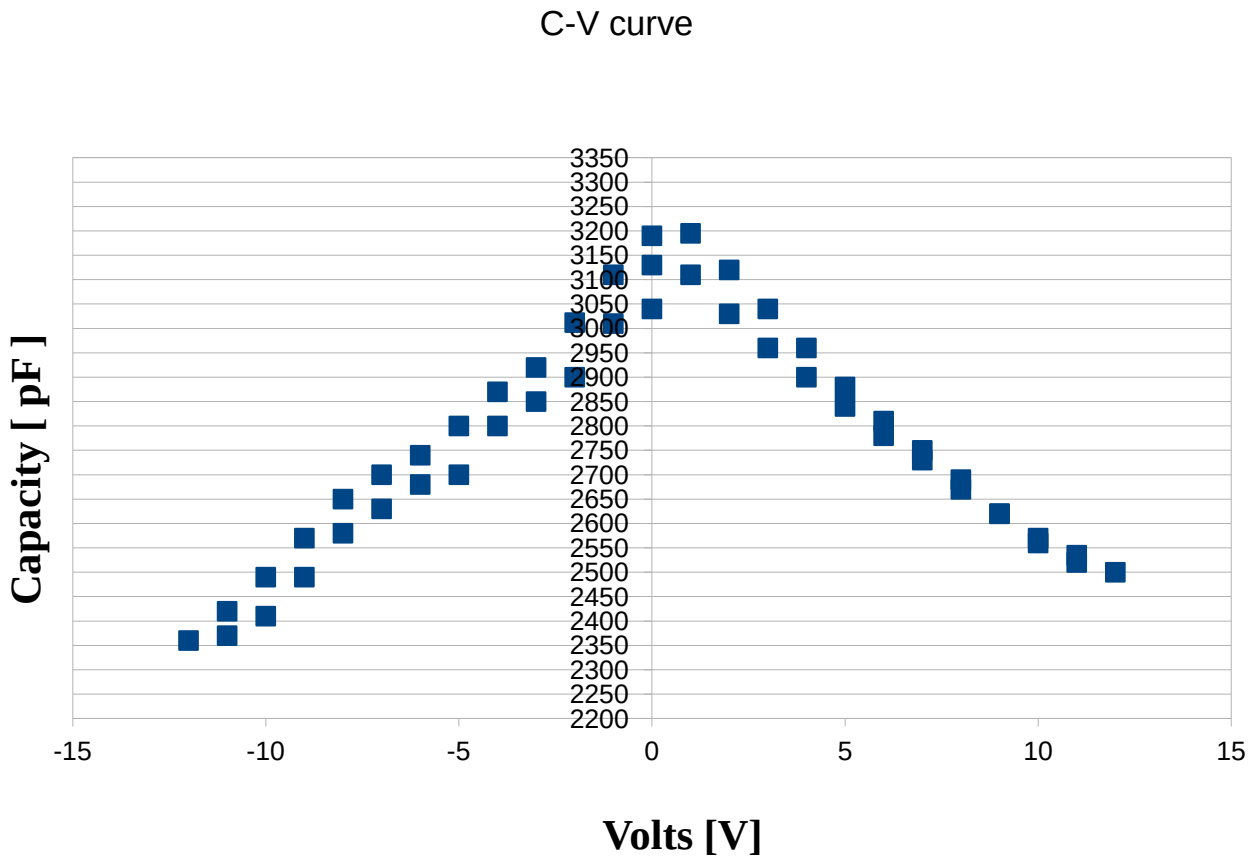

Fig. 70: C-V curve for 1µm PNZT 1%Nb substrate annealed at 700°C for 30min

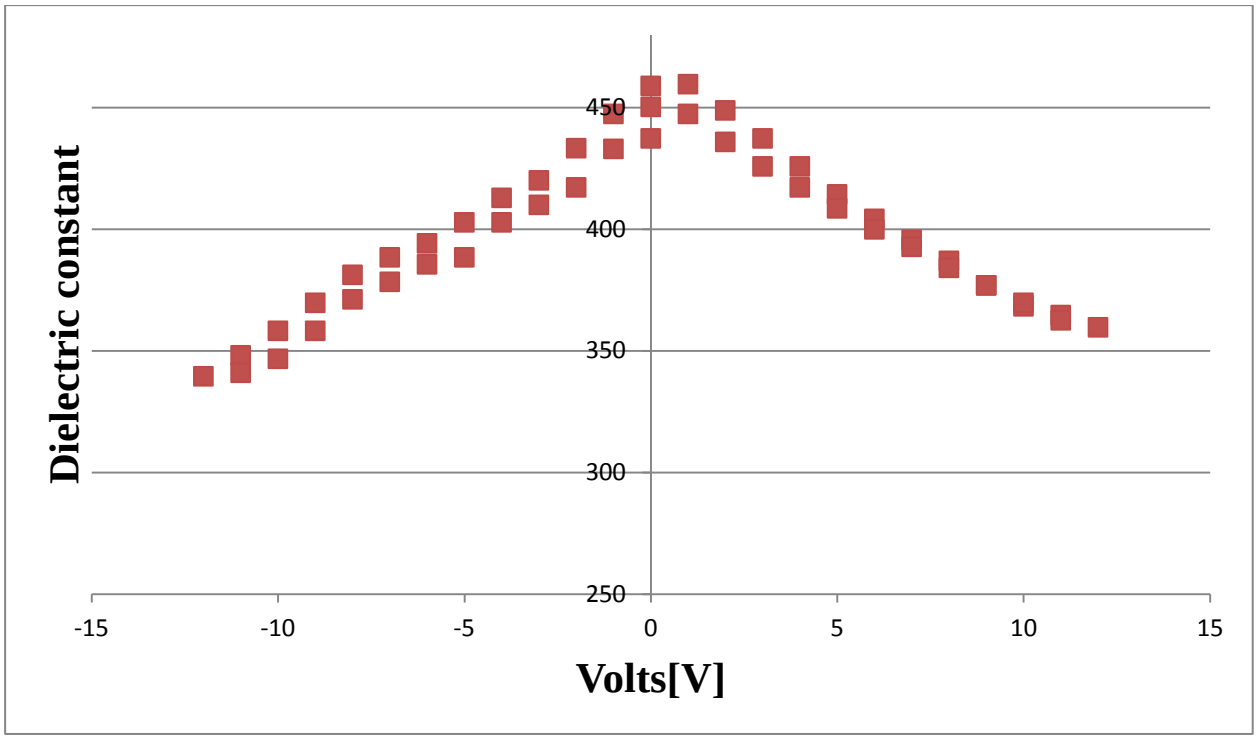

Fig. 71: ε-V curve for 1µm PNZT 1%Nb substrate annealed at 700°C for 30min

Also these films show ferroelectricity and the C-V curves have the typical butterfly shape of ferroelectric materials, Fig.70 and 71. The curves are less symmetric than in the previous case. In particular the values obtained for positive DC bias are slightly higher than those obtained for negative DC bias, and the positive wing of the C-V curve is narrower than the positive for both the curves. The value of the dielectric constant at 0V is 459. The maximum value is obtained at 1V and corresponds to a dielectric constant of 460.

6.6.3 ELECTRICAL CHARACTERIZATION OF PNZT 2%Nb FILMS

Also in the case the sample has a good density, uniformity, homogeneity and absence of cracks. The sample was annealed at 750°C for 30minutes. The XRD and optical microscope analysis have shown that the crystallization behavior of these films is very similar to the one of the PZT and PNZT 1%Nb and the films crystallized with a strong (110) preferential orientation. Using a capacimeter set with the parameter described before, the capacitance of the capacitor fabricated has been measured and the C-V curve has been plotted, fig.72. Moreover, knowing the area of the electrodes and the thickness of the deposited films is possible to find out the value of the dielectric constant and the ε-V curves, fig.73. In this case the electrodes area is 700.000 μm^2 and

the film thickness is considered to be 1 µm because the capacitance is calculated for two equals capacitors in series. Each capacitor is made by a PZT film composed by two layers of approximately 0.25 µm each.

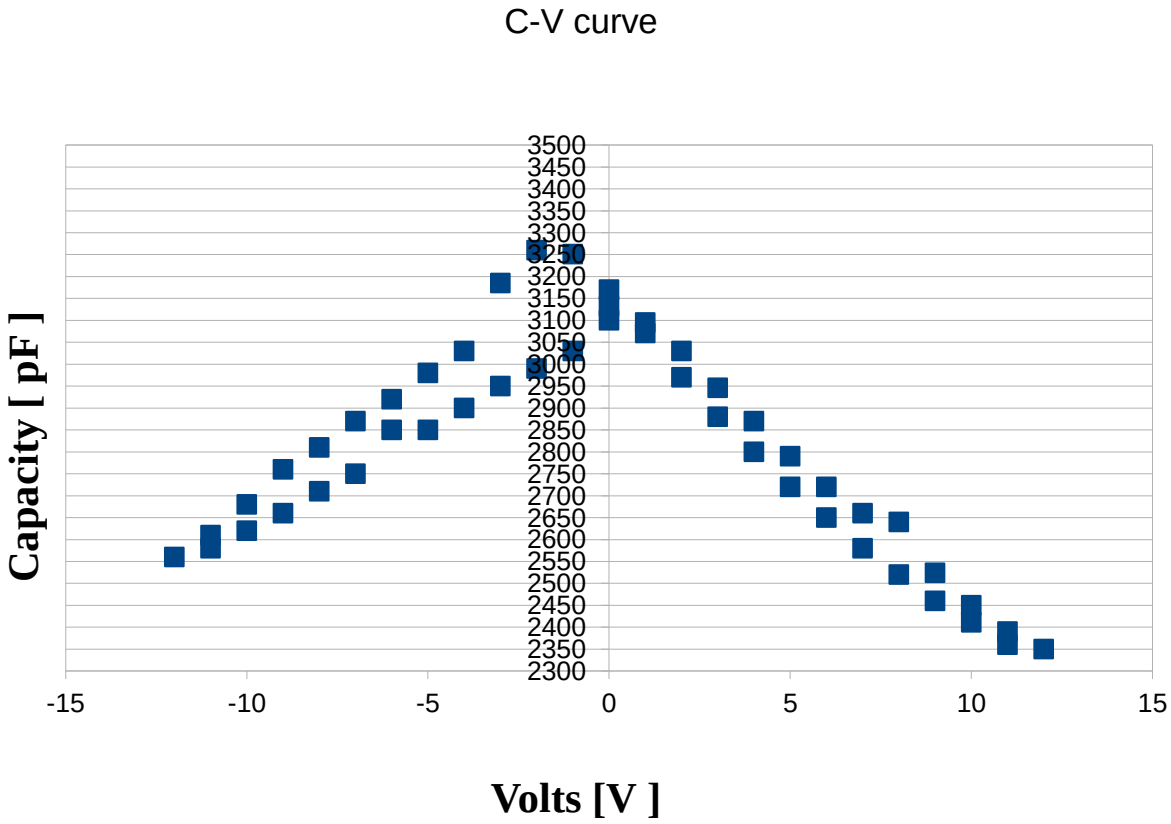

Fig. 72: C-V curve for 1µm PNZT 2%Nb substrate annealed at 750°C for 30min

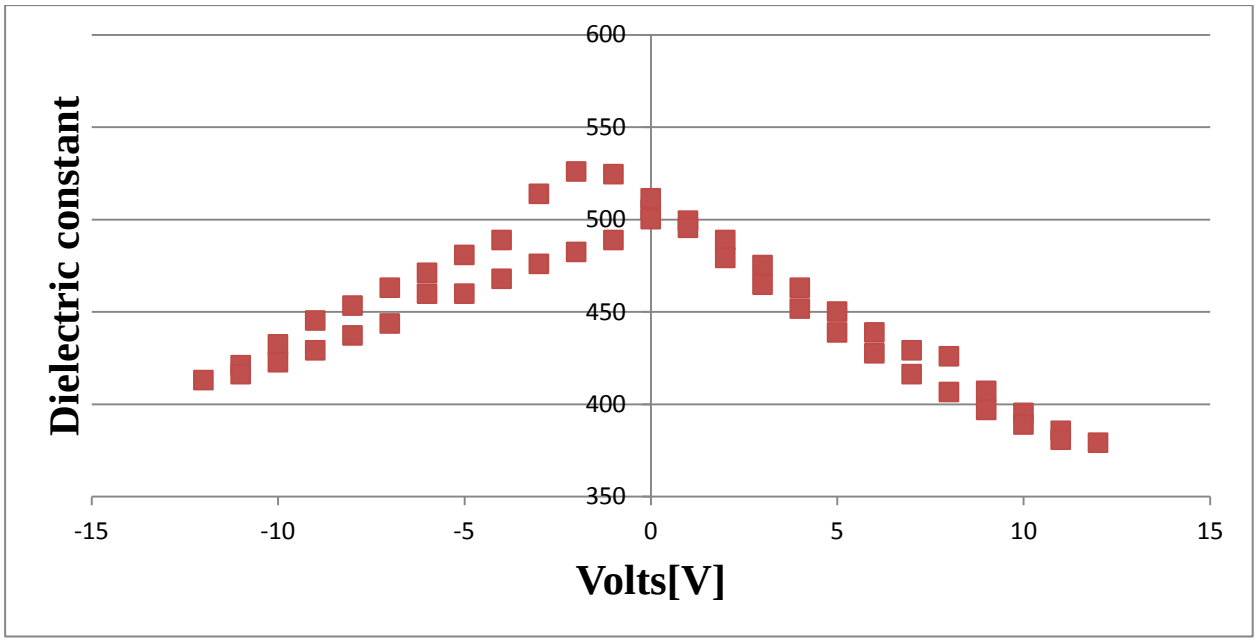

Fig. 73: ε-V curve for 1µm PNZT 2%Nb substrate annealed at 750°C for 30min

Even in this case there is a butterfly shape. The curves display a quite symmetric shape similar to the previous case. The values obtained for positive DC bias are slightly lower than those ones obtained for negative DC bias, and the positive wing of the C-V curve is narrower than the positive for both the curves. In this case the value of capacitance at 0V is 511 and the maximum value of capacitance is 526 obtained at 2 Volts for negative DC bias.

6.6.4 ELECTRICAL CHARACTERIZATION OF PNZT 3%Nb FILMS

The thin films obtained from the solution containing 3% of Niobium are very rich of cracks and microcracks. This is due to the fact that they were obtained at high temperature and therefore there is a good chance of obtaining cracked film. However the density and the homogeneity of the films allow us to verify the ferroelectric property using a capacimeter. The XRD and optical microscope analysis have shown that the crystallization behavior of these films is very similar to the one of the PZT and PNZT1%Nb and the films crystallized with a strong (110) preferential orientation. The capacitance and the dielectric constant of the capacitor have been measured and the C-V and ε-V curves have been plotted, fig.74 and 75. In this case the electrodes area is 785.000 μm^2 and the film thickness is considered to be 1 µm because the capacitance is calculated for two equals capacitors in series. Each capacitor is made by a PZT film formed by two layers of approximately 0.25 µm each.

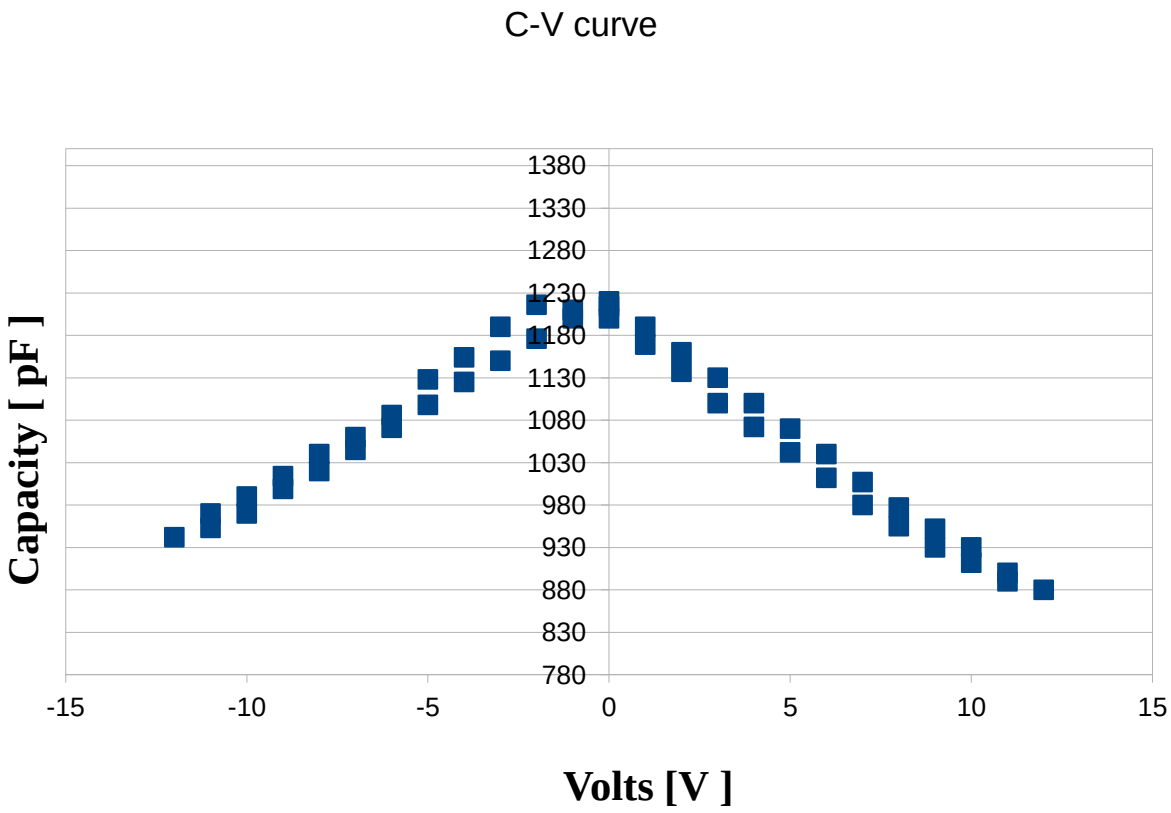

Fig. 74: C-V curve for 1µm PNZT 3%Nb substrate annealed at 825°C for 30min

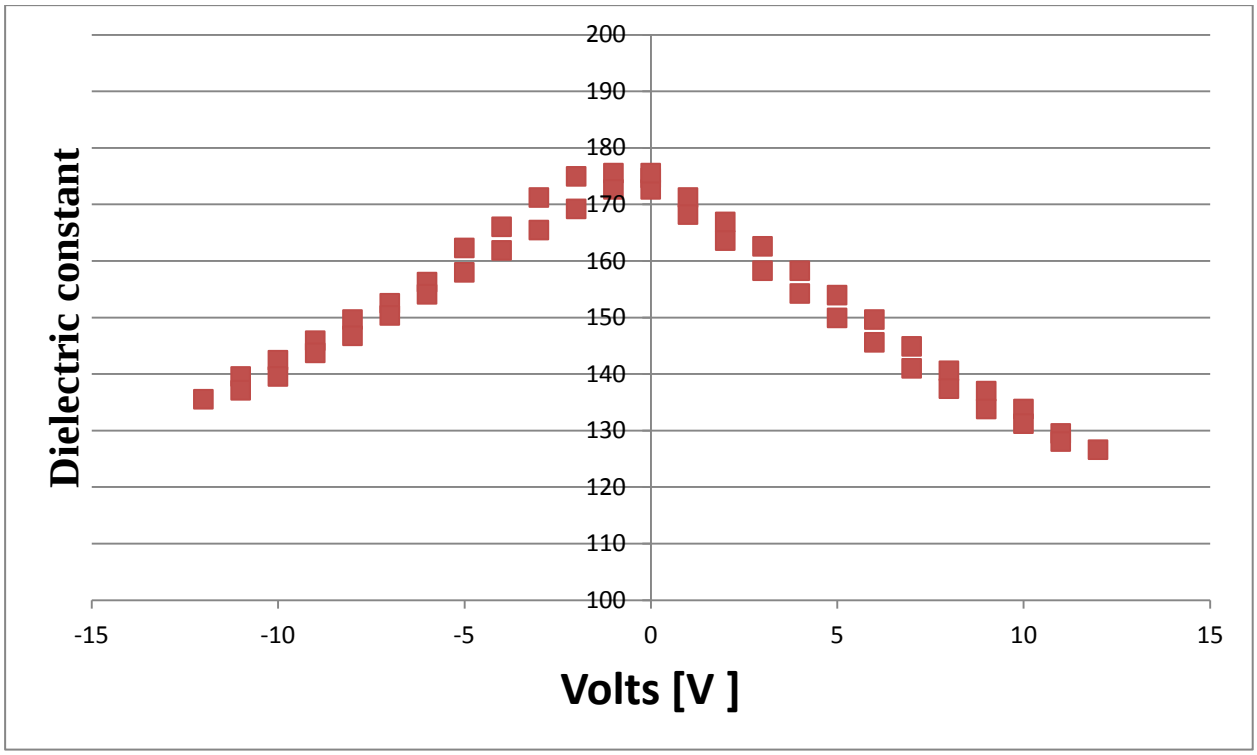

Fig. 75: curve for 1µm PNZT 3%Nb substrate annealed at 825°C for 30min

The butterfly shape is clearly evident, and the curves show a good symmetry. The value of the dielectric constant at 0V is 176 and this is also the maximum value. However, the center of the hysteresis loops is not located at zero bias voltage, but shifted toward the negative bias voltage. It is suggested that a internal bias field at the interface between the bottom electrode and PZT films was induced by the difference of thermal history of the top and bottom electrodes or entrapment of space charges, e.g., oxygen vacancies in the interface between electrode and film [37].

After showing the ferroelectric behaviour, some consideration must be done. The thin film with the best property in term of dielectric constant and value of capacitance is the PZT thin film. The values obtained matches with the literature[37]. As we mentioned previously, the introduction of Nb on bulk PZT ceramics induces a modification in films microstructure, space charge density, oxygen and lead vacancies density and in domain wall mobility. So, we can expect to observe some modifications in ferroelectric properties of PZT thin films by Nb doping. However we can see from the results that the ferroelectric properties are much less lower than the ferroelectric properties of the PZT undoped. It was proved by compositional analysis that the thin films doped with Niobium contain an high amount of Niobium with regards to the ideal composition, and we

said that this is probably due to the presence of some Niobium oxides on the surface of the film. It is possible that this oxides slow down the movement of the wall domain and this result in a decrease of the ferroelectric property of the sample. Speaking about the PNZT it was proved by the results that the ferroelectric properties increase with the increase in the amount of Niobium until it reaches 2%. After this value of doping the sample shows very low value of capacitance and dielectric constant. A possible explanation is the fact that as we said before, the PNZT 3%Nb requires an annealing temperature higher than 800°C. At this temperature the films always present cracks and microcracks and this defect are deleterious for the ferroelectric properties. Another explanation could be the fact that after a certain amount, the Niobium slows down the movement of the wall domain. Tab.4 shows the mean and the maximum value of dielectric constant obtained.

Tab. 4: mean value and maximum value of dielectric constant

	Dielectric constant (mean value)	**dielectric constant(max)**
PZT	656	946
PNZT 1%Nb	399	460
PNZT 2%Nb	451	526
PNZT 3%Nb	153	176

CHAPTER VII

7 CONCLUSIONS AND FURTHER WORKS

A method to synthesize and deposit via solution deposition technique Nb-doped Lead Zirconate Titanate (PNZT) thin films with a composition of $PbNb_x(Zr_{0.52}Ti_{0.48})_{1-x}O_3$ has been developed in this work. PZT material is widely used in the microelectronic industry to produce actuators, sensors, transducers and MEMS devices with high performances and therefore it's fundamental to develop a production process that has to be as simple as possible and that has to guarantee good films quality and high performances. Moreover the use of the less hazardous chemicals as possible is another important parameter that has to be taken into account when developing a production plan. First of all a new route to synthesize the PNZT sol-gel precursors solutions has been developed and secondly an appropriate thermal treatment to obtain fully crystallized films has been chosen. A simple method to obtain homogeneous and stable sol gel solutions has been developed Using Lead acetate 3-hydrated, Zirconium propoxide, Titanium isopropoxide and Niobium(V) ethoxide as metals precursors. Acetic acid and propanol have been used as solvent. An improvement offered by this method is the use of solvents which are less toxic than the commonly used 2-Methoxyethanol and the procedure to obtain the final sol-gel solution is definitely simpler. Following the procedures described in the thesis, homogeneous and stable sol gel solutions have been prepared. In the chemistry of the prepared solutions acetic acid has both the role of solvent and chelating agent, that is fundamental to modify the metals alkoxides in solution, lowering their tendency towards hydrolysis and condensation and consequently preventing the solution from gelification and metals precipitation. With this composition the sol gels have shown high stability over long periods and the metals precipitation has been avoided. Four different solutions have been prepared varying the Nb composition. The first solution was prepared adding 0% of Nb to produce a simple PZT solution, then we add 1% of Nb, in the third solution there was 2% of Nb and 3% of Nb in the last one. After the sol gels synthesis, the prepared solutions have been spinned coated on $Pt/TiO_2/SiO_2/Si$ substrates. A proper thermal

treatment has been performed on the deposited films and it includes a drying step at 150°C, a firing step at 370°C and an annealing step at a temperature higher than 650°C. For the drying and firing steps the process time has been set at 5 minutes and the effects of different annealing times on the films crystallization have been studied. A proper thermal treatment must prevent any type of films cracking and elements diffusion from the substrate to the PZT layer, and it must assure a fully films crystallization into a ferroelectric perovskite phase. For the solutions containing 0%, 1% and 2% of Niobium, uniform, dense and crack free PZT films with a fully perovskite crystallographic structure has been obtained, tuning the annealing times and temperature. The solution containing 3% of Nb had a fully perovskite structure but a problem of formation of cracks and micro cracks occurred due to the high temperature used in the process. For all the solutions, the PNZT films crystallized into a polycrystalline structure but with a strong (110) preferential orientation, which is the most thermodynamically stable phase. The thickness of a PNZT mono layer was around 0,25 μm, as demonstrated by SEM analysis. Double layer films have been deposited for all the four different solutions, using for each one those combinations of annealing temperature and annealing time that guarantee the formation of fully crystallized films with good morphology. More exactly 30 minutes are used for all the different solution, 650°C for the PZT film, 700°C for the PNZT 1%Nb, 750°C for the PNZT 2%Nn and 825°C for the PNZT 3%Nb. Then a compositional analysis was made. The analysis shows that the PZT undoped has a composition very close to the ideal one, but in the PZT Nb-doped there is an higher value of Niobium than expected, this is probably due to the fact that some Niobium oxides grow up on the ceramic interface. Finally, top gold electrodes have been patterned, using cold sputtering deposition, on the deposited double layer films, obtaining in this way a metal/PZT/metal structure that is suitable for electrical measurements. The electrical characterization has been done analyzing the C-V and the ε-V curves of the capacitors fabricated. These curves have shown a non linear relation between the capacitance and the applied voltage and a butterfly shape that is typical of ferroelectric materials. Observing these curves it can be concluded that all the films deposited behave as ferroelectric and so the scope of this work has been reached. The C-V curves were not always symmetric and this phenomenon is due to fact that different materials were used to build the top and bottom electrode. The dielectric constants of these films can be extrapolated and the mean values found are 656 for the PZT thin film, 399 for the PNZT 1%Nb, 451 for the PNZT 2%Nb and 153 for the PNZT 3%Nb. The value of the dielectric constant of the PZT thin film is in agreement with the literature, the values of the PZT Nb-doped are lower than expected. A possible explanation is that the Niobium oxides described before slows down the wall domain mobility and this results in a decrease of the

ferroelectric property. It is important to underline that no piezoelectric and polarization measurement was done, therefore further works should be done to fully understand the properties of these ferroelectric thin films. Other important works can be done to solve the problem of the excess of Niobium in the final composition, in order to avoid the formation of Niobium oxides on the surface. A possible way to solve this problem is the use of a solution with a different composition from the ideal one. Also the use of different solvent and precursors must to be take into consideration, in fact the solution used in this thesis require high temperature to activate the transformation from pyrochlore phase to perovskite phase. High temperature is deleterious for the film as we said before it could bring to crack formation, especially for the PNZT 3% Nb.

REFERENCES

[1] Chidambaram, N., Mazzalai, A., & Muralt, P. (2012). Measurement of effective piezoelectric coefficients of PZT thin films for energy harvesting application with interdigitated electrodes. *IEEE Transactions on Ultrasonics, Ferroelectrics, and Frequency Control, 59*(8), 1624-1631.

[2] Kayasu, V., & Ozenbas, M. (2009). The effect of nb doping on dielectric and ferroelectric properties of PZT thin films prepared by solution deposition. *Journal of the European Ceramic Society, 29*(6), 1157-1163

[3] Giacomo Gafforelli, "Deposition of PZT on silicon substrate ", Ph.D. School of Materials Engineering: Material for Electronics Applications , Politecnico of Milano.

[4] Taeyun Kim, "Lead Zirconate Titanate (PZT) based thin film capacitors for embedded applications", PhD dissertation, Graduate Faculty of North Carolina State University, Department of Material Science and Engineering, Raleigh, 2003.

[5] Ruangchalermwong, C., Li, J., Zhu, Z., Lai, F., & Muensit, S. (2009). Enhanced ferro- and piezoelectric properties in (100)-textured nb-doped pb(ZrxTi1 - x)O3 films with compositions at morphotropic phase boundary.*Thin Solid Films, 517*(24), 6599-6604.

[6] Chilibon, I., & Marat-Mendes, J. (2012). Ferroelectric ceramics by sol-gel methods and applications: A review. *Journal of Sol-Gel Science and Technology, 64*(3), 571-611.

[7] Taeyun Kim, "Lead Zirconate Titanate (PZT) based thin film capacitors for embedded applications", PhD dissertation, Graduate Faculty of North Carolina State University, Department of Material Science and Engineering, Raleigh, 2003.

[8] Matthieu Cueff , "Micro-actionneurs Piézoélectriques" , Thesis project, École Doctorale Electronique, Electrotechnique, Automatique et Traitement du Signal, Universitè de Grenoble, France, November 2011 pag 21

[9] S. Somiya, F. Aldinger, N. Claussen, R.M. Spriggs, K. Uchino, K. Koumoto, M. Kaneno, 2003, ELSEVIER academic press, *Handbook of Advanced Ceramics* VOLUME II Processing and their Applications pag 108

[10] Jaffe, B., Cook, W.R. and Jaffe, H., Piezoelectric Ceramics, Academic press, London and new York, (1971)

[11] S. Somiya, F. Aldinger, N. Claussen, R.M. Spriggs, K. Uchino, K. Koumoto, M. Kaneno, 2003, ELSEVIER academic press, *Handbook of Advanced Ceramics* VOLUME II Processing and their Applications pag 111-117

[12] Morgana electroceramics, resources, 2013 Guide to Piezoelectric & Dielectric Ceramic chapter 1

[13] Isupov, V. A. (1983). Some aspects of the physics of piezoelectric ceramics. *Ferroelectrics, 46*(3-4), 217-225.

[14] *Robert B. Heimann 2010 WILEY-VCH Verlag GmbH & Co.KGaA, Weinheim*, Classic and Advanced Ceramics From Fundamentals to Applications classic and advanced ceramics pag 25

[15] *Robert B. Heimann 2010 WILEY-VCH Verlag GmbH & Co.KGaA, Weinheim*, Classic and Advanced Ceramics From Fundamentals to Applications classic and advanced ceramics pag 271

[16] Morgana electroceramics, resources, 2013 Guide to Piezoelectric & Dielectric Ceramic chapter 2

[17] Brett Harold Piekarski. Lead Zirconate Titanate thin films for piezoelectric actuation and sensing of mems resonator. Dissertation submitted to the Faculty of the Graduate School of the University of Maryland, College Park in partial fulfillment of the requirements for the degree of Doctor of Philosophy 2005

[18] C. Jefferey Brinker, George W. Scherer, 1990 Sol-gel science The Physics and Chemistry of Sol-Gel Processing ELSEVIER academic press pag 7-8-9

[19] Heinz K. Henisch, 1970, THE PENNSYLVANIA STATE UNIVERSITY PRESS, Crystal growth in gels (Penn. State uiv 1970 p41

[20] C. Jefferey Brinker, George W. Scherer, 1990 Sol-gel science The Physics and Chemistry of Sol-Gel Processing ELSEVIER academic press pag 1

[21] Yi, G., & Sayer, M. (1996). Acetic acid/water based sol-gel PZT process I: Modification of zr and ti alkoxides with acetic acid. *Journal of Sol-Gel Science and Technology, 6*(1), 65-74.

[22] Yi, G., & Sayer, M. (1996). Acetic acid/water based sol-gel PZT process II: Formation of a water based solution. *Journal of Sol-Gel Science and Technology, 6*(1), 75-82.

[23] Zhang, Q., Huang, Z., & Whatmore, R. W. (2002). Studies of lead zirconate titanate sol ageing part I: Factors affecting particle growth. *Journal of Sol-Gel Science and Technology, 23*(2), 135-144.

[24] Guanghua Yi, Zheng Wu and Michael Sayer, "Preparation of Pb(Zr,Ti)O3 thin films by sol gel processing: Electrical, optical, and electrooptic properties" , *Journal Applied Physics*, 64 (5).

[25] Boyle, T. J., Dimos, D., Schwartz, R. W., Alam, T. M., Sinclair, M. B., & Buchheit, C. D. (1997). Aging characteristics of a hybrid sol-gel pb(zr,ti)O3 precursor solution. *Journal of Materials Research, 12*(4), 1022-1030

[26] Brian Leclerc, Process Optimization for Sol-Gel PZT Films Queen's University Kingston, Ontario, Canada March 1999

[27] Bhuiyan, M. S., Paranthaman, M., & Salama, K. (2006). Solution-derived textured oxide thin films - A review. *Superconductor Science and Technology, 19*(2), R1-R21.

[28] Piezoelectric coefficients of $Pb(Zr,Ti)O_3$ ceramics as a function of composition close to the morphotropic phase boundary [PhD dissertation, Graduate Faculty of North Carolina State University, Department of Material Science and Engineering, Raleigh, 2003

[29] Zhu, W., Fujii, I., Ren, W., & Trolier-Mckinstry, S. (2012). Domain wall motion in A and B site donor-doped pb (zr 0.52 ti 0.48) O 3 films. *Bio 2011, , 95.* (9) pp. 2906-2913.

[30] Julia Vivian Martinez, "Fabrication, materials and characterization for Efficient MEMS power generation", *Thesis of Master of science in Materials science and Engineering, Washington State University, School of Mechanical and Materials Engineering,* August 2004

31] K.D. Budd, S.K. Dey, and D.A. Payne, (1985). Sol-gel processing of PbTiO3, PbZrO3, PZT, and PLZT thin films. *Proc. Ceramic Proc.* 36, pg. 107-121

[32] S.K. Dey, K.D. Budd and D.A. Payne. (1988). Thin film ferroelectrics of PZT by

sol-gel processing. *IEEE Trans. UFFC 35(1), p.80* 49

[33] M. Sayer. PIEZOELECTRIC THIN FILM DEVICES. (1991). Department of Physics, Queen's University Kingston, Ontario, *IEEE* 1051-0117/91/0000-059, Ultrasonic symposium.

[34] Qin, H. Zhu, J. Jin, Z. & Wang Y.. (2000) .PZT thin films with preferred-orientation induced by external stress., *Thin Solid Films,* 379, pg. 72-75.

[35] Birnie, D. P. I.,II, & Manley, M. (1997). Combined flow and evaporation of fluid on a spinning disk. *Physics of Fluids, 9*(4), 870-870.

[36] Guanghua Yi and Michael Sayer; "SOL GEL PROCESSING OF THICK PZT FILMS" , Department of Physics, Queen's University Kingston, Ontario, Canada.

[37] Souza, E. C. F., Simões, A. Z., Cilense, M., Longo, E., & Varela, J. A. (2004). The effect of nb doping on ferroelectric properties of PZT thin films prepared from polymeric precursors. *Materials Chemistry and Physics,88*(1), 155-159.

[38] Kurchania, R., & Milne, S. J. (2003). Effect of niobium modifications to PZT (53/47) thin films made by a sol-gel route. *Journal of Sol-Gel Science and Technology, 28*(1), 143-150.

[39] Kayasu, V., & Ozenbas, M. (2009). The effect of nb doping on dielectric and ferroelectric properties of PZT thin films prepared by solution deposition. *Journal of the European Ceramic Society, 29*(6), 1157-1163.

[40] Sumio Sakka, "HANDBOOK of SOL–GEL SCIENCE and TECHNOLOGY: Processing, Characterization and Applications", *VOLUME I: Sol-gel processing*, volume editor: Hiromitsu Kozuka, Kansai University,Suita, Osaka, Japan

[41] S.K. Pandey, A.R. James, R. Raman, S.N. Chatterjee, Anshu Goyal,Chandra Prakash, T.C. Goel, (2005).Structural, ferroelectric and optical properties of PZT thin films., *Physica B* 369

(2005) p.g 135–142, Elsevier

[42] K. K. Uprety, L. E. Ocola, and O. Auciello, (2007).Growth and characterization of transparent Pb(Zi,Ti)O3 capacitor on glass substrate. *Journal Applied Physics* 102, 084107 , American Institute of Physics